ASSESSMENT OF SLOPE STABILITY FOR A SEGMENT (Km: 25+600-26+000) OF ANTALYA-KORKUTELİ HIGHWAY

A THESIS SUBMITTED TO
THE GRADUATE SCHOOL OF NATURAL AND APPLIED SCIENCES
OF
MIDDLE EAST TECHNICAL UNIVERSITY

BY

HURİYE ASLI ARIKAN

IN PARTIAL FULFILLMENT OF THE REQUIREMENTS
FOR
THE DEGREE OF MASTER OF SCIENCE
IN
GEOLOGICAL ENGINEERING DEPARTMENT

JUNE 2010

I hereby declare that all information in this document has been obtained and presented in accordance with academic rules and ethical conduct. I also declare that, as required by these rules and conduct, I have fully cited and referenced all material and results that are not original to this work.

Name, Last name : Huriye Aslı Arıkan

Signature :

ABSTRACT

ASSESSMENT OF SLOPE STABILITY FOR A SEGMENT
(KM: 25+600-26+000) OF ANTALYA-KORKUTELİ HIGHWAY

Arıkan, Huriye Aslı

M.Sc., Department of Geological Engineering

Supervisor: Prof. Dr. Tamer Topal

June 2010, 94 pages

The cut slopes at a segment between Km 25+600 and 26+000 of the Antalya-Burdur Breakaway-Korkuteli State Road to be newly constructed have slope instability problems due to the existence of highly jointed limestone.

The purpose of this study is to investigate the engineering geological properties of the units exposed at three cut slopes, to assess stability of the cut slopes, and to recommend remedial measures for the problematic sections.

In this respect, both field and laboratory studies have been carried out. The limestone exposed at the cut slopes are beige to gray, fine grained, fossiliferous, and highly jointed. It has two joint sets and a bedding plane

as main discontinuities. The kinematic analysis indicates that planar failure is expected at Km: 25+900. Limit equilibrium analysis show that the cut slopes with bench have no slope instability problems except rockfalls which endanger the traffic safety. In this thesis it is recommended to covering the cut slope with wire mesh and fibre reinforced shotcrete

Keywords: Highway, Limestone, Kinematic Analysis, Limit Equilibrium Analysis, Rock-Fall, Rock Slope, Korkuteli

ÖZ

ANTALYA-KORKUTELİ KARAYOLUNUN BİR KESİMİ (KM: 25+600-26+000) İÇİN ŞEV DURAYLILIĞININ DEĞERLENDİRİLMESİ

Arıkan, Huriye Aslı

Yüksek Lisans, Jeoloji Mühendisliği Bölümü

Tez Yöneticisi: Prof. Dr. Tamer Topal

Haziran 2010, 94 sayfa

Yeni yapılacak Antalya-Burdur Ayrımı Korkuteli Yolunun Km:25+500-26+000 arasındaki kesiminde bulunan ve çok çatlaklı kireçtaşı içinde yer alan kaya yarma şevlerinde, şev duraysızlık problemleri bulunmaktadır.

Bu çalışmanın amacı, kaya yarma şevlerde bununan birimlerin mühendislik jeolojisi özelliklerini incelemek, şev stabilitesini değerlendirmek ve problemli kesimler için çözüm önermektir.

Bu çerçevede, saha ve laboratuvar çalışmaları yapılmıştır. Kaya yarma şevlerde, bej-gri, ince taneli fosilli ve çok çatlaklı kireçtaşı bulunmaktadır. Ana süreksizlikler olarak, kayaçta iki eklem takımı ve bir tabaka mevcuttur. Yapılan kinematik analizlere göre, Km: 25+900'de düzlemsel

kayma beklenmektedir. Trafik güvenliğini tehlikeye düşürecek kaya düşmeleri dışında, limit denge analizlerine göre palyeli şevlerde herhangi bir duraysızlık problemi bulunmamaktadır. Bu tezde, palyeli kaya yarma şevler için, tel kafes ve fiberle güçlendirimiş şatkrit kullanılması önerilmektedir.

Anahtar kelimeler: Karayolu, Kireçtaşı, Kinematik Analiz, Limit Denge Analizi, Kaya Düşmesi, Kaya Şevi, Korkuteli

To My Dear Mother, Father and My Grandfather

ACKNOWLEDGEMENTS

I am greatly indebted to Prof.Dr. Tamer Topal for his guidance, very encouraging supervision, interest, patience and his endless helps.

Many thanks to all my instructors for giving the best information.

I am grateful to Geol. Eng. Tahir Tanju Ökten and Geol. Eng. Mehmet Besim Hanedar at Form-Beril for their support during the thesis studies, all the field work studies, the laboratory supports and information and knowledge sharing.

I want to thank to my dear friend Esin Şişman for her help, productive suggestions and discussions, especially in the research part. Also for her friendship and all kinds of helps and supports for years.

I would like to thank to all my friends, especially Ulaş Canatalı, Balkın Çoker and Nazan Çapoğlu for all their supports and helps and especially their friendship during the stressful preparation stage.

Finally, I would like to thank my family, my mom and dad, for their unlimited patience, support and encouragement in every step I took both in this study and all through my life. I also would like to thank to my grandfather and my grandmother for their support and willingness for finishing this degree.

TABLE OF CONTENTS

ABSTRACT……iv

ÖZ……vi

ACKNOWLEDGEMENTS……ix

TABLE OF CONTENTS……x

LIST OF TABLES……xiii

LIST OF FIGURES……xiv

CHAPTER

1. INTRODUCTION……1

    1.1. Purpose and Scope……1

    1.2. Location and Properties of the Road……2

    1.3. Vegetation and Climate……5

    1.4. Methods of Study……7

    1.5. Previous Studies……8

2. GEOLOGY AND SEISMICITY OF THE STUDY AREA……10

    2.1. Geology of the Study Area……10

    2.2. Seismicity of the Study Area……13

3. ENGINEERING GEOLOGICAL PROPERTIES OF THE LIMESTONE

EXPOSED AT Km: 25+600-26+000……16

3.1. Engineering Geological Properties of Limestone at Km: 25+600……23

3.2. Engineering Geological Properties of Limestone at Km: 25+900……27

3.3. Engineering Geological Properties of Limestone at Km: 26+000……31

4. KINEMATIC ANALYSES OF THE CUT SLOPES……35

4.1. Kinematic Analysis of the Cut Slope at Km: 25+600……35

4.2. Kinematic Analysis of the Cut Slope at Km: 25+900……38

4.3. Kinematic Analysis of the Cut Slope at Km: 26+000……42

5. LIMIT EQUILIBRIUM AND ROCKFALL ANALYSES OF THE SLOPE ……45

5.1. Limit Equilibrium Analysis of the Cut Slope for Planar Failure at Km: 25+900……46

5.2. Limit Equilibrium Analysis of the Cut Slope for Mass Failure at Km: 25+900……46

5.3. Rockfall Analysis of the Cut Slope……58

5.3.1. Rockfall Analysis of the Cut Slopes in the Current Situation……58

5.3.2. Rockfall Analysis of the Cut Slope at Km: 25+600……62

5.3.3. Rockfall Analysis of the Cut Slope at Km: 25+900……69

5.3.4. Rockfall Analysis of the Cut Slope at Km: 26+000……76

6. DISCUSSION.....84

7. CONCLUSIONS AND RECOMMENDATIONS.....90

REFERENCES.....92

LIST OF TABLES

TABLE

Table 3.1. Orientations of the major discontinuity sets at Km:25+600…26

Table 3.2. Orientations of the major discontinuity sets at Km:25+900…28

Table 3.3. Orientations of the major discontinuity sets at Km:26+000…32

Table 5.1. Parameters used in the rockfall analysis for the cut slopes…58

Table 6.1. Comparison of the factor of safety values from the limit equilibrium analysis at Km: 25+900……85

Table 6.2. Rockfall run-out distances for the cut slopes……86

Table 6.3. Types of rockfall movements at the cut slopes ……87

Table 6.4. Comparison of the catch barrier distances from the road ……88

LIST OF FIGURES

FIGURES

Figure 1.1. Satellite view of the study area……3

Figure 1.2. Location and transportation map of the study Area……4

Figure 2.1. Geological map of the study area (modified from MTA)……11

Figure 2.2. A view from Yeniceboğazıdere formation……12

Figure 2.3. A view from Limestone Unit……13

Figure 2.4. Earthquake zoning map of the study area and its close vicinity with recorded epicenters ……34

Figure 2.5. Earthquake acceleration map of Turkey for the stability analyses of slopes……35

Figure 3.1. The geological plan (Scale: 1/1000) showing the borehole (SK-1 and SK-2) locations near Yenice bridge at Km: 26+600-26+700)……17

Figure 3.2. Borehole log of SK-1 at Yenice bridge……18

Figure 3.3. Borehole log of SK-2 at Yenice bridge……19

Figure 3.4. Photograph of the oriented samples taken from the field……19

Figure 3.5. Summary report for the direct shear test……21

Figure 3.6. Mohr-Coulomb failure criterion of the limestone based the

test results.....22

Figure 3.7. A view from limestone facing north at Km: 25+600.....23

Figure 3.8. Pole plot and contour diagram of the discontinuities at Km: 25+600.....24

Figure 3.9. Rose diagram of the discontinuities at Km: 25+600.....25

Figure 3.10. Dominant discontinuity sets at Km: 25+600.....25

Figure 3.11. A view from the limestone facing north at Km: 25+600.....26

Figure 3.12. A view from the limestone facing north at Km: 25+900.....27

Figure 3.13. Pole plot and contour diagram of the discontinuities at Km: 25+900.....29

Figure 3.14. Rose diagram of the discontinuities at Km: 25+900.....29

Figure 3.15. Dominant discontinuity sets at Km: 25+900.....30

Figure 3.16. A view from the limestone at Km: 25+900.....30

Figure 3.17. A view from the limestone facing north at Km: 26+000.....31

Figure 3.18. Pole plot and contour diagram of the discontinuities at Km: 26+000.....33

Figure 3.19. Rose diagram of the discontinuities at Km: 26+000.....33

Figure 3.20. Dominant discontinuity sets at Km: 26+000.....34

Figure 3.21. Discontinuities developed in the limestone at Km: 26+000 34

Figure 4.1. Photograph showing main discontinuities developed in the

limestone at Km: 25+600.....36

Figure 4.2. Kinematic analysis of the cut slope for planar failure at Km: 25+600.....36

Figure 4.3. Kinematic analysis of the cut slope for wedge failure at Km: 25+600.....37

Figure 4.4. Kinematic analysis of the cut slope for toppling failure at Km: 25+600.....37

Figure 4.5. Photograph showing main discontinuities developed in the limestone at Km: 25+900.....38

Figure 4.6. Kinematic analysis of the cut slope for planar failure at Km: 25+900.....39

Figure 4.7. Elimination of the planar failure kinematically by flattening of the slope at Km: 25+900.....39

Figure 4.8. Kinematic analysis of the cut slope for wedge failure at Km: 25+900.....40

Figure 4.9. Elimination of the wedge failure kinematically by flattening of the slope at Km: 25+900.....41

Figure 4.10. Kinematic analysis of the cut slope for toppling failure at Km: 25+900.....41

Figure 4.11. Photograph showing main discontinuities developed in the limestone at Km: 26+000.....42

Figure 4.12. Kinematic analysis of the cut slope for planar failure at Km: 26+000.....43

Figure 4.13. Kinematic analysis of the cut slope for wedge failure at Km: 26+000……44

Figure 4.14. Kinematic analysis of the cut slope for toppling failure at Km: 26+000……44

Figure 5.1. Limit equilibrium analysis of the cut slope with discontinuity controlled failure surface using current highway slope geometry……47

Figure 5.2. Limit equilibrium analysis of the cut slope with all surfaces analysed……47

Figure 5.3. Limit equilibrium analysis of cut slope with surfaces showing factor of safety only less than 1.1……48

Figure 5.4. Limit equilibrium analysis of the flattened cut slope by 7^{o}…49

Figure 5.5. Limit equilibrium analysis of the slope with bench……49

Figure 5.6. Limit equilibrium analysis of the slope with rock bolting…50

Figure 5.7. Limit equilibrium analysis of the slope with the rock bolting and all surfaces analysed……48

Figure 5.8. GSI value of the limestone rock mass selected from the Roclab software……52

Figure 5.9. The outputs of RocLab software for cut slope analyzed……53

Figure 5.10. Limit equilibrium analysis of the cut slope for mass failure with current slope geometry……54

Figure 5.11. Limit equilibrium analysis of the cut slope for mass failure with all possible failure surfaces……54

Figure 5.12. Limit equilibrium analysis of the cut slope for mass failure after slope flattening……55

Figure 5.13. Limit equilibrium analysis of the cut slope for mass failure after slope flattening with all possible failure surfaces ……56

Figure 5.14. Limit equilibrium analysis of the cut slope with bench for mass failure……57

Figure 5.15. Limit equilibrium analysis of the cut slope with bench and all possible failure surfaces for mass failure……57

Figure 5.16. Rockfall analysis with 10 kg block for current slope condition ……59

Figure 5.17. Rockfall analysis with 60 kg block for current slope condition ……59

Figure 5.18. Rockfall analysis with 150 kg block for current slope condition……60

Figure 5.19. Rockfall analysis with 10 kg block and barrier solution for current slope condition……61

Figure 5.20. Rockfall analysis with 60 kg block and barrier solution for current slope condition……61

Figure 5.21. Rockfall analysis with 150 kg block and barrier solution for current slope condition……62

Figure 5.22. Rockfall analysis with 10 kg block and slope flattening solution at Km: 25+600……63

Figure 5.23. Rockfall analysis with 60 kg block and slope flattening solution at Km: 25+600……63

Figure 5.24. Rockfall analysis with 150 kg block and slope flattening solution at Km: 25+600……64

Figure 5.25. Rockfall analysis with 10 kg block and bench solution at Km: 25+600……64

Figure 5.26. Rockfall analysis with 60 kg block and bench solution at Km: 25+600……65

Figure 5.27. Rockfall analysis with 150 kg block and barrier solution for current slope condition……65

Figure 5.28. Rockfall analysis (10 kg block) with slope flattening and barrier solution at Km: 25+600……66

Figure 5.29. Rockfall analysis (60 kg block) with slope flattening and barrier solution at Km: 25+600……67

Figure 5.30. Rockfall analysis (150 kg block) with slope flattening and barrier solution at Km: 25+600……67

Figure 5.31. Rockfall analysis (10 kg block) with bench and barrier solution at Km: 25+600……68

Figure 5.32. Rockfall analysis (60 kg block) with bench and barrier solution at Km: 25+600……68

Figure 5.33. Rockfall analysis (150 kg block) with bench and barrier solution at Km: 25+600……69

Figure 5.34. Rockfall analysis (10 kg block) with slope flattening solution at Km: 25+900……70

Figure 5.35. Rockfall analysis (60 kg block) with slope flattening solution at Km: 25+900……70

Figure 5.36. Rockfall analysis (150 kg block) with slope flattening solution at Km: 25+900……71

Figure 5.37. Rockfall analysis (10 kg block) with bench solution at Km: 25+900……71

Figure 5.38. Rockfall analysis (60 kg block) with bench solution at Km: 25+900……72

Figure 5.39. Rockfall analysis (150 kg block) with bench solution at Km: 25+900……72

Figure 5.40. Rockfall analysis (10 kg block) with slope flattening and barrier solution at Km: 25+900……73

Figure 5.41. Rockfall analysis (60 kg block) with slope flattening and barrier solution at Km: 25+900……74

Figure 5.42. Rockfall analysis (150 kg block) with slope flattening and barrier solution at Km: 25+900……74

Figure 5.43. Rockfall analysis (10 kg block) with bench and barrier solution at Km: 25+900……75

Figure 5.44. Rockfall analysis (60 kg block) with bench and barrier solution at Km: 25+900……75

Figure 5.45. Rockfall analysis (150 kg block) with bench and barrier solution at Km: 25+900……76

Figure 5.46. Rockfall analysis (10 kg block) with slope flattening solution at Km: 26+000……77

Figure 5.47. Rockfall analysis (60 kg block) with slope flattening solution at Km: 26+000……77

Figure 5.48. Rockfall analysis (150 kg block) with slope flattening solution at Km: 26+000……78

Figure 5.49. Rockfall analysis (10 kg block) with bench solution at Km: 26+000……78

Figure 5.50. Rockfall analysis (60 kg block) with bench solution at Km: 26+000……79

Figure 5.51. Rockfall analysis (150 kg block) with bench solution at Km: 26+000……79

Figure 5.52. Rockfall analysis (10 kg block) with slope flattening and barrier solution at Km: 26+000……80

Figure 5.53. Rockfall analysis (60 kg block) with slope flattening and barrier solution at Km: 26+000……81

Figure 5.54. Rockfall analysis (150 kg block) with slope flattening and barrier solution at Km: 26+000……81

Figure 5.55. Rockfall analysis (10 kg block) with bench and barrier solution at Km: 26+000……82

Figure 5.56. Rockfall analysis (60 kg block) with bench and barrier solution at Km: 26+000……82

Figure 5.57. Rockfall analysis (150 kg block) with bench and barrier solution at Km: 26+000……83

CHAPTER 1

INTRODUCTION

1.1. Purpose and Scope

Antalya-İzmir State Highway is becoming important due to increase in traffic, especially related to tourism. However, the present road from the Antalya-Burdur Breakaway-Korkuteli (Km: 25+500-63+500) is out of standard and now cannot take additional traffic load. Therefore, a new road project with widening of the existing one is initiated. The new road will be part of the Antalya-İzmir State Highway with 2x2 lane motorway. It has 22.00-26.00 m of platform width.

Various lithologies and several natural or cut-slopes exist along the highway route. The field studies reveal that the section of the Antalya-Burdur Breakaway-Korkuteli highway from Km: 25+600 to 26+000 is located in limestone and has three slopes having slope instability problems.

The purpose of this study is to investigate the engineering geological properties of the limestone exposed at Km: 25+600-26+000, to assess stability of the slopes for different mode of failures, and to suggest necessary remedial measures that can be adopted in practice.

In order to accomplish this task, a detailed field study including engineering description of the limestone and scan-line survey was

conducted. The samples taken were tested in the laboratory. The data obtained from both the field and the laboratory were used for kinematic, limit equilibrium and rockfall analysis.

1.2. Location and Properties of the Road

Antalya-Korkuteli State Road starts at Km: 25+578 at the north of Thermessos National Park. At Km: 26+660, it crosses the Yeniceboğazı Stream by a bridge and makes curves through NW. Km: 31+550, Bayatbademleri Junction comes and it continues parallel to the Cinli Stream through west. At Km: 38+000, it passes the Naldöken Junction, and curves to SW at the Gölcük Alluvium Plateau. At 2 km south of the Söğütçük Village, it curves to W again, and passes from the Canavar Gate, and reaches the Bayat Junction. At Km: 49+600, it reaches to Yazır Junction, and at Km: 54+450, it crosses Marzuman Stream with a bridge and continues parallel to the stream. It leaves the present road at Km: 55+030, turns from the S and W of Korkuteli. Finally, the road turns to W and end at Fethiye at Km: 63+603 (Figures 1.1 and 1.2).

The properties of the project are given below:

Road Type and Class: State Road, 1st Class

Lane Number and Width: 2x2, 3.50 m

Platform Width: 22.00-26.00 m

Refuge Width: 2.00-4.00 m

Expropriation Width: 40.00-50.00 m

Sidewalk Width: 3.00 m

Bench Width: 5.00 m

Figure 1.1. Satellite view of the study area (from Google Earth, 2010)

Figure 1.2. Location and transportation map of the study area (GDH)

1.3. Vegetation and Climate

The climate of Antalya is generally of Mediterranean type. It is hot and dry in the summers and warm and wet in the winters. In the inner parts of the region, "Cold Mid-Continental" climate is dominant.

The average temperature in the summers is between 28 and 36 °C. At the midday, temperature gets hotter than 40 °C. In January, the average temperature changes between 10 and 20 °C. Snow is not seen in the city. Frost is almost never seen. When the weather is not rainy, it is clear and sunny. In Antalya, where the average relative humidity is % 64, the average temperature of sea water is 17.6 °C in January, 18.0 °C in April, 27.7 °C in August and 24.5 °C in October. On the coast of Antalya, summertime is long and hot. Even in winters, the temperature is cool to warm. While the rain is unavailable in summer, downpour of rain is frequent in December and January, but rare during the months of fall and spring. Barely 40-50 days of the year are overcast and rainy. Antalya is one of the rare regions which are available for tourism with average 300 sunny days during the year and the yearly average temperature of 18.7 °C. It is possible to have a swim at least for the nine months of the year (Antalya Municipality, 2007a).

Lemur, which is suitable for extreme summer draughts and stays green during the wintertime, is dominant from the shore to the heights of 500-600 m. Ryegrass, arbutus, sandalwood, wild strawberries and oleander are common among lemur which has a maximum height of 3-5 m. Between the altitude of 600-1200 m, there appears the mixed or hillside forests where Pinus brutia and oak are widespread. Oak groves are seen between Pinus brutia, and on higher altitudes Aleppo pine and black pine begins to appear. Between the altitudes of 1200-2100 m there is a zone of high forests which consists of cedar, fir, scotch pine,

beech, and various juniper types. Especially in the Western Taurus, there are wholesome cedar forests. Above the altitude of 2000 m coniferous trees become sparse and short. This zone ends between 2100-2300 m, and passes through high hayricks, so called the alpine meadows, which consists of colorful flowers and does not run dry during summertime. In the high plains of Teke Plateau, steppe plants have grown out due to the destruction of oak trees. In the forests of Antalya extending to 946.466 hectares, there are types of herb and tree like fir, oak, ashen, elm, arbutus, sycamore, wild pear, linden, wild and inoculated olive, kermes oak, dyer's oak, sandalwood, gumwood, myrtle, Melia azaderach, daphne, Phllyrea, agnus-castus, oleander, carob, hop-hornbeam, heather, spruce, dyer's rocket, genista, thyme, popper, spurge, thorny myrtle, musk thistle, dead nettle, sage, saffron, Kanadisches Berufkraut, Sarcopoterium spinosum L., Asphodelus, asparagus, chrysanthemum (Antalya Municipality, 2007b).

The area of Korkuteli district is 2471 km^2. Its altitude from the shoreline is 1020 m, and its climate is Mediterranean with the ratio of ¼, and Lake District type continental with the ratio of ¾. The four seasons are apparent in the district and the average temperature is -5 °C in wintertime and 25 °C in summertime (Antalya Agriculture, 2007).

There is a terrain structure consisting of plains and hills at the back side of the Beydağları facing towards Mediterranean. Naturally, the slopes and feet of Beydağları is covered with pine groves, shrubbery and forests; on the other side plains are used for agricultural means. In the district 101.465 hectares are agricultural fields, 5800 hectares are lawn and pasture, 100.339 hectares are forests and shrubbery, 351 hectares are water surface, and 40.313 hectares are residential and non-agricultural areas. 116 hectares of the agricultural field is located within the area of the forests (Antalya Agriculture, 2007).

1.4. Methods of Study

The study has been carried out in several stages. The first stage was to perform a detailed literature survey. In this part, previous studies completed around the study area have been obtained and the fundamental theories related to engineering geology and slope instability have been searched.

Secondly, the field studies were carried out. It includes field description of the engineering geological properties of the limestone, performing scan-line surveys at three cut slopes and obtaining nine oriented samples with discontinuities.

Thirdly, laboratory studies were performed on the rock samples obtained from the field. Unit weight and uniaxial compressive strength of the limestone, and shear strength parameters (cohesion and internal friction angle) of the discontinuities are measured in accordance with ISRM (1981).

Then, the discontinuity orientation data were analyzed with DIPS (2004) software to assess the dominant discontinuity sets. Limit equilibrium analyses for three cut slopes were performed with SLIDE (2004) software for different slope geometries and without/with remedial measures. Rockfall analyses were performed to assess the possibility if a detached rock for different weights reaches the highway to endanger the highway traffic.

Finally, all of these analyses were evaluated together to recommend possible remedial measures for the Km: 25+600-26+000 section of the planned road.

1.5. Previous Studies

Although many studies are done around the Antalya Region, there are only few studies in this particular Antalya-Korkuteli region. The first geological study in the Korkuteli Road was done by Colin (1962). He studied in a very wide region around Fethiye-Antalya-Kaş and Finike, and the defined the Beydağları formation and the Alakırçay Group which crop out along the Antalya-İzmir Satate Highway route.

Şenel et al. (1994) studied this region and gave detailed explanation about the Beydağları formation. They have revealed the contact information for this unit. This work was related to the study area in only one unit.

Şenel (1997) gave a detailed explanation about almost all of the units that can be seen along the planned road. In this study, the Beydağları formation was explained in detail. He mentioned the Söbütepe formation (Upper Paleocene-Lower Eocene) which outcrops at the road and said the lower boundary of this unit is discordant. In this study, Antalya nappes were also given in detail. In this part of the study, some details of Tilkideliğitepe formation, Yeniceboğazıdere formation and Limestone Unit are given in details. He also described the Alakırçay nappe and the Alakırçay Group. All of these units outcrop in the planned road. However, the Limestone Unit of Şenel (1997) is seen at the three cut slopes that are studied in this thesis.

FORM Jeoteknik (2008) carried out a geological and geotechnical study in the proposed Antalya-Burdur Breakaway-Korkuteli State Road Km: 25+500-63+500. They prepared geological and engineering geological maps, and the geological profile for the area. Beril Drilling Co drilled many boreholes and trial pits along the planned road in 2006, 2 of which are very close to the thesis area. FORM Jeoteknik (2008) evaluated the data obtained from the field and laboratory and carried out some kinematic and stability analysis of earth and cut slopes. Geological and engineering geological assessment of the planned road

for the cut-slopes and the embankments were also done. The author of this thesis was also involved at all stages of the project for FORM-Beril Co during the geotechnical investigations.

There are other studies not directly related to the study area but related to the region. Pisoni (1967) mentioned about the Kaş limestone (Maastrichtian-Lutetian), Pınarbaşı formation (Lower Miocene) and Felenkdağı conglomerate (Lower Miocene). Poisson and Poignant (1974) studied the Katrandağı formation (Cenomanian). They also studied on the Karabayır formation (Miocene and Cretaceous-Paleogene) around Korkuteli.

CHAPTER 2

GEOLOGY AND SEISMICITY OF THE STUDY AREA

2.1. Geology of the Study Area

Although various lithological units are exposed along the Antalya-Burdur Breakaway-Korkuteli highway (Figure 2.1), the Limestone unit belonging to Çataltepe Nappe is the main lithological unit of the highway segment studied in this thesis.

The Çataltepe Nappe consists of three formations, namely Tilkideliğitepe formation (TRt), Yeniceboğazıdere Formation (JKy), and the Limestone Unit (JKyk).

The Tilkideliğitepe formation (TRt) contains massive, partly thin-medium-thick layered, greenish gray to light brown marls, and limestone lenses and blocks rich in macro fossils. The lower boundary of this formation is tectonic and the upper boundary is concordant with the Yeniceboğazıdere formation. The thickness of this unit is about 100 meters. The formation has been deposited in shelf environment. The age of the formation is Norian based on its fossil content (Şenel, 1977).

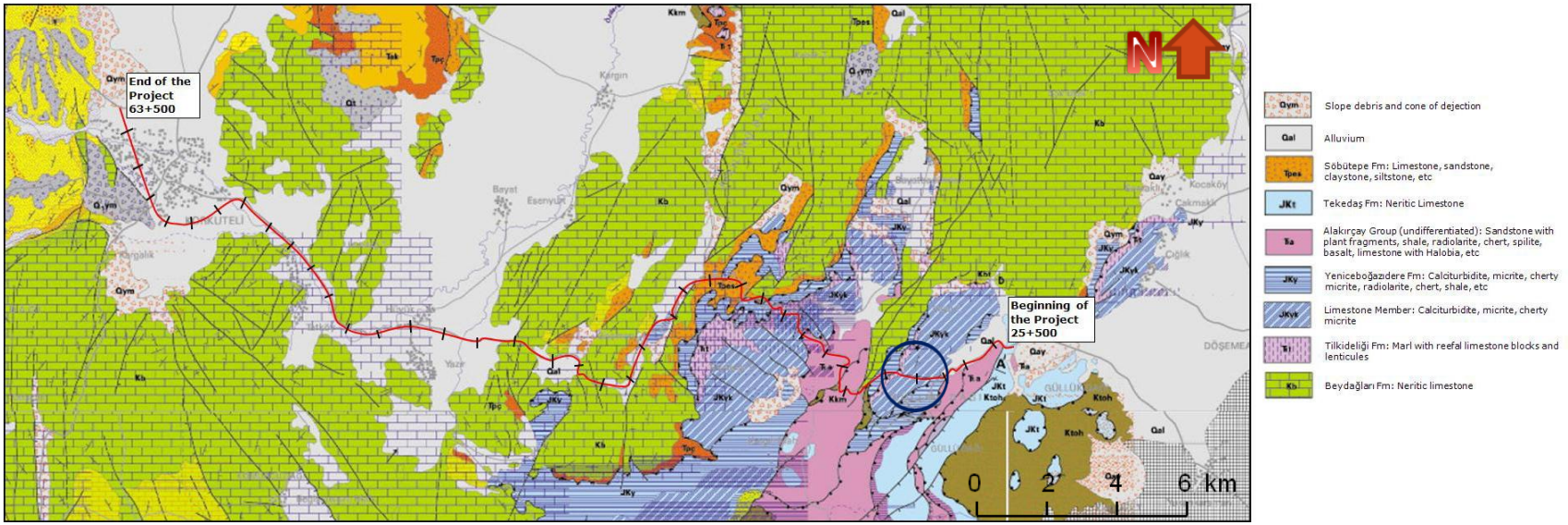

Figure 2.1 Geological map of the study area (modified from MTA, 2004)

The Yeniceboğazıdere formation (JKy) is composed of calciturbidite, chert, radiolarite, shale and limestone and was named by Poisson (1977). The formation is thin-medium bedded, beige to greenish gray, and includes micrite with chert, calciturbidite, radiolarite, shale and silicified limestone. A distinct layer due to the red-pink micritic limestone at the bottom of the unit can also be seen (Figure 2.2).

Figure 2.2. A view from the Yeniceboğazıdere formation.

Thick calciturbidite, limestone and silicified limestone of the Yeniceboğazıdere formation is subgrouped as Limestone Unit (JKyk). This unit includes thin-medium bedded, beige to gray micrite, cherty micrite and calciturbidites (Figure 2.3). The dominant rock type is calciturbidite and most of these rocks are silicified. The unit has a thickness more than 300 m. The age of the limestone unit is accepted as Jurassic-Cretaceous based on its fossil content (Şenel, 1977).

Figure 2.3. A view from the limestone unit.

2.2. Seismicity of the Study Area

The study area is located in the 2nd degree earthquake zone (Figure 2.4) according to the Earthquake Zones of Turkey Map (GDDA, 1996). There are no major earthquakes recorded from 1900 to 2010 in the

study area. However, 25 earthquakes having a magnitude of greater than 3.0 have been recorded near the study area (Figure 2.4)

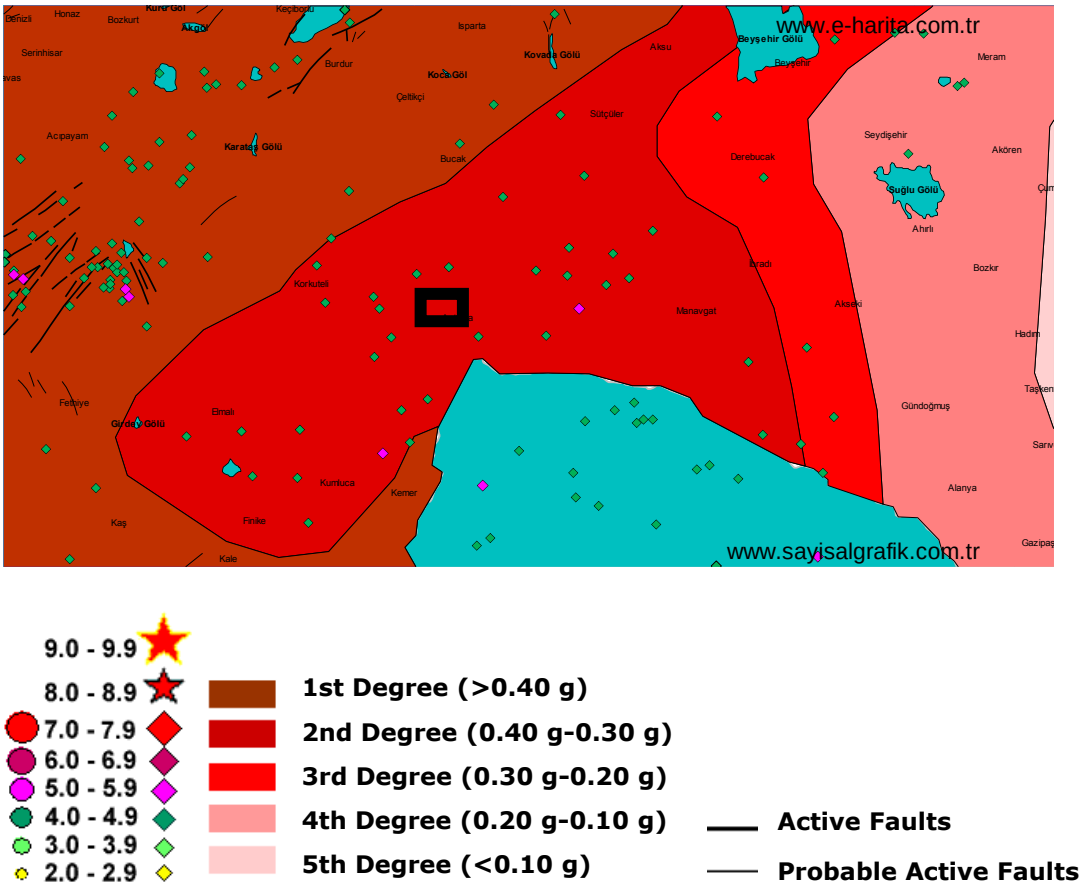

Figure 2.4. Earthquake zoning map of the study area and its close vicinity with recorded epicenters (GDDA, 1996).

In the projects of infrastructure, maximum horizontal ground acceleration value may range from 0.4g to 0.3 g for the 2nd degree earthquake zones. However, the acceleration value for stability analysis is reduced by 1/2 to 1/3 of the peak values. Based on the seismic coefficient map (Figure 2.5) of General Directorate of Highways (GDH, 2007), an acceleration value of 0.15g is considered for the studied three cut slopes during the stability analyses of this thesis.

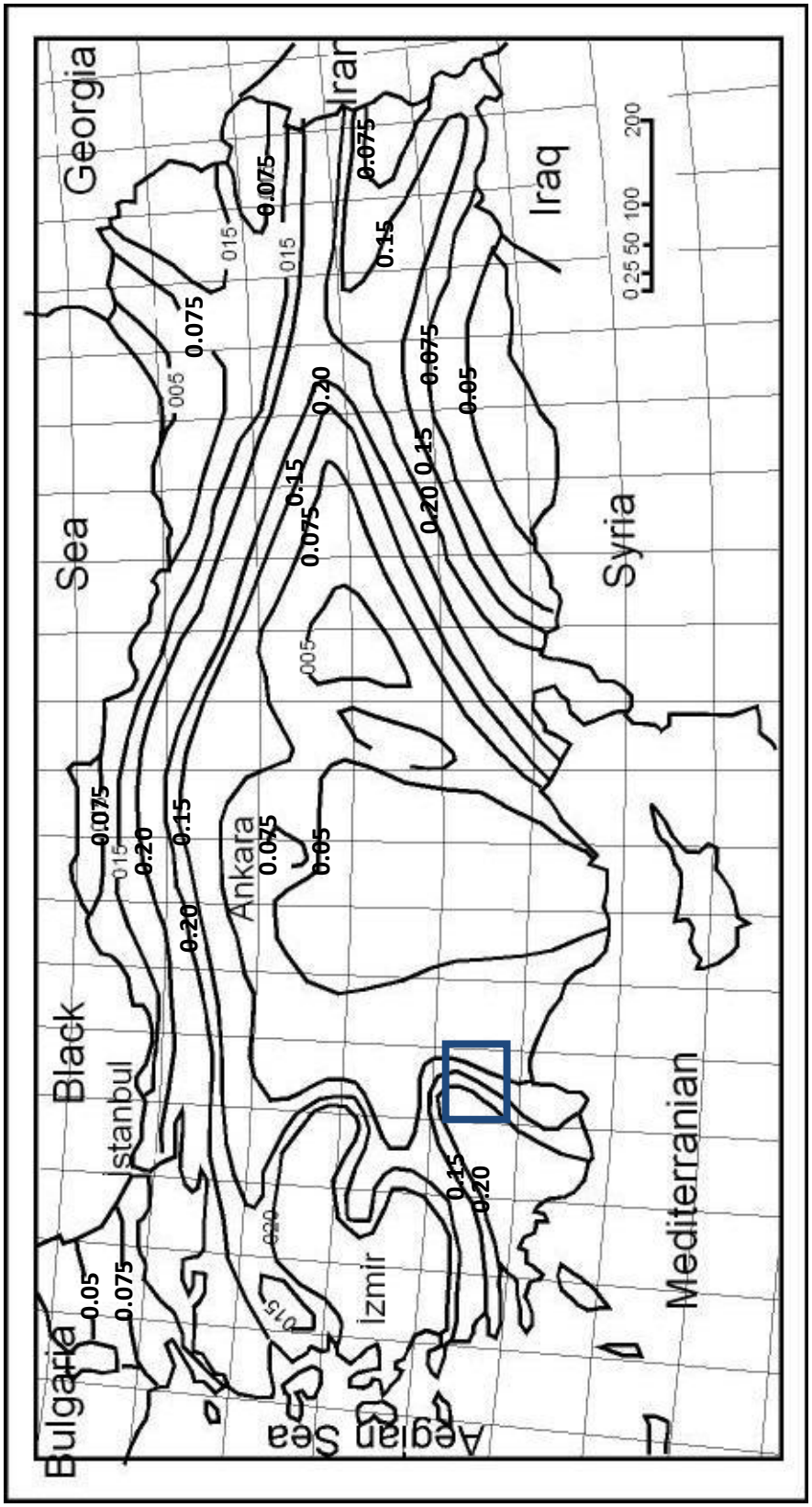

Figure 2.5. Earthquake acceleration map of Turkey for the stability analyses of slopes (GDH, 2007)

CHAPTER 3

ENGINEERING GEOLOGICAL PROPERTIES OF THE LIMESTONE EXPOSED AT KM: 25+600-26+000

In this chapter, the engineering geological properties of the limestone belonging to the Çataltepe nappe at Km: 25+600-26+000 section of the highway will be given. At three sections of the highway where slope instability problems exist, field descriptions (material and mass) of the limestone were done. Scanline-surveys (each for a length of at least 30 m) along natural rock exposures were performed in accordance with Priest (1993) at suitable locations near the highway. The directional data obtained from the surveys were evaluated by using DIPS (2004) software of Rocscience. The data are plotted through Schmidt net using the lower hemisphere projection. Diagrams for pole and contour plots, rose diagram and dominant discontinuity sets are determined for this part of the road in three cut slopes.

Twelve oriented samples were taken from the field for laboratory testing. The laboratory tests were conducted at the Department of Geological and Mining Engineering of METU). Unit weight and uniaxial compressive strength of the limestone, and shear strength parameters (cohesion and internal friction angle) along the discontinuities were determined following the procedures given in ISRM (1981).

During the project studies in this area, two boreholes were drilled close to the thesis area (Figure 3.1) by Beril Co in 2006. The simplified borehole logs mainly showing the lithological variations are given in Figures 3.2 and 3.3. Although there are some minor lithological variations, the rock is essentially beige and partly sandy and silicified limestone.

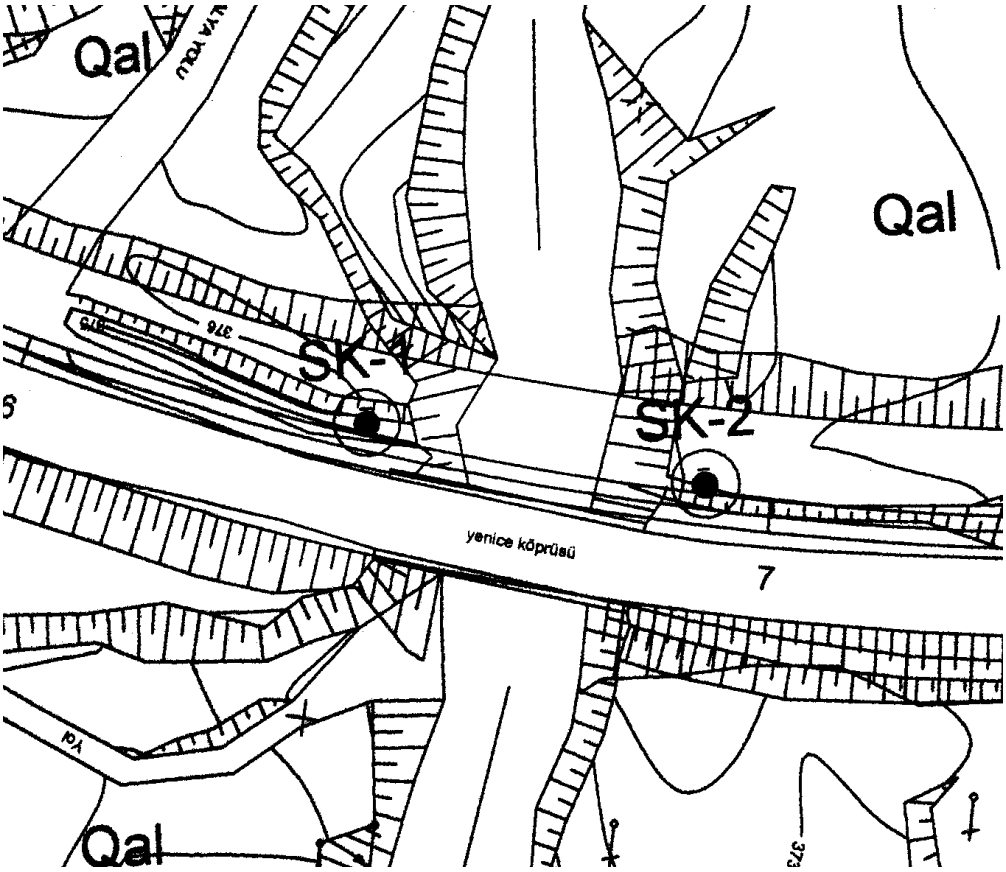

Figure 3.1. The geological plan (Scale: 1/1000) showing the borehole (SK-1 and SK-2) locations near Yenice bridge at Km: 26+600-26+700).

SONDAJ YERİ / *Boring Location* **:**	**YENİCE BRIDGE -1**
SONDAJ DER. / *Boring Depth* **:**	**10,00 m**

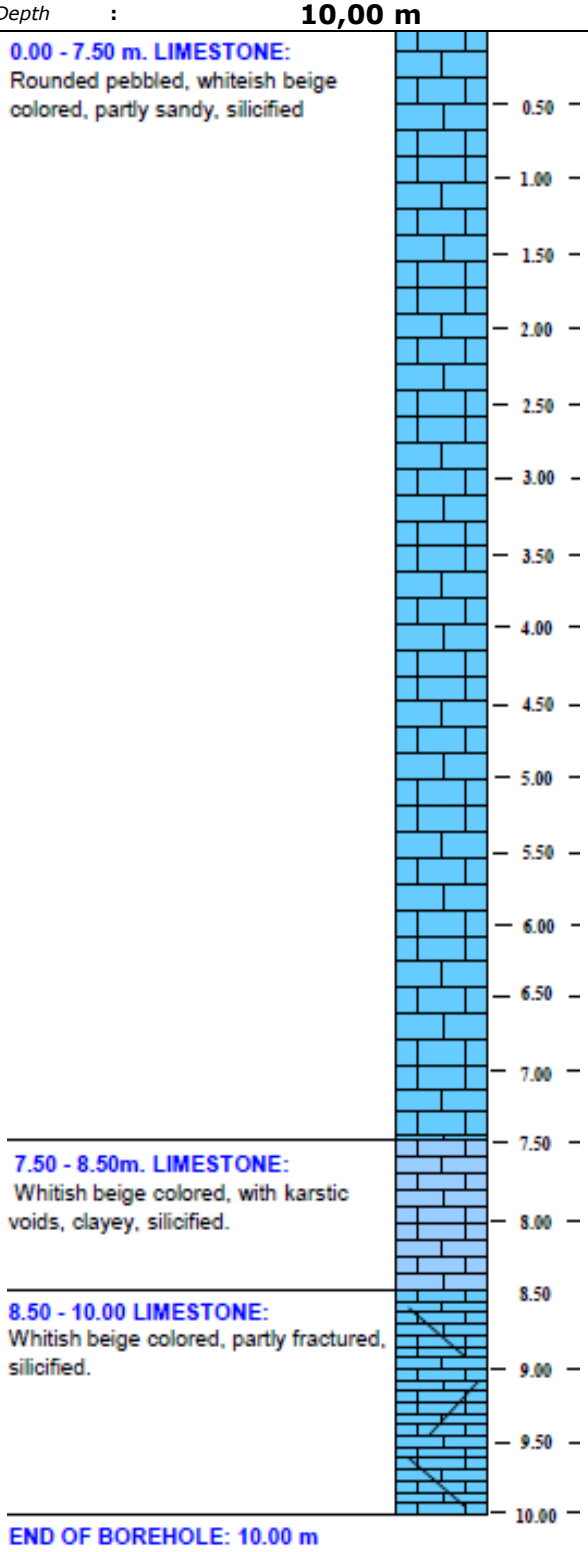

Figure 3.2. Borehole log of SK-1 at Yenice bridge.

SONDAJ YERİ / *Boring Location* **:**	**YENİCE BRIDGE-2**
SONDAJ DER. / *Boring Depth* **:**	**15,00 m**

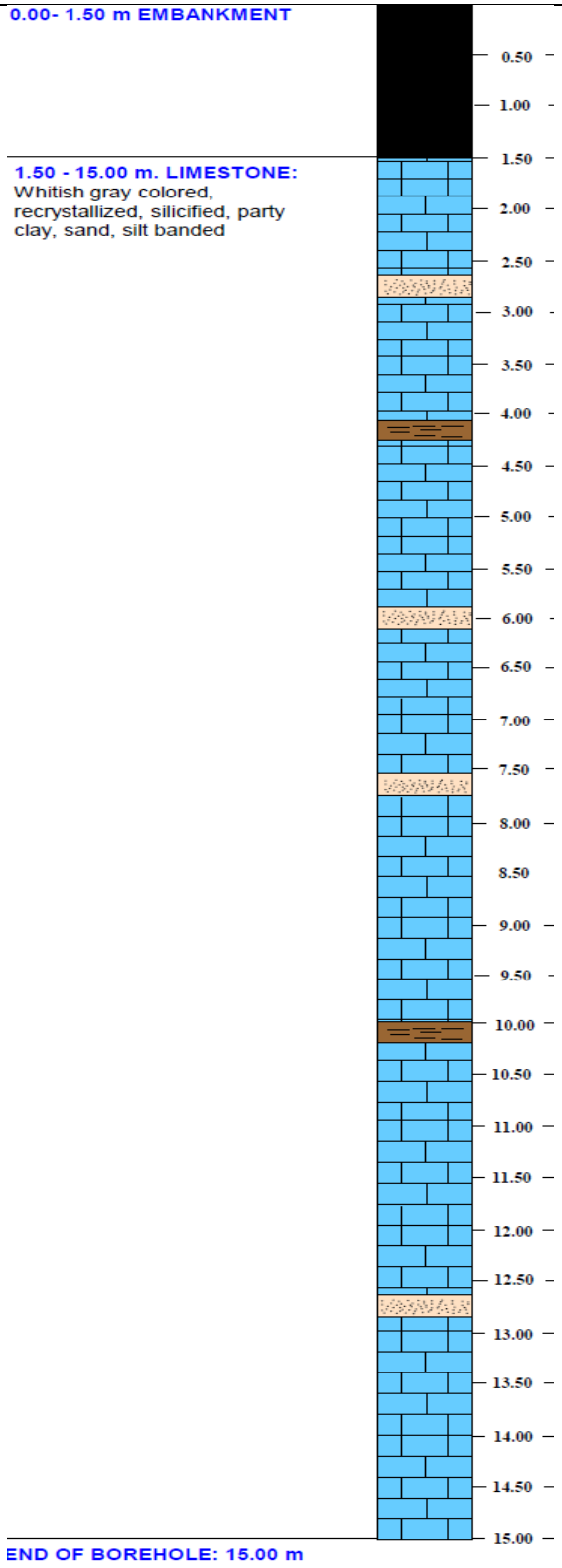

Figure 3.3. Borehole log of SK-2 at Yenice bridge.

Eight of the twelve oriented block samples from Km: 25+600, Km:25+900 and Km:26+000 were containing discontinuities (Figure 3.4). Direct shear tests were carried out in the Mining Engineering Department of the Middle East Technical University (METU). Cohesion (c) and friction angle (ø) were determined by the tests.

Figure 3.4. Photograph of the oriented samples taken from the field.

The unit weight and uniaxial compressive strength tests on intact rock were performed on five samples. The results reveal that the unit weight of the limestone is 25 kN/m^3. However, the uniaxial compressive strength of the rock is found to be 50 MPa which is a value at the boundary between medium strong and strong rock according to ISRM (1981).

The direct shear tests were performed on four different normal loads (0.5 kN, 1 kN, 2kN and 4 kN). Two tests were performed for each normal load value using different samples. Then, shear stresses are

determined for each normal load. The test data for average peak and residual shear stress values, and the test results (cohesion and internal friction angle) are presented in Figures 3.5 and 3.6. According to the test results, the peak cohesion and internal friction angle along the discontinuities are 2.65 MPa and 35.45°. On the other hand, the residual cohesion and internal friction angle of the discontinuities are 1.85 MPa and 34.17°. The test results show that very low reduction in shear strength parameters for the discontinuities exists.

DIRECT SHEAR TEST FOR DISCONTINUITY

REPORT

Surface Area	Normal Load	Peak Shear Load	Residual Shear Load	Normal Stress	Peak Shear Stress	Residual Shear Stress
cm^2	kN	kN	kN	MPa	MPa	MPa
29.361	0.5	0.75	0.60	1.736	2.604	2.083
23.396	1.0	1.50	1.25	4.357	6.536	5.446
29.530	2.0	2.50	2.10	6.904	8.630	7.249
27.025	4.0	3.40	3.10	15.088	12.825	11.693

Shear Strength Envelope	Cohesion (MPa)	Friction Angle (°)
Peak	2.651	35.445
Residual	1.852	34.167

Notices:

- Due to the manometer limits, lowest normal stress value is 1.736 MPa.
- Residual shear stress values are obtained after taking the specimens to original positions.

Figure 3.5. Summary report for the direct shear test.

Peak Shear Strength Envelope for Mohr-Coulomb Failure Criterion

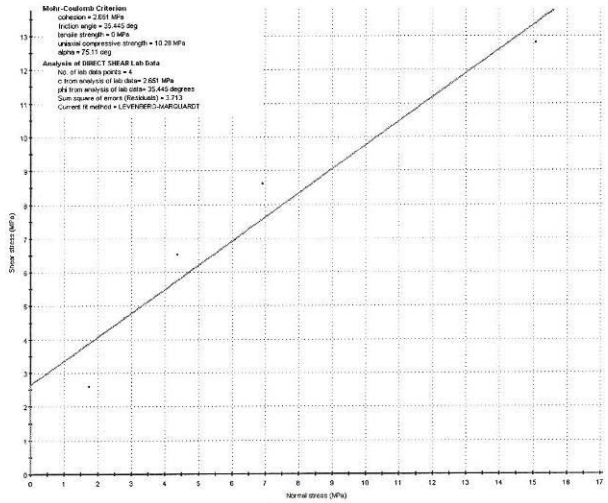

Residual Shear Strength Envelope for Mohr-Coulomb Failure Criterion

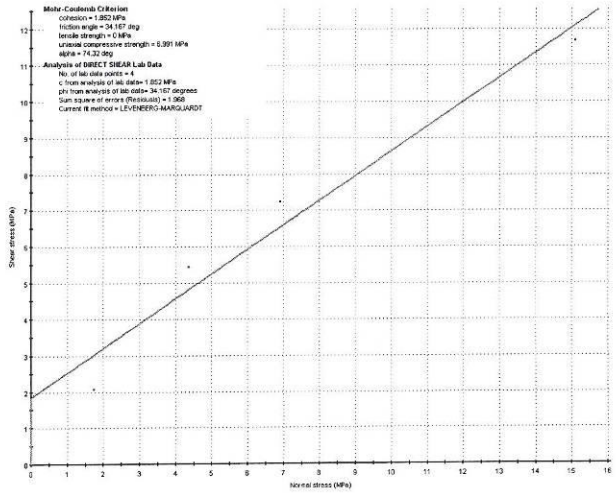

Figure 3.6. Mohr-Coulomb failure criterion of the limestone based the test results.

3.1. Engineering Geological Properties of the Limestone at Km: 25+600

The limestone at this locality is beige to gray, fine grained (micritic), fossiliferous, and highly jointed (Figure 3.7). Fifty six discontinuity measurements were taken during the scan-line survey carried out for a length of nearly 30 meters. The joints and bedding plane constitute the major discontinuities at this location.

Figure 3.7. A view from the limestone facing north at Km: 25+600.

The discontinuities generally have close to wide (60 mm-1000 mm) spacing, tight to partly open (0.1 mm-0.5 mm) aperture, planar rough to undulating rough discontinuity surfaces, slightly weathered mainly in

the form of discoloration along discontinuity surfaces although some karstic cavities exists near the surface, medium strong and strong. The discontinuities have practically no infill material except upper 1 m. On the other hand, the discontinuities are locally filled by secondary calcite. Most of the discontinuities (bedding planes and joints) have high persistence mainly greater than 10 m, but one of the joint set is bed confined. No groundwater seepage was encountered at this location.

Orientation data (dip amount/dip direction) are processed through DIPS (2004) using lower hemisphere and Schmidt net. Pole plot and contour diagram, rose diagram and the dominant discontinuity sets are shown in Figures 3.8-3.10.

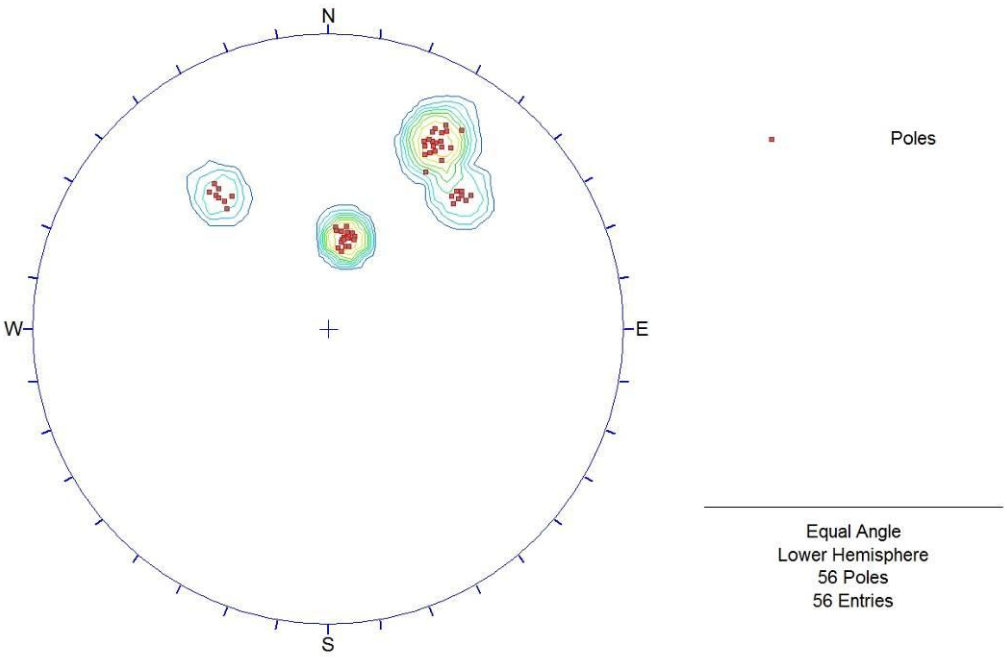

Figure 3.8. Pole plot and contour diagram of the discontinuities at Km: 25+600.

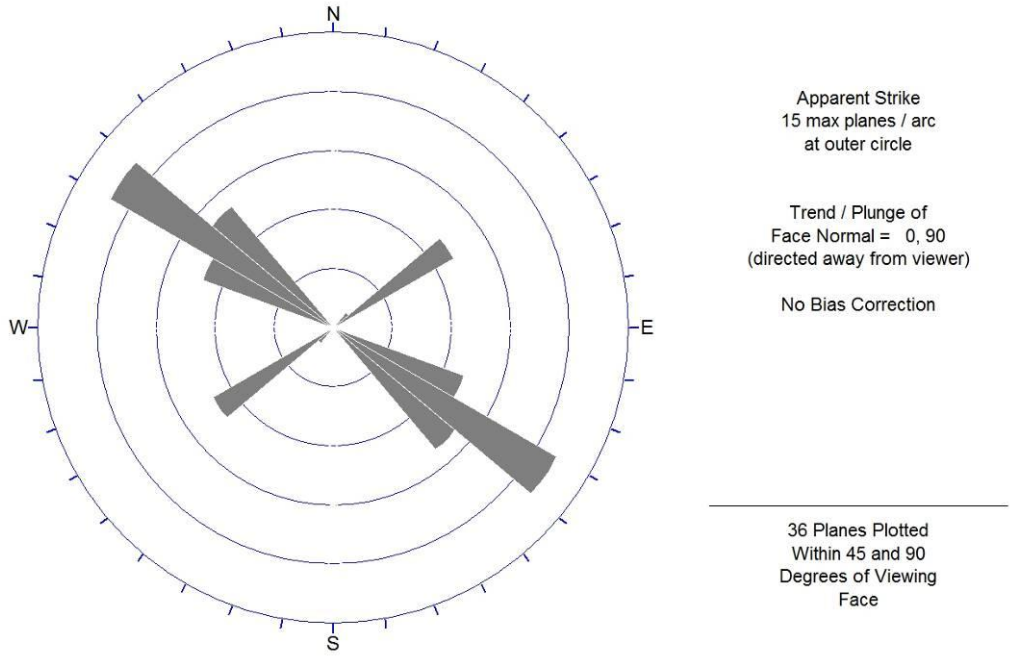

Figure 3.9. Rose diagram of the discontinuities at Km: 25+600

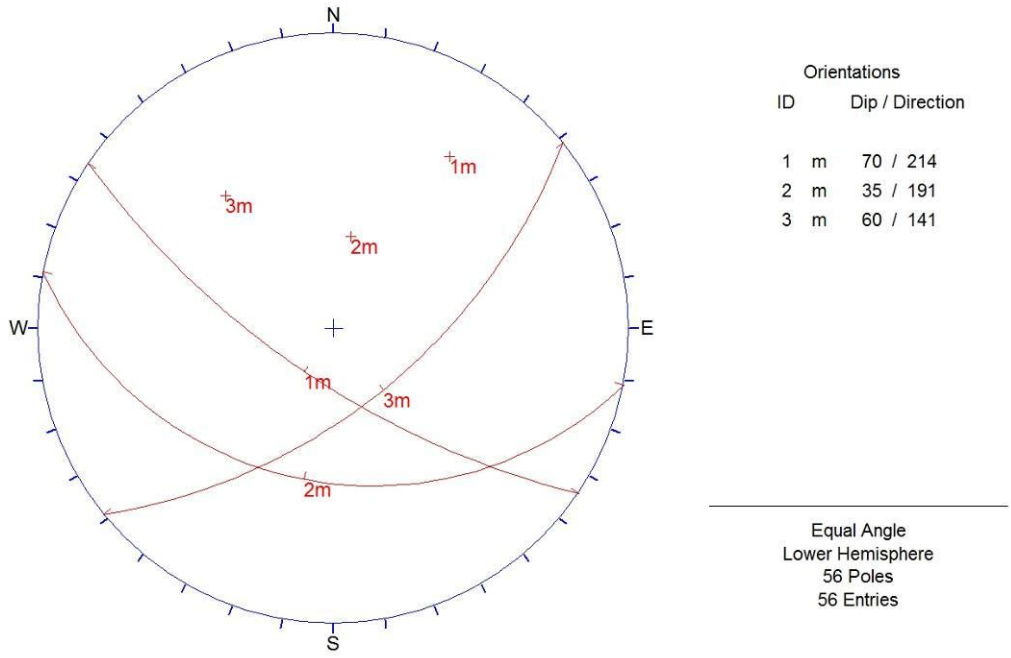

Figure 3.10. Dominant discontinuity sets at Km: 25+600.

Based on the discontinuity analysis, there are two dominant joint sets and one bedding plane (Figure 3.11). The orientation data of the discontinuities are presented in Table 3.1. The joint sets (J1 and J2) have dip amount/dip direction of poles of 35/191 and 60/141. On the other hand, dip amount/dip direction of the bedding plane (BP) is 70/214.

Table 3.1. Orientations of the major discontinuity sets at Km: 25+600.

Discontinuity Sets	**Dip Amount**	**Dip Direction**
Discontinuity Set 1 (BP)	70	214
Discontinuity Set 2 (J1)	35	191
Discontinuity Set 3 (J2)	60	141

Figure 3.11. A view from the limestone facing north at Km: 25+600.

3.2. Engineering Geological Properties of Limestone at Km: 25+900

The limestone at this locality is very similar to the one observed at Km:25+600. The rock is beige to gray, fine grained, and highly jointed (Figure 3.12). One hundred fourty eight discontinuity measurements were taken during the scan-line survey carried out for a length of nearly 30 meters. The joints and bedding plane constitute the major discontinuities at this location.

Figure 3.12. A view from the limestone facing north at Km: 25+900.

The discontinuities generally have close to wide (60 mm-1000 mm) spacing, tight to partly open (0.1 mm-0.5 mm) aperture, planar rough to undulating rough discontinuity surfaces, slightly weathered mainly in

the form of discoloration along discontinuity surfaces although some karstic cavities exists near the surface, medium strong and strong. The discontinuities have practically no infill material except upper 0.5 m. On the other hand, the discontinuities are locally filled by secondary calcite. Most of the discontinuities (bedding planes and joints) have high persistence mainly greater than 10 m. However, one of the joint set is bed confined which has very low (0.3-<1m) persistence. Groundwater seepage was not seen during the field study around this cut slope.

Orientation data (dip amount/dip direction) are evaluated by DIPS (2004) software using lower hemisphere and Schmidt net. Pole plot and contour diagram, rose diagram and the dominant discontinuity sets are shown in Figures 3.13-3.15.

Based on the discontinuity analysis, there are two joint sets and one bedding plane at this location (Figures 3.15 and 3.16). The orientation data of the discontinuities are presented in Table 3.2. The joint sets have dip amount/dip direction of 25/135 and 57/256. On the other hand, dip amount/dip direction of the bedding plane is 55/345.

Table 3.2. Orientations of the major discontinuity sets at Km: 25+900.

Discontinuity Sets	**Dip Amount**	**Dip Direction**
Discontinuity Set 1 (BP)	55	345
Discontinuity Set 2 (J1)	25	135
Discontinuity Set 3 (J2)	57	256

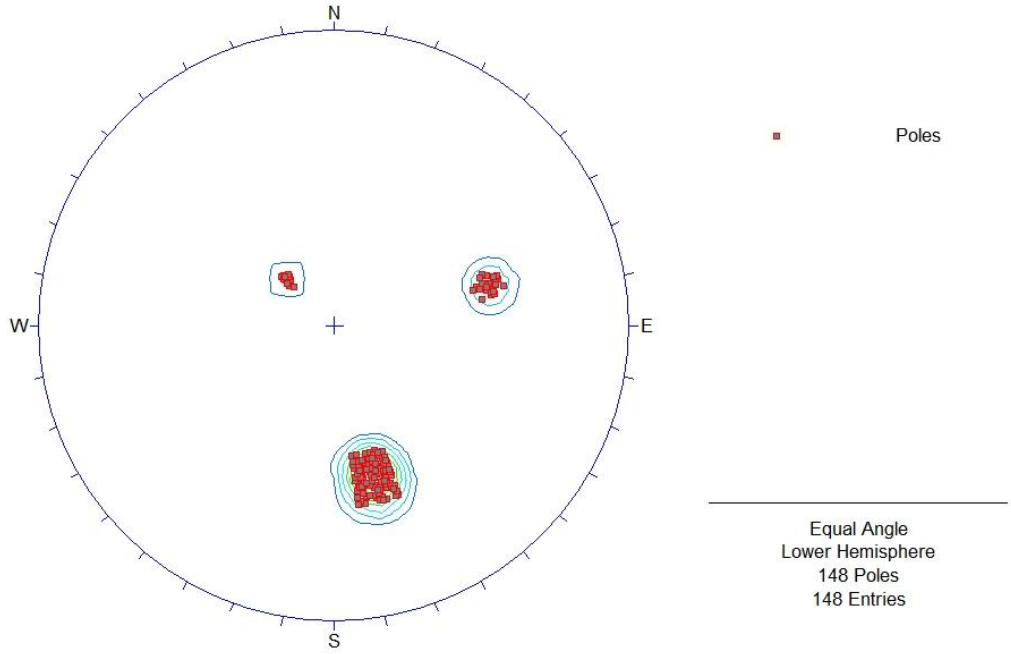

Figure 3.13. Pole plot and contour diagram of the discontinuities at Km: 25+900.

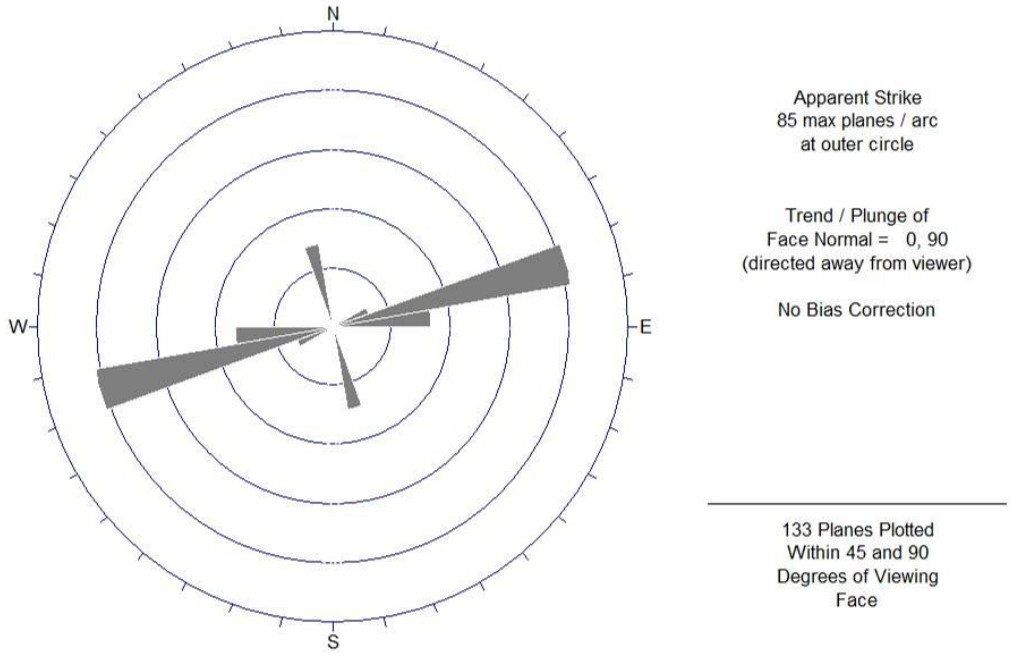

Figure 3.14. Rose diagram of the discontinuities at Km: 25+900.

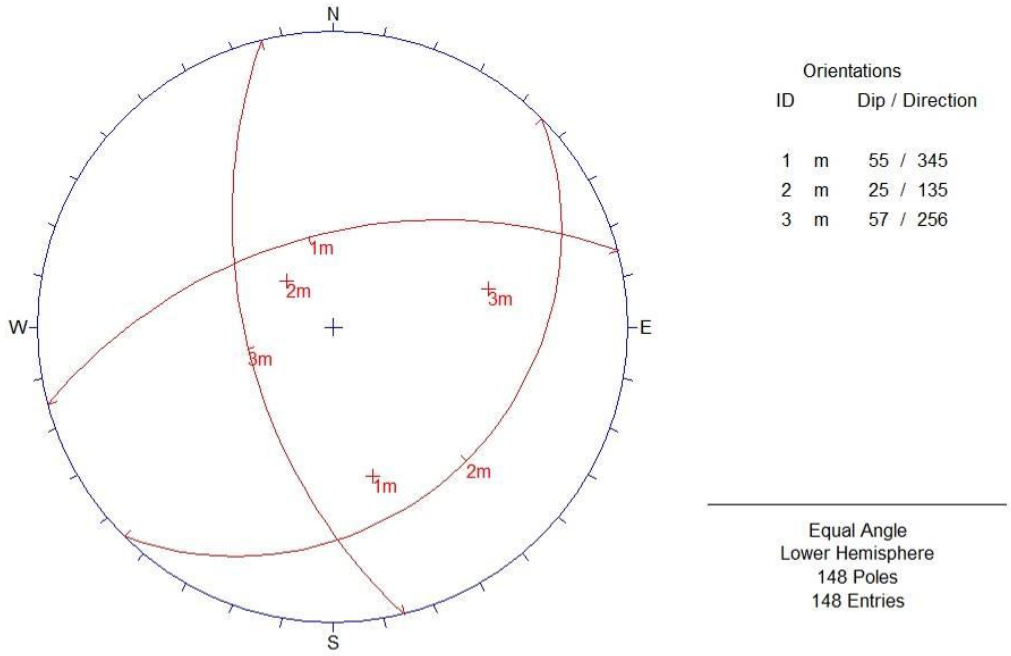

Figure 3.15. Dominant discontinuity sets at Km: 25+900.

Figure 3.16. A view from the limestone at Km: 25+900.

3.3. Engineering Geological Properties of Limestone at Km: 26+000

The limestone at this locality is also very similar to the one observed at Km:25+600 and 25+900. The rock is beige to gray, fine grained, and highly jointed (Figure 3.17). Seventy six discontinuity measurements were taken during the scan-line survey carried out for a length of nearly 30 meters. Similar to other two locations, the joints and bedding plane constitute the major discontinuities at this location.

Figure 3.17. A view from the limestone facing north at Km: 26+000.

The discontinuities have close to wide (60 mm-1000 mm) spacing, tight to partly open (0.1 mm-0.5 mm) aperture, planar rough to undulating rough discontinuity surfaces. The weathering is dominant only near the

surface. It is slightly weathered mainly in the form of discoloration along discontinuity surfaces. The rock is medium strong and strong. Except local calcite infilling, the discontinuities have practically no infill material. Most of the discontinuities (bedding planes and joints) have high persistence mainly greater than 10 m. However, one of the joint set is bed confined which has very low (0.3 - <1m) persistence. Groundwater seepage was not detected at this locality.

Dip amount/dip direction of the discontinuities evaluated by DIPS (2004). Pole plot and contour diagram, rose diagram and the dominant discontinuity sets are shown in Figures 3.18-3.20.

Based on the discontinuity analysis, it is found that two dominant joint sets and one bedding plane exist at this location (Figures 3.20 and 3.21). The orientation data of the discontinuities are presented in Table 3.3. The joint sets have dip amount/dip direction of 40/335 and 84/268. On the other hand, dip amount/dip direction of the bedding plane is 45/175.

Table 3.3. Orientations of the major discontinuity sets at Km: 26+000.

Discontinuity Sets	**Dip Amount**	**Dip Direction**
Discontinuity Set 1 (J1)	40	335
Discontinuity Set 2 (J2)	84	268
Discontinuity Set 3 (BP)	45	175

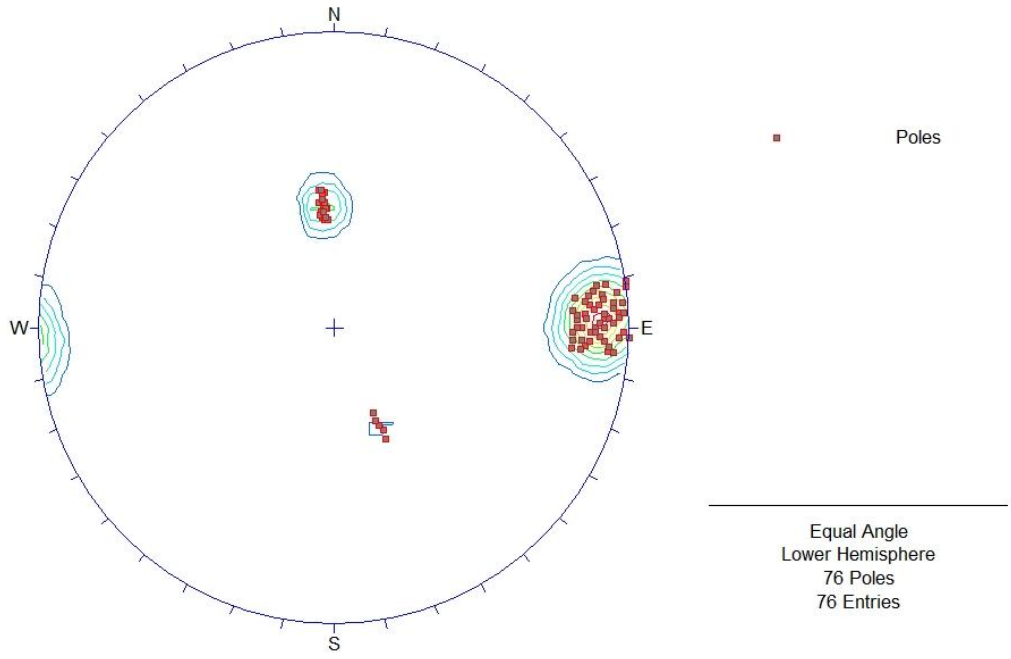

Figure 3.18. Pole plot and contour diagram of the discontinuities at Km: Km: 26+000.

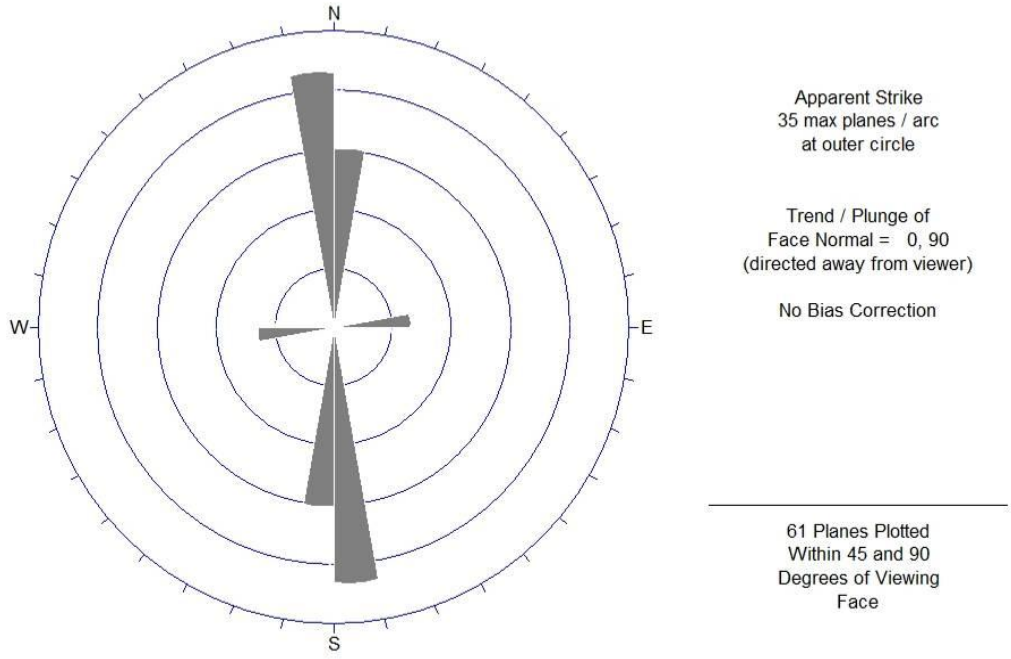

Figure 3.19. Rose diagram of the discontinuities at Km: 26+000.

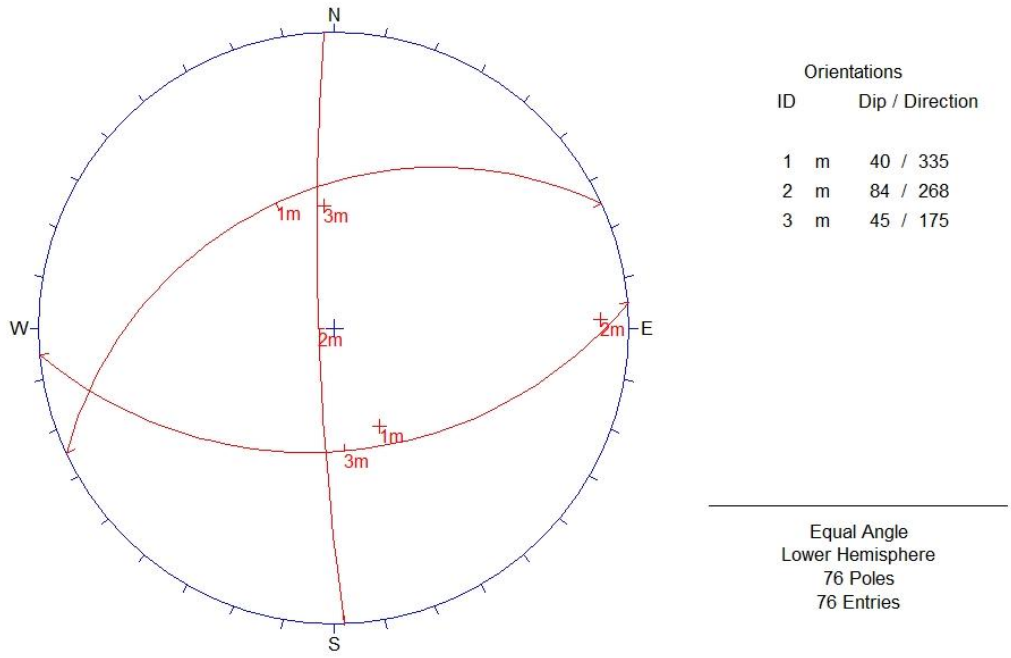

Figure 3.20. Dominant discontinuity sets at Km: 26+000.

Figure 3.21. Discontinuities developed in the limestone at Km: 26+000.

CHAPTER 4

KINEMATIC ANALYSES OF THE CUT SLOPES

In this chapter, kinematic analyses of the cut slopes for Km: 25+600 - 26+000 part of the road are given. The kinematic analyses are carried out according to the procedure described in Hoek and Bray (1981) and Turner and Schuster (1996). The kinematic analyses are done for planar, wedge and toppling failures, separately. For the friction angle, 35° found from the direct shear tests is used.

4.1. Kinematic Analysis of the Cut Slope at Km: 25+600

At this location, two joint sets and a bedding plane form the main discontinuities (Figure 4.1). The kinematic analysis for planar failure performed at Km: 25+600 shows that except one joint set, no plane failure is expected. Nevertheless, the poles of this problematic joint set partly fall within the daylight envelope. Since the difference of the strikes between the slope (64/240) and the discontinuity (35/191) is more than 20°, no planar failure is expected at this location (Figure 4.2). According to the kinematic analysis for wedge and toppling failures (Figures 4.3 and 4.4), the cut slope is stable for both cases.

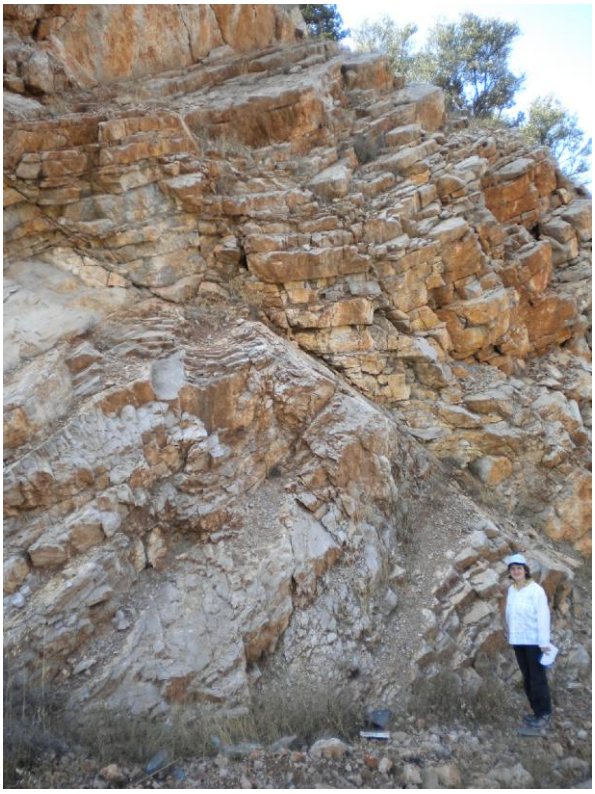

Figure 4.1. Photograph showing main discontinuities developed in the limestone at Km: 25+600.

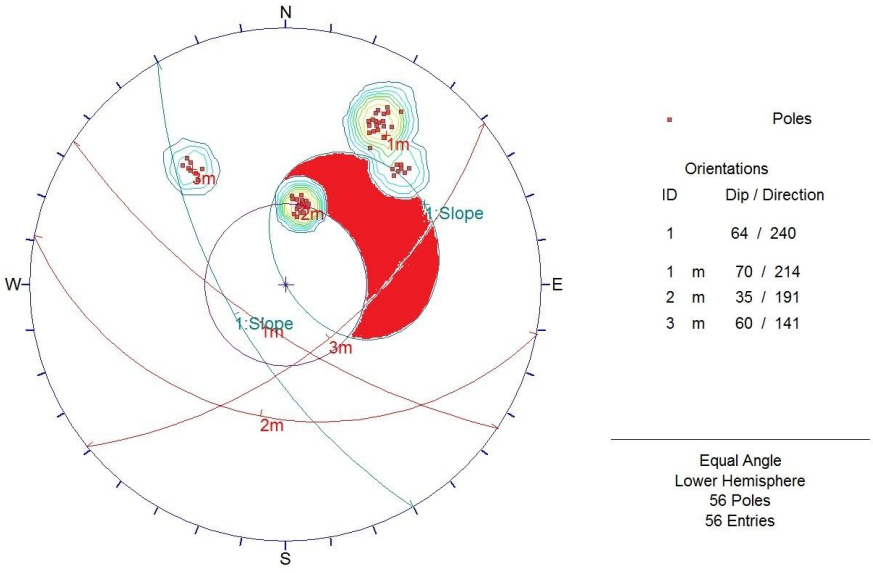

Figure 4.2. Kinematic analysis of the cut slope for planar failure at Km: 25+600.

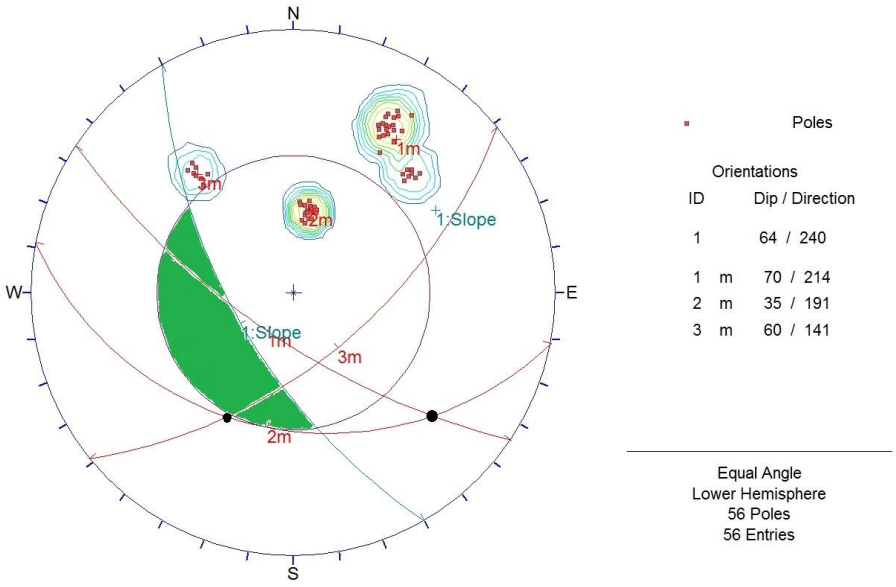

Figure 4.3. Kinematic analysis of the cut slope for wedge failure at Km: 25+600.

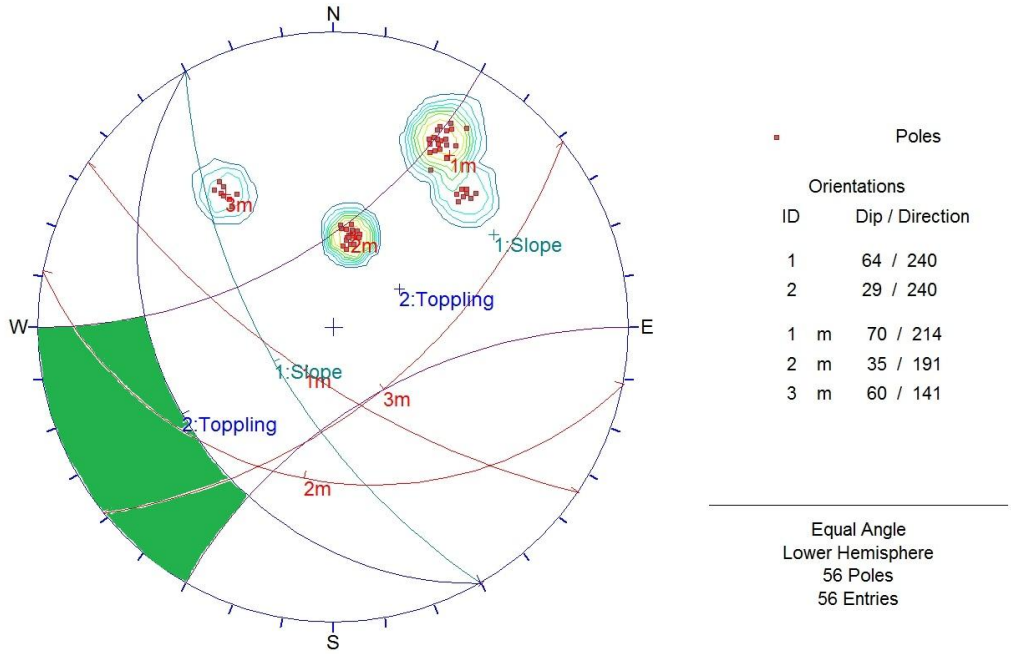

Figure 4.4. Kinematic analysis of the cut slope for toppling failure at Km: 25+600.

As a summary, according to the kinematic analyses carried out, this part of the cut slope does not have any planar, wedge or toppling failures. Therefore, the limit equilibrium analysis which will be discussed in Chapter 5 of this thesis is not performed for this part of the study area.

4.2. Kinematic Analysis of the Cut Slope at Km: 25+900

Two joint sets and a bedding plane also form the main discontinuities at Km: 25+900 (Figure 4.5). The slope amount and its direction for the cut slope at this location is 64/250. The kinematic analysis for plane failure performed at Km: 25+900 shows that the poles of one joint set (57/256) falls within the daylight envelope. Therefore, planar failure controlled by the joint is likely to occur at this location (Figure 4.6). In order to eliminate this problem, a slope flattening of 10° may be recommended (Figure 4.7).

Figure 4.5. Photograph showing main discontinuities developed in the limestone at Km: 25+900.

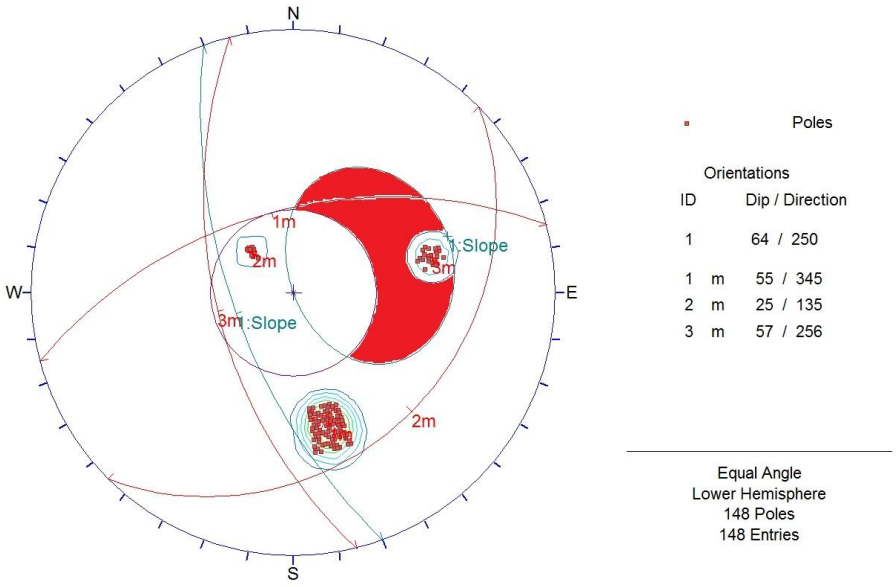

Figure 4.6. Kinematic analysis of the cut slope for planar failure at Km: 25+900.

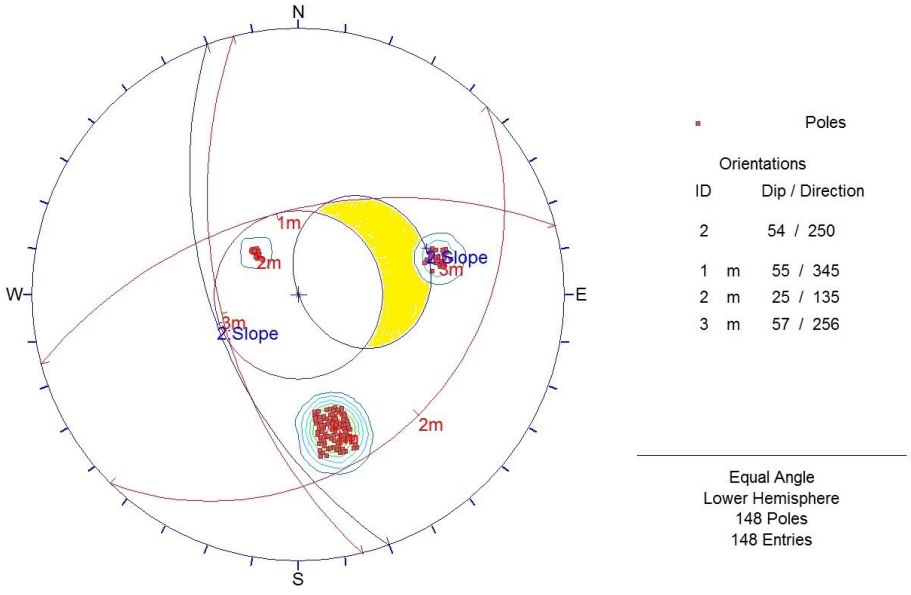

Figure 4.7. Elimination of the planar failure kinematically by flattening of the slope at Km: 25+900.

The kinematic analysis for wedge failure performed at Km: 25+900 shows that the intersection of the bedding plane (55/345) and joint set 2 (25/135) falls within the danger zone. Therefore, wedge failure is likely to occur at this location (Figure 4.8). In order to eliminate this problem, a slope flattening of 8° is suggested (Figure 4.9). The kinematic analysis for toppling failure reveals that no toppling failure is likely at this cut slope (Figure 4.10).

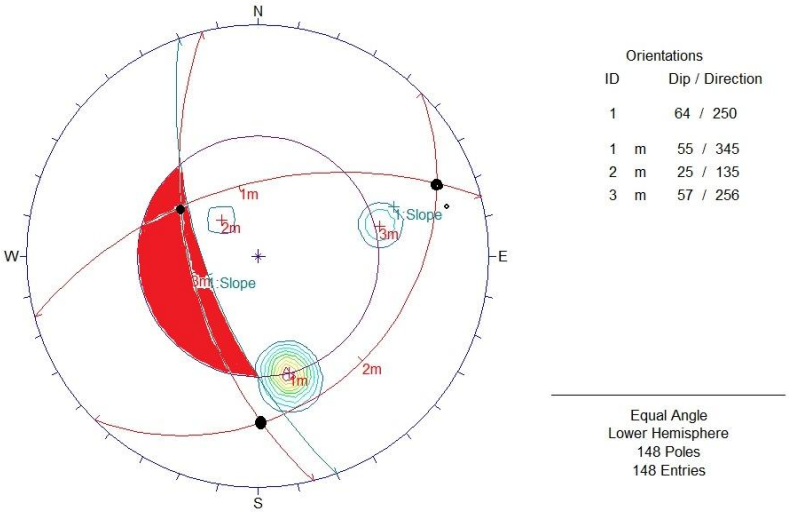

Figure 4.8. Kinematic analysis of the cut slope for wedge failure at Km: 25+900.

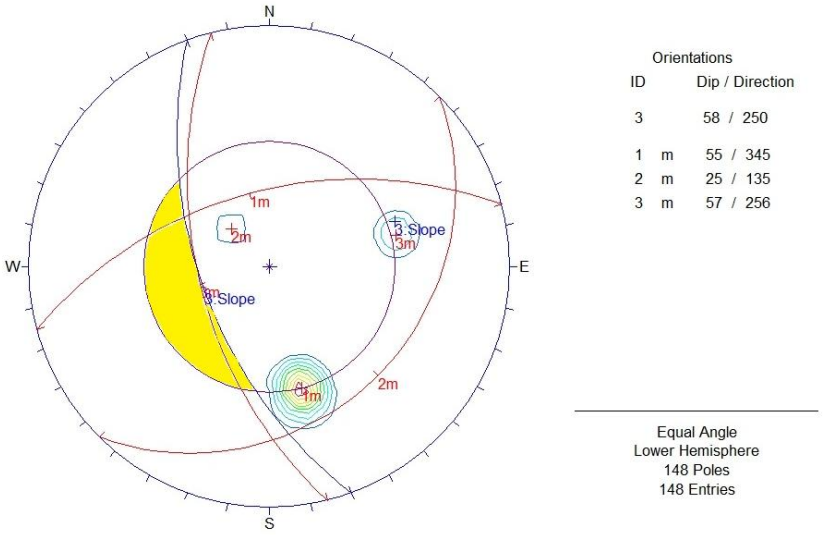

Figure 4.9. Elimination of the wedge failure kinematically by flattening of the slope at Km: 25+900.

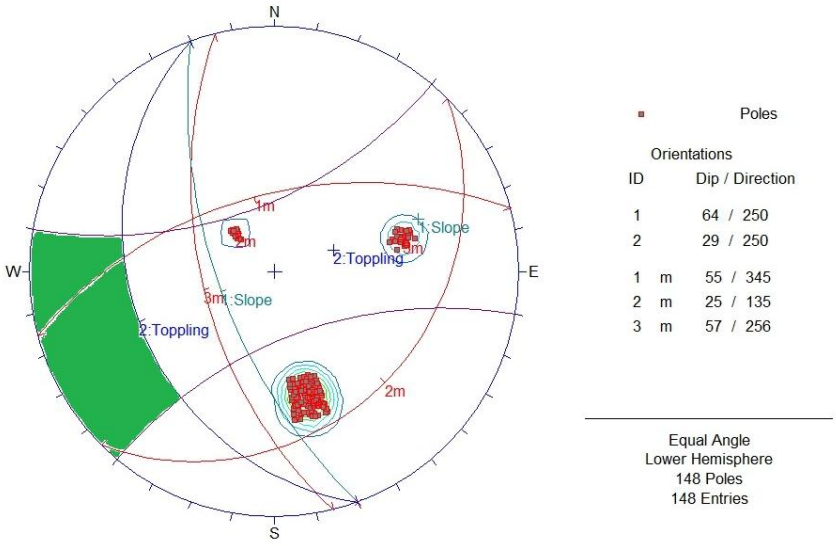

Figure 4.10. Kinematic analysis of the cut slope for toppling failure at Km: 25+900.

As a summary, according to the kinematic analysis carried out at Km:25+900, the cut slope does not have any toppling failures, but the planar and wedge failures are likely to occur. 10° of slope flattening will eliminate both risks. Therefore, only kinematic analysis is performed for this part of the study area.

4.3. Kinematic Analysis of the Cut Slope at Km: 26+000

Similar to the other two cut slopes, two joint sets and a bedding plane also form the main discontinuities at Km: 25+900 (Figure 4.11). The kinematic analysis for plane failure performed at Km: 26+000 shows that although poles of the joint (J2) partly fall within the daylight envelope, its dip amount is steeper than the slope angle (Figure 4.12). Thus, this discontinuity is not daylighting. So, no planar failure is expected at this location.

Figure 4.11. Photograph showing main discontinuities developed in the limestone at Km: 26+000.

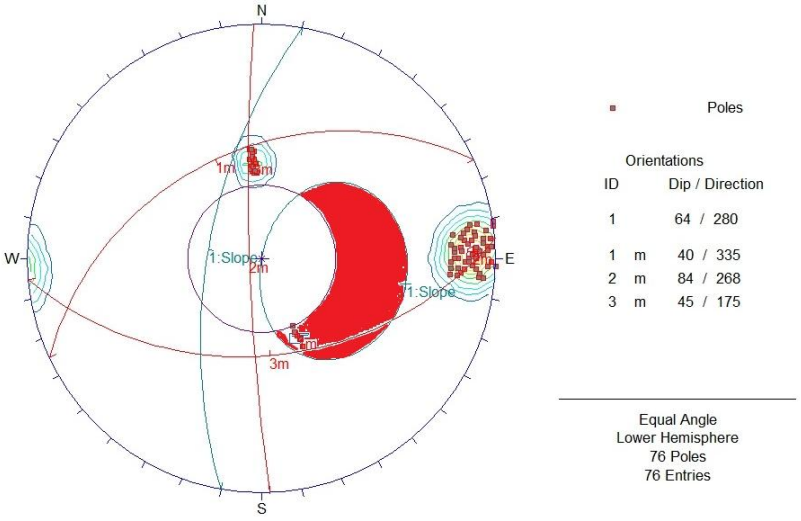

Figure 4.12. Kinematic analysis of the cut slope for planar failure at Km: 26+000.

According to the kinematic analysis, this part of the highway is safe as per the wedge or toppling failure analyses (Figures 4.13-4.14). As a summary, this part of the cut slope does not have any wedge or toppling failures. Furthermore, for the planar failure, the critical joint does not daylight. Therefore, the limit equilibrium analysis is not performed in Chapter 5 for this part of the study area.

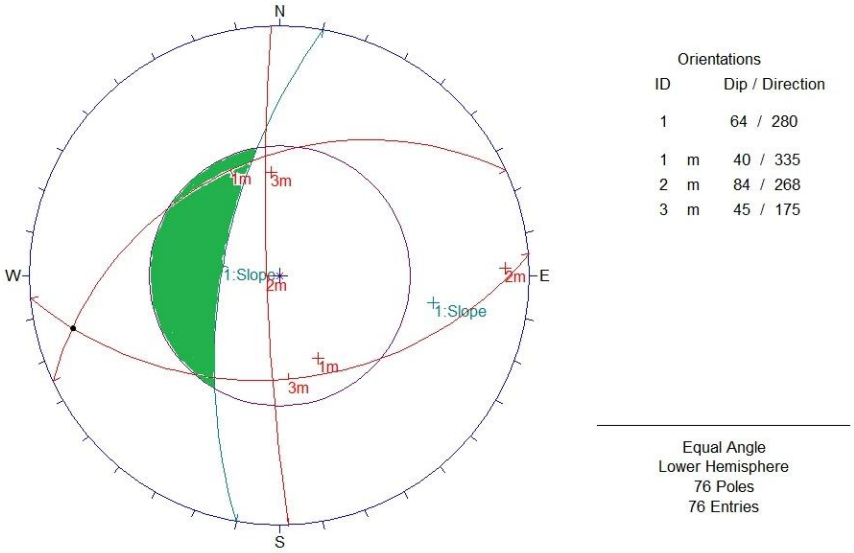

Figure 4.13. Kinematic analysis of the cut slope for wedge failure at Km: 26+000.

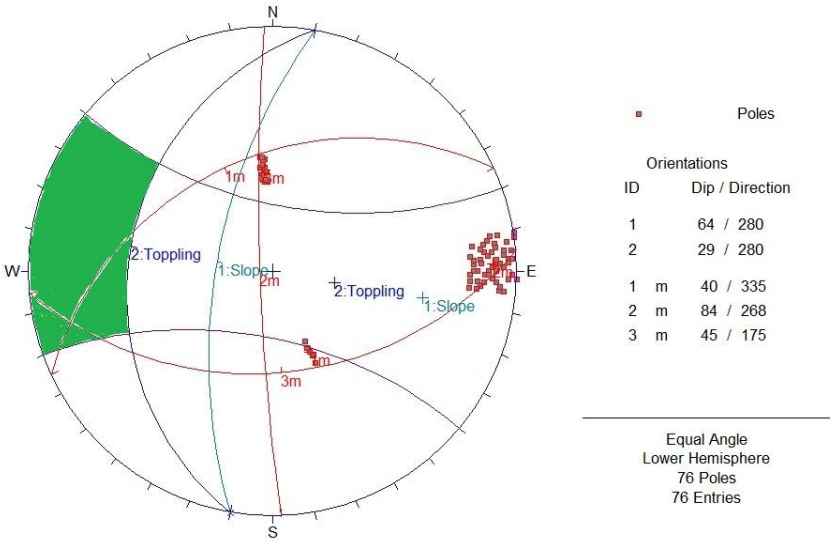

Figure 4.14. Kinematic analysis of the cut slope for toppling failure at Km: 26+000.

CHAPTER 5

LIMIT EQUILIBRIUM AND ROCKFALL ANALYSES OF THE SLOPE

This chapter includes the limit equilibrium and rockfall analysis of the cut slopes at Km: 25+600-26+000 part of the road. Based on the kinematic analysis and field observations, the main concern was the possibility of the planar failure at Km: 25+900 and rockfall which may adversely affect the highway. In order to eliminate these risks, a series of analyses using SLIDE (2004) and RocFall (2004) software programs were performed.

For the slope stability analysis, the seismicity coefficient is taken as 0.15 for all conditions as taken from General Directorate of Highways. Additionally, the cut slope is analyzed only for dry case since no groundwater was encountered at the slope. Two different of analyses using the SLIDE software were carried out. Firstly, the planar failure analyses of the cut slope at Km: 25+900 were done. For this purpose, non-circular analysis with a failure surface controlled by the discontinuity was performed. Thirty slices were used for the analysis. The shear strength parameters obtained from the direct shear test for the discontinuities were adopted in the analysis. Based on the result, the slope was analyzed with some remedial measures such as slope flattening, adding a bench, or strengthening methods with rock bolts. The aim was to achieve a safe slope, and for this purpose the factor of

safety of the final cut slope was aimed as minimum 1.1 for long term analyses suggested by GDH (1995), Cornforth (2005) and Topal and Akın (2009). Since there are small pieces and highly jointed structure in the limestone, secondly, mass failure analysis was carried out. The aim of this analysis was to find out if there is massive slide of the rock mass.

For the rockfall analysis, RocFall (2004) software program by Rocscience was used. This analysis is important because the slopes in the study area are high and the rocks were blocky. In this type of high rock slopes, it is generally expected to have rockfalls if the rock is highly jointed. For this purpose a series of analysis was run for the different block masses of the rock representing the real field conditions with the same angle of the slope for the current situation. After completing the limit equilibrium analyses with remedial measures, the rockfall analyses are done again in order to see the effects and differences of flattening the slope or bench.

5.1. Limit Equilibrium Analysis of the Cut Slope for Planar Failure at Km: 25+900

According to the analysis carried out, this part is found to be the most problematic part of the highway. It is not safe in the current situation due to a very low factor of safety of 0.50 with seismic coefficient (Figures 5.1-5.3).

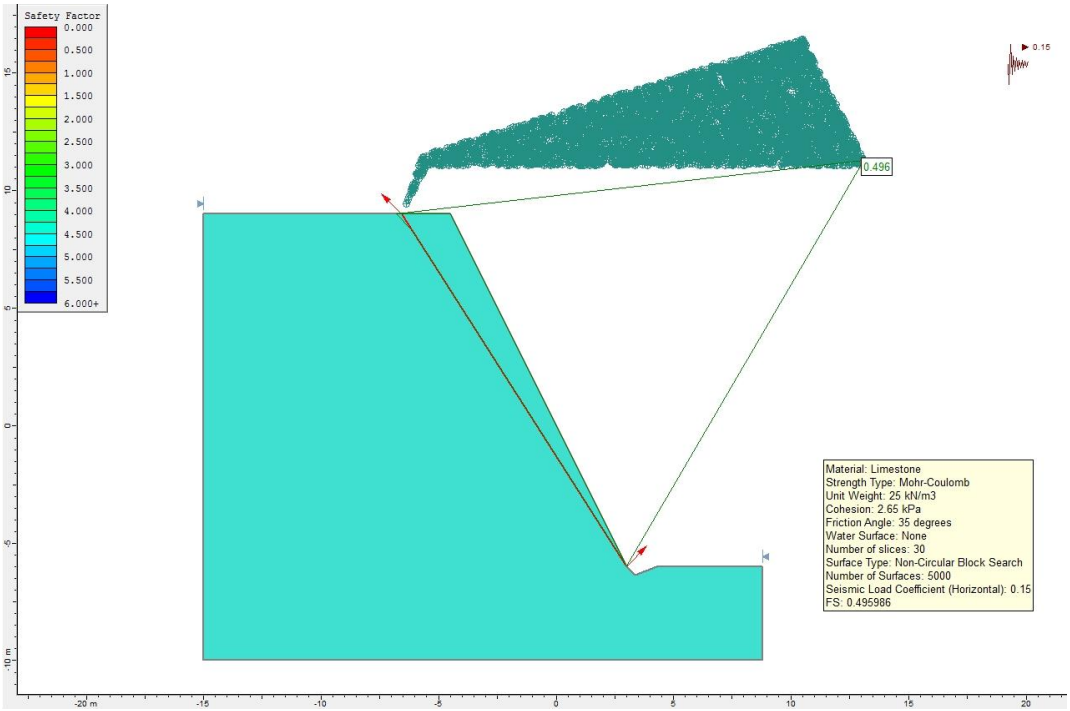

Figure 5.1. Limit equilibrium analysis of the cut slope with discontinuity controlled failure surface using current highway slope geometry.

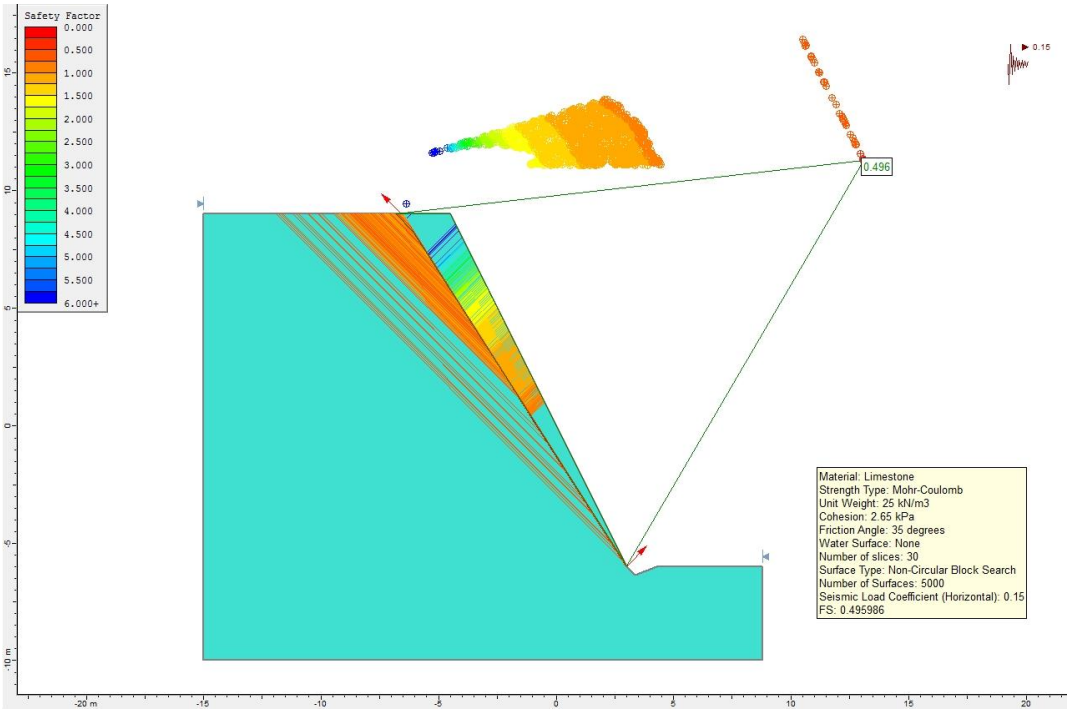

Figure 5.2. Limit equilibrium analysis of the cut slope with all surfaces analysed.

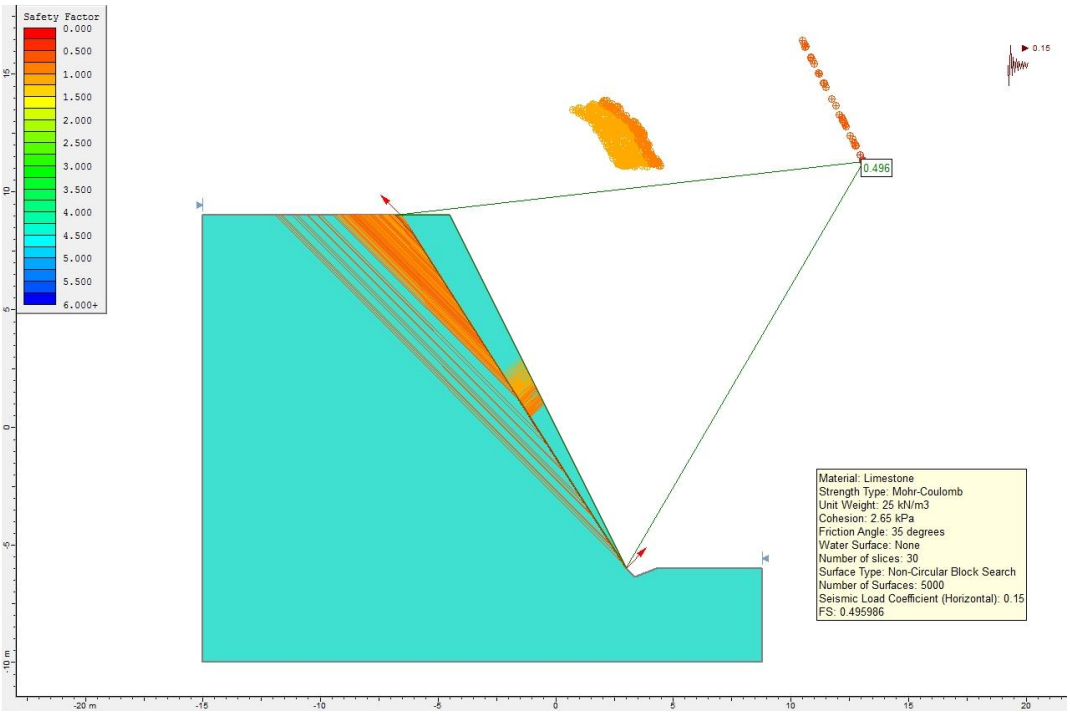

Figure 5.3. Limit equilibrium analysis of cut slope with surfaces showing factor of safety only less than 1.1.

As a remedial solution slope flattening has been utilized. The slope angle of this part is 64°. Based on the analysis (Figure 5.4), the desired factor of safety is achieved in case the cut slope is flattened by 7°, thus forming a new slope with 57°.

Another option was to try benches. The height of the bench was 10 meters from the road elevation. The horizontal length of the bench is suggested as 5 meters. The limit equilibrium analysis with bench of the slope yields a stable slope (Figure 5.5).

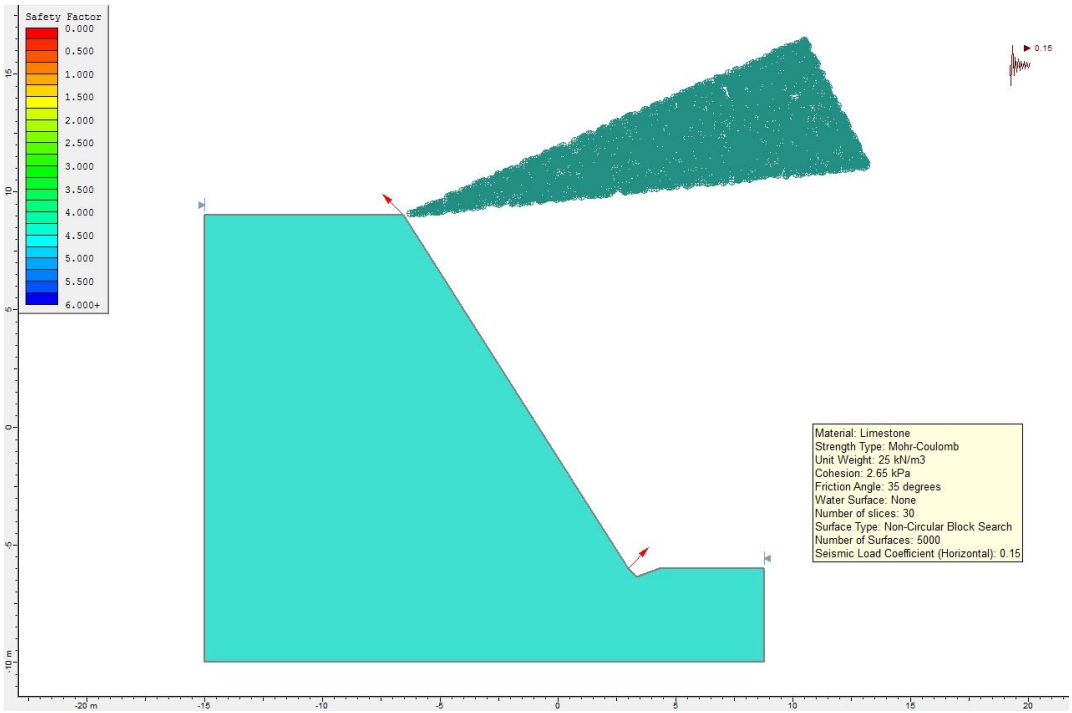

Figure 5.4. Limit equilibrium analysis of the flattened cut slope by 7°.

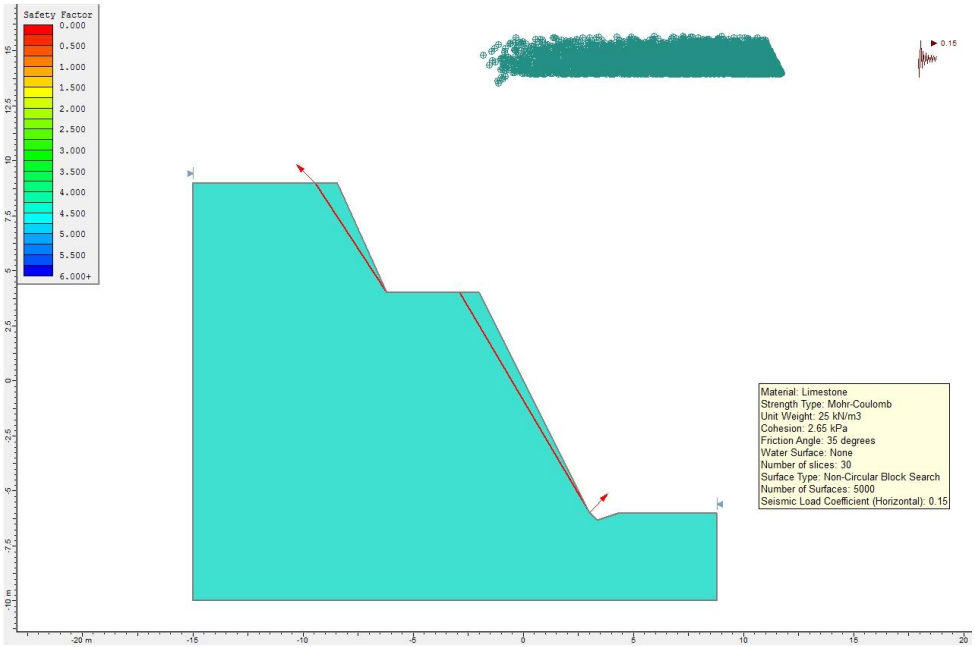

Figure 5.5. Limit equilibrium analysis of the slope with bench.

The third option as a remedial solution was the use of rock bolts. For the limit equilibrium analysis with rock bolt, the optimum configuration of the rock bolt is found to be as follows: the distance between the bolts is 2 meters, the length of the bolts is 4 meters, the bolts are placed with 8° angle from the horizontal, the capacity of the bolt is 75 kN and the rock bolt type is end-anchored. The resultant factor of safety with the used of the above mentioned rock bolts is found to be 1.11 (Figures 5.6-5.7).

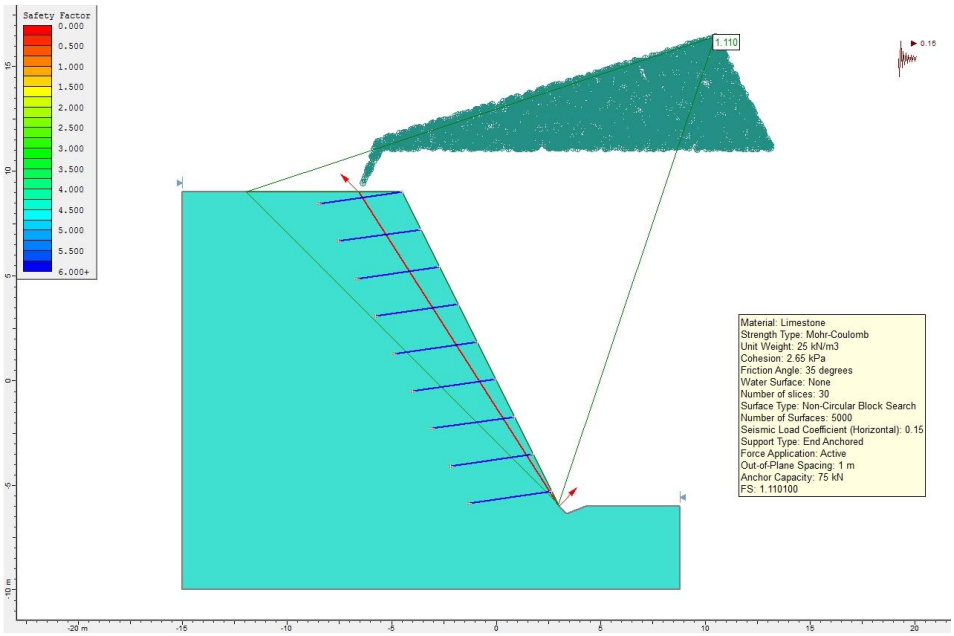

Figure 5.6. Limit equilibrium analysis of the slope with rock bolting.

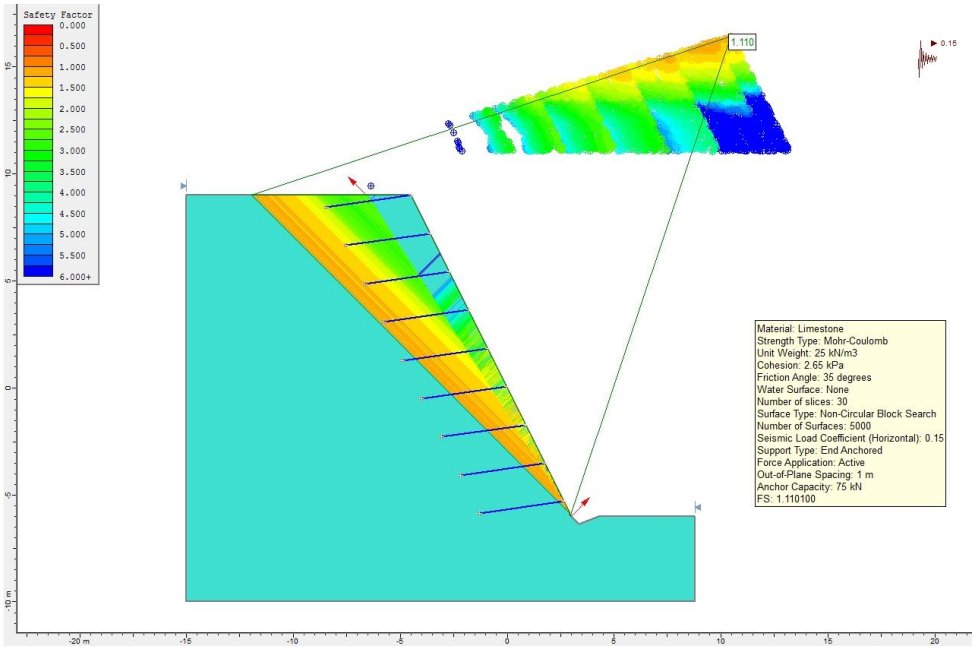

Figure 5.7. Limit equilibrium analysis of the slope with the rock bolting and all surfaces analysed.

5.2. Limit Equilibrium Analysis of the Cut Slope for Mass Failure at Km: 25+900

The aim of this analysis is to find out if there is massive failure in the cut slope at Km: 25+900. In order to carry out the analyses, RocLab (2007) software program of Rocscience was used to get the instantaneous cohesion (c) and the friction angle (ø) values for the specific slope height. The input and the output values used for the analysis were as follows:

Inputs:

- Intact Uniaxial Compressive Strength (sigci): 50

- GSI (Geological Strength Index): 55 (Figure 5.8)

- Intact Rock Parameter (mi): 8 (Micritic limestone)

- Disturbance Factor (D): 0.7 (Good blasting slope)

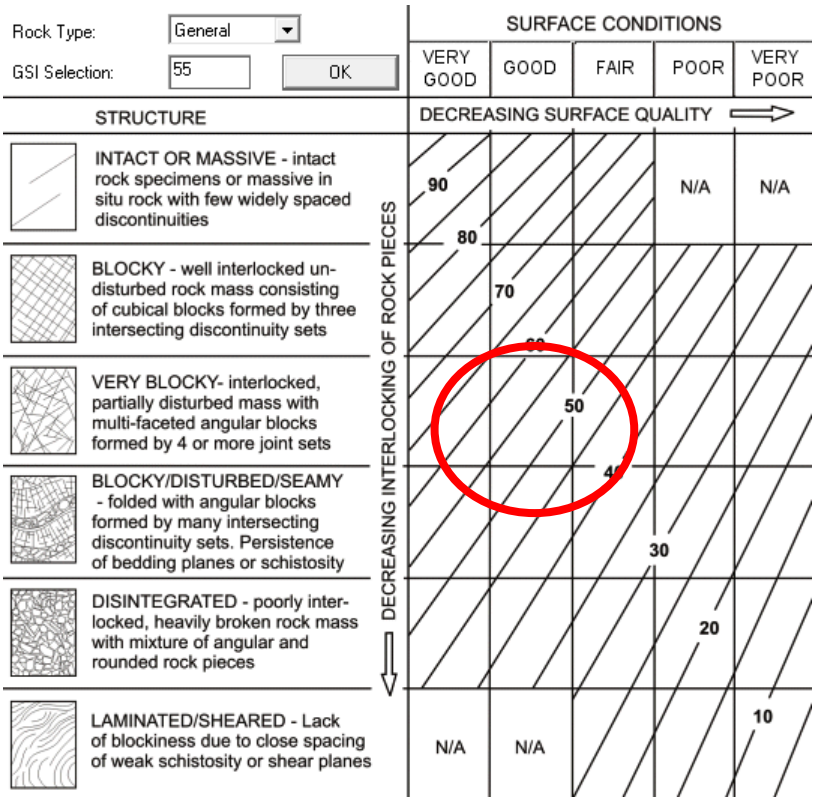

Figure 5.8. GSI value of the limestone rock mass selected from the Roclab software.

Outputs (Figure 5.9):

- Cohesion (c): 0.302 MPa

- Internal Friction Angle (ø): 51.55°

- Uniaxial Compressive Strength (UCS): 1.868 MPa

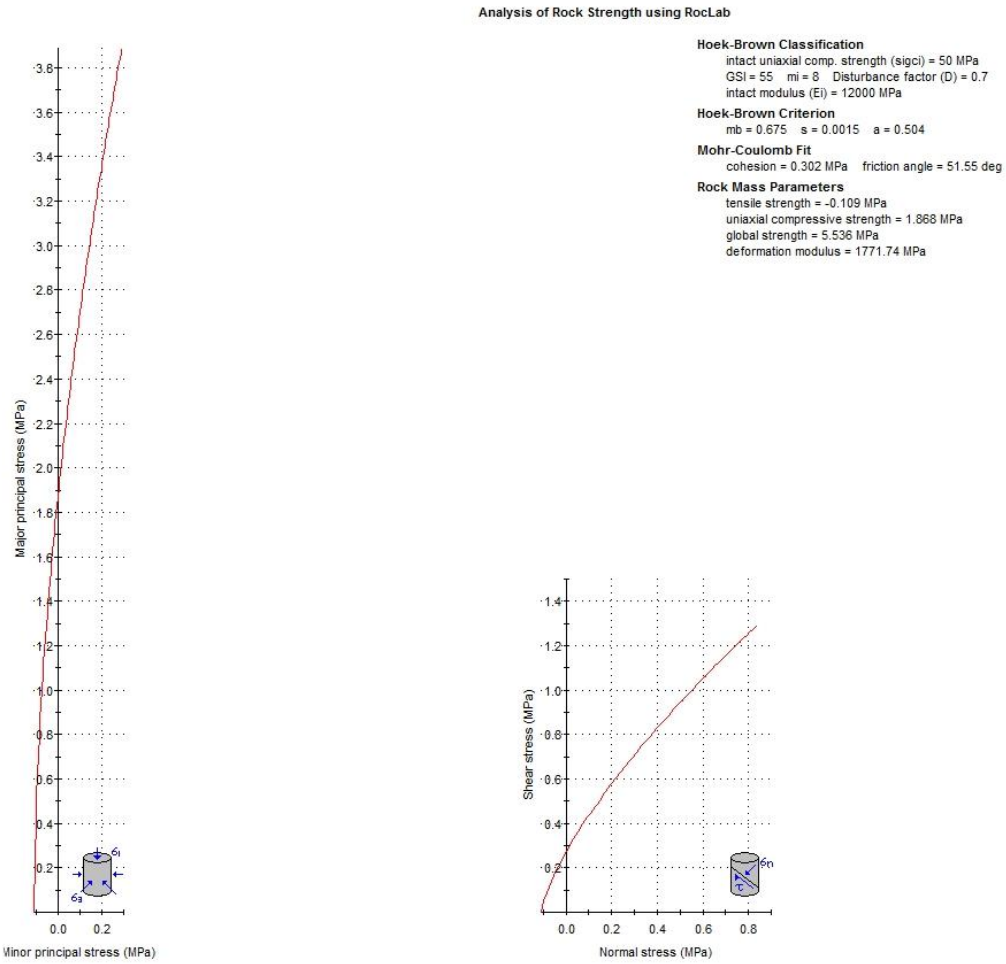

Figure 5.9. The outputs of RocLab software for cut slope analyzed.

After obtaining the instantaneous cohesion (c) and the internal friction angle (ø) values from the RocLab software program, SLIDE software was run again in order to analyze the mass failure risk. The seismicity coefficient is also taken as 0.15 and the slope is analyzed for dry case only. According to the analysis carried out, this part is completely safe in current situation having a factor safety of 5.03 (Figures 5.10-11).

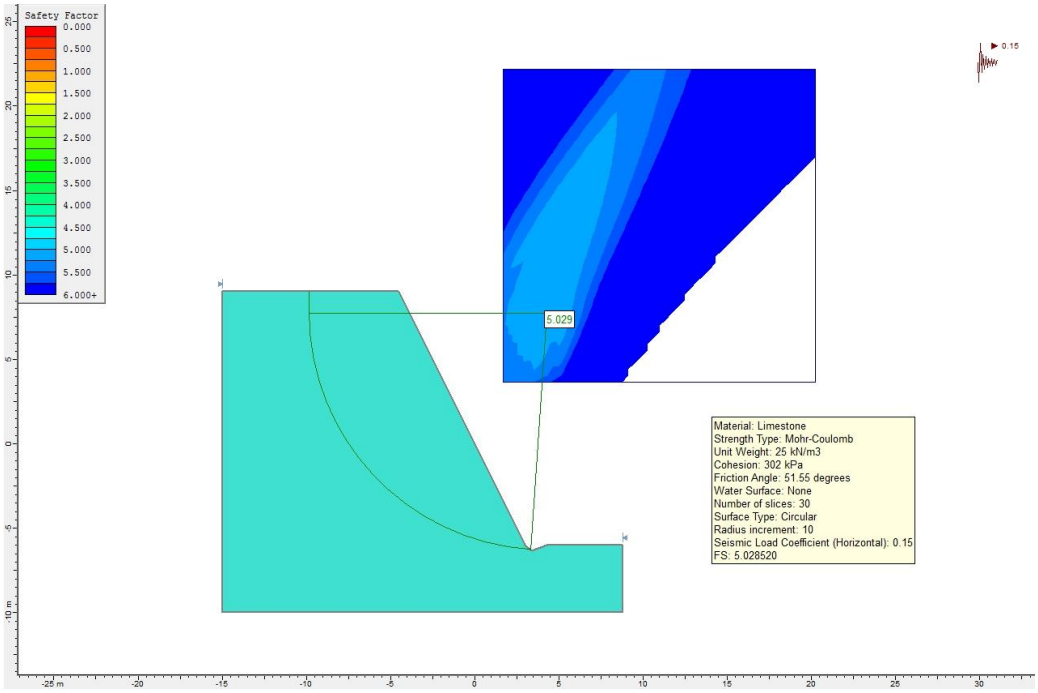

Figure 5.10. Limit equilibrium analysis of the cut slope for mass failure with current slope geometry.

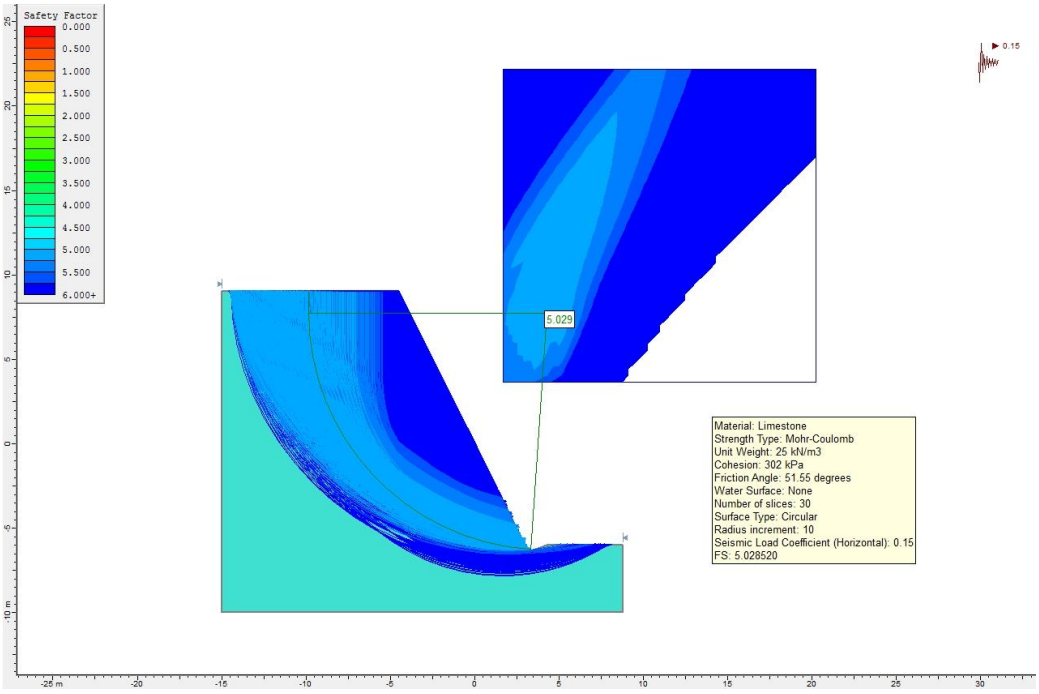

Figure 5.11. Limit equilibrium analysis of the cut slope for mass failure with all possible failure surfaces

As a remedial solution for Km: 25+900, slope flattening has been suggested. In order to see the effects of this remedial solution for the mass failure, limit equilibrium analysis is done. The slope angle of this part was 64° but for the slope flattening solution of Km:25+900, it was changed as 57°. The resultant factor of safety is found to be 5.27 (Figures 5.12 and 5.13).

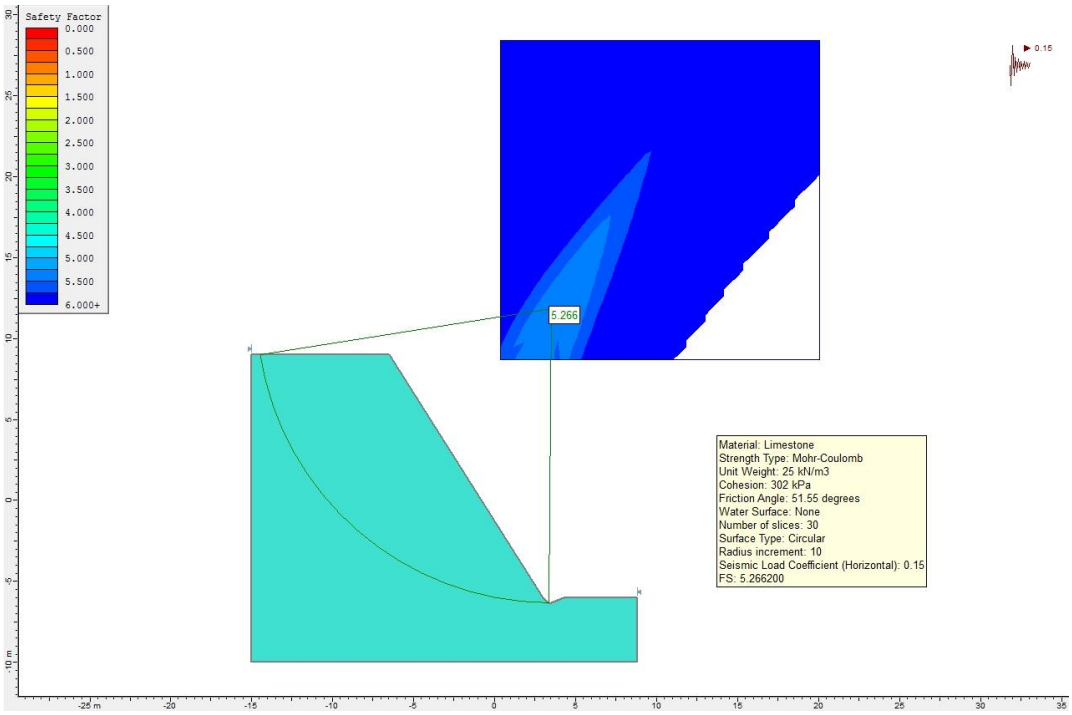

Figure 5.12. Limit equilibrium analysis of the cut slope for mass failure after slope flattening.

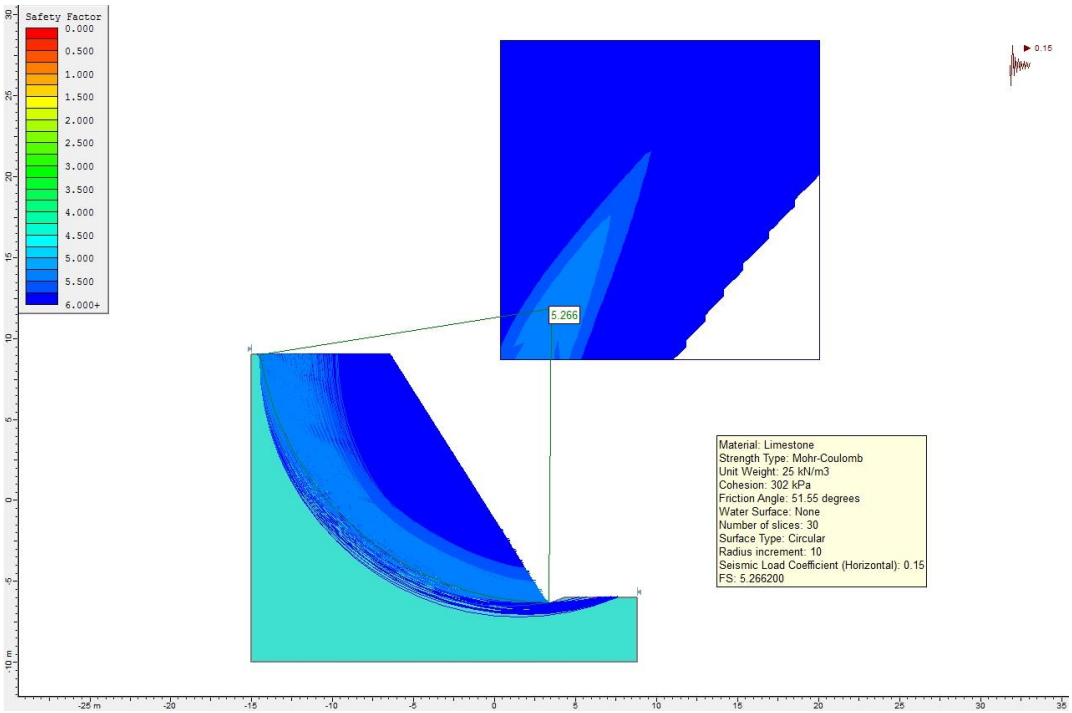

Figure 5.13. Limit equilibrium analysis of the cut slope for mass failure after slope flattening with all possible failure surfaces.

As another remedial solution for Km: 25+900, bench has been suggested. In order to see the effects of this remedial solution for the mass failure, limit equilibrium analysis is also done. Another reason to run the limit equilibrium analysis for mass failure in bench solution is that according to the General Directorate of Highway, the slopes cannot be higher than 10 meters without benches. The height of the bench is planned as 10 meters from the road elevation. The horizontal length of the bench is suggested as 5 meter, as indicated before. The resultant factor of safety is found to be 5.56 (Figures 5.14 and 5.15).

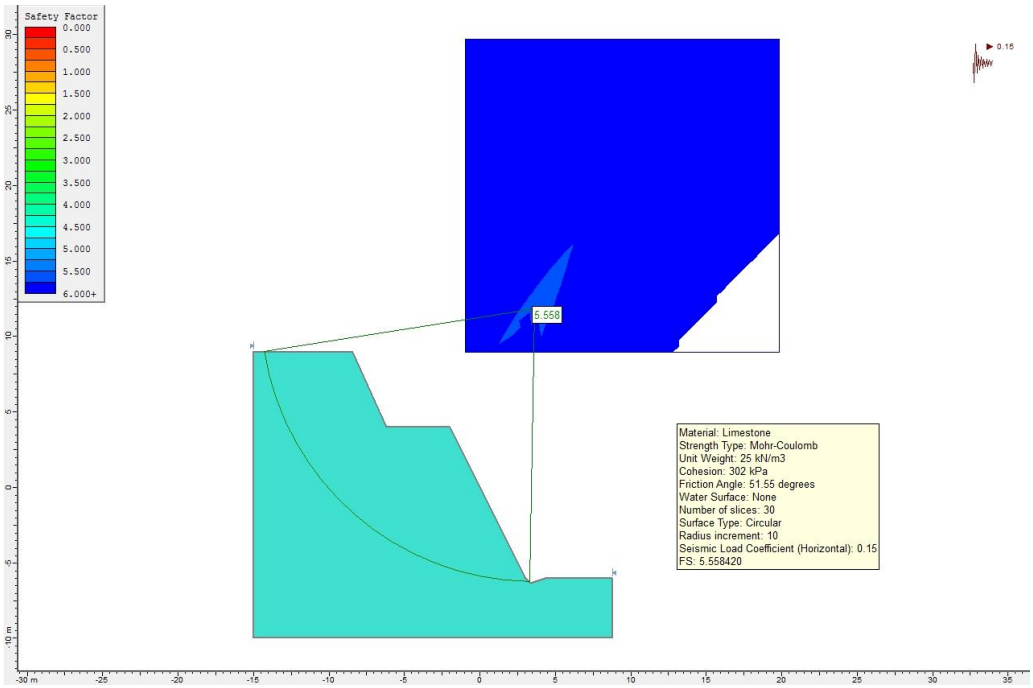

Figure 5.14. Limit equilibrium analysis of the cut slope with bench for mass failure.

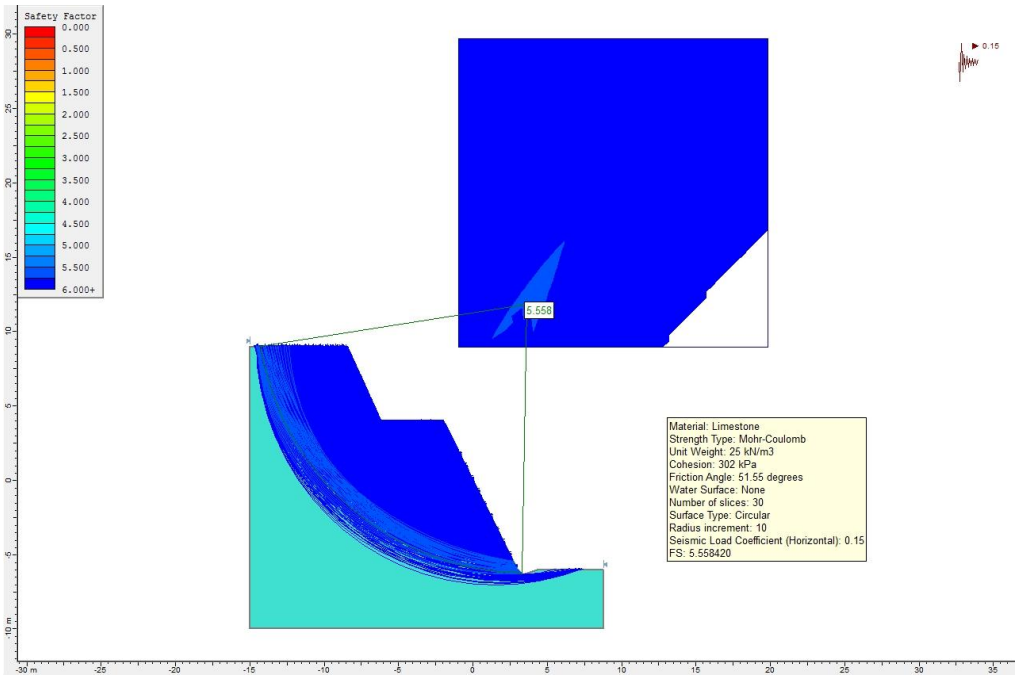

Figure 5.15. Limit equilibrium analysis of the cut slope with bench and all possible failure surfaces for mass failure.

5.3. Rockfall Analysis of the Cut Slope

For the rockfall analysis, RocFall software program by Rocscience was used. This analysis was important in this study because the slopes in the study area are high and the limestone is blocky. For such cut slopes, it is generally expected to have rockfalls reaching the highway and adversely affecting the driver's safety.

In this study, firstly, block sizes observed in the field (10 kg, 60 kg, 150 kg) are considered. Then, suitable parameters are selected for rockfall analysis (Table 5.1). A ditch with real dimensions is considered in the profile.

Table 5.1. Parameters used in the rockfall analysis for the cut slopes.

Parameters	Value
Coefficient of normal restitution	0.315 ± 0.064
Coefficient of tangential restitution	0.712 ± 0.116
Friction angle (degrees)	35 ±2
Slope roughness	2 ±1
Initial velocity (m/sec)	1.5 ± 0.15
Number of throw	1000 rocks
Minimum velocity cut-off (m/sec)	0.1
Sampling interval	50

5.3.1. Rockfall Analysis of the Cut Slopes in the Current Situation

The rockfall analyses using the parameters given in Table 5.1 for the current cut slopes are performed for 10 kg, 60 kg and 150 kg blocks. The results indicate that the rocks are likely to reach the highway (Figures 5.16-5.18) and this is not an acceptable condition for the driver's safety.

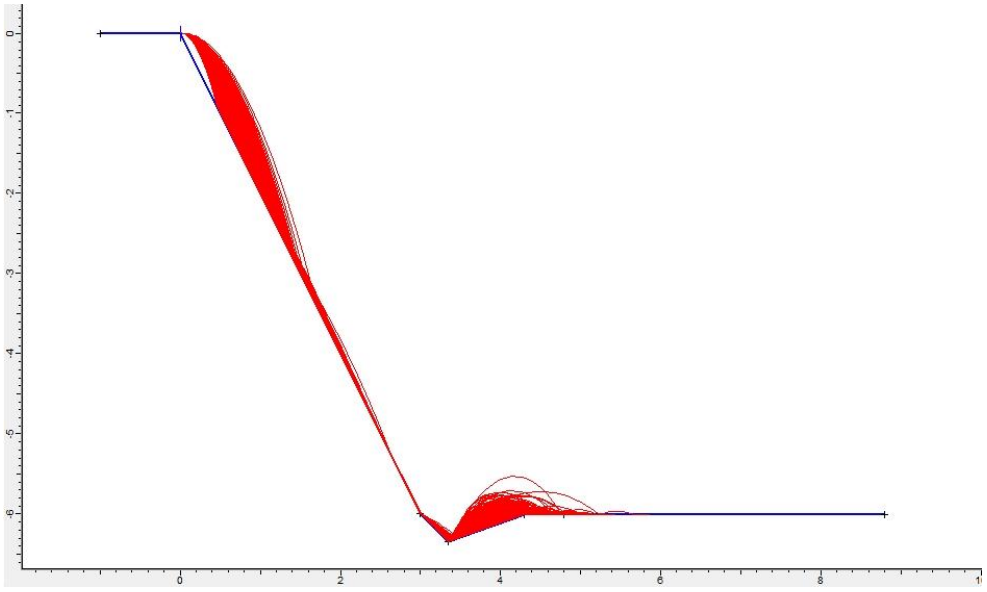

Figure 5.16. Rockfall analysis with 10 kg block for current slope condition.

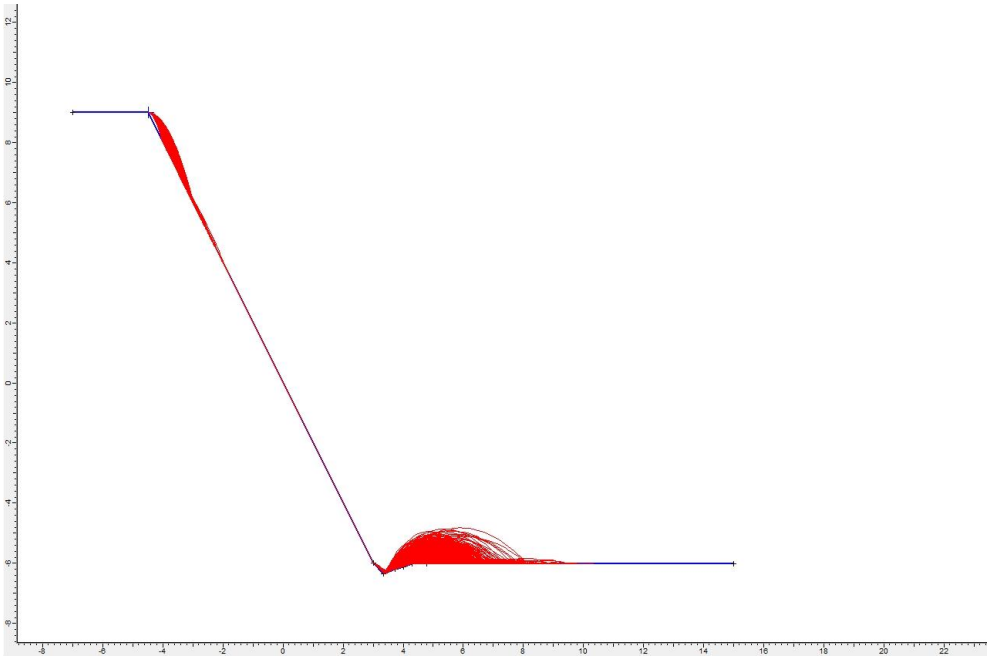

Figure 5.17. Rockfall analysis with 60 kg block for current slope condition.

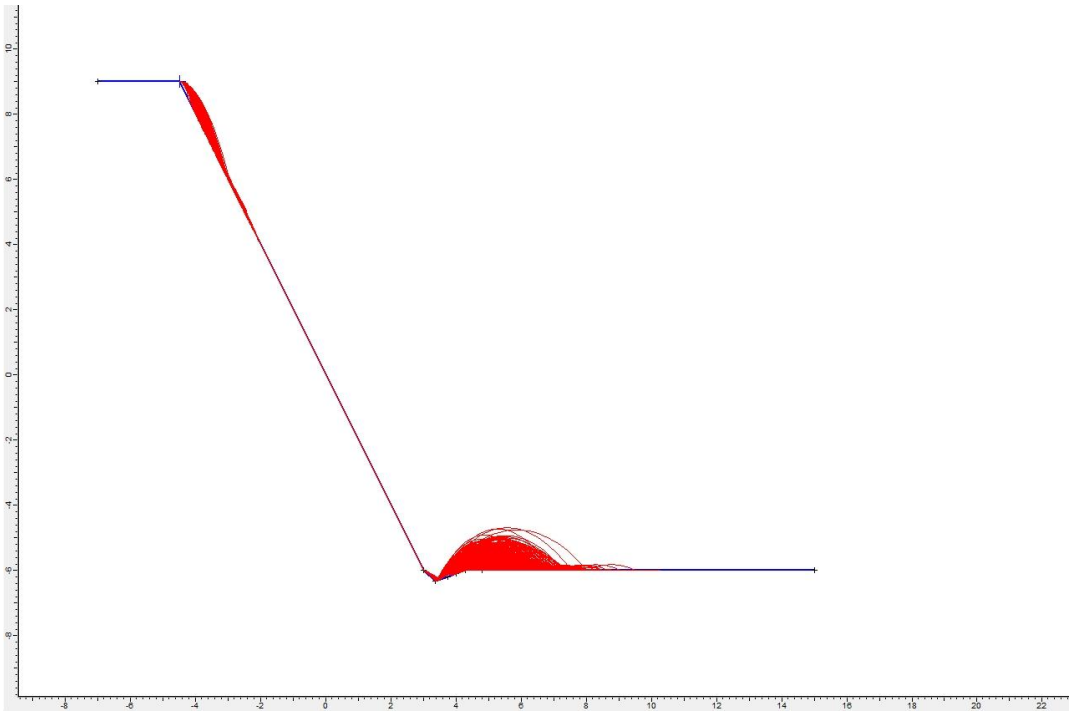

Figure 5.18. Rockfall analysis with 150 kg block for current slope condition.

As a solution, catch barrier can be implemented if the slope geometry is not modified. In order to see the behavior of the limestone blocks, the rockfall analysis is also done with the barrier (Figures 5.19-21). As can be seen from the figures, the barrier works well, but it should be installed very close to the road which is not desired in engineering practice.

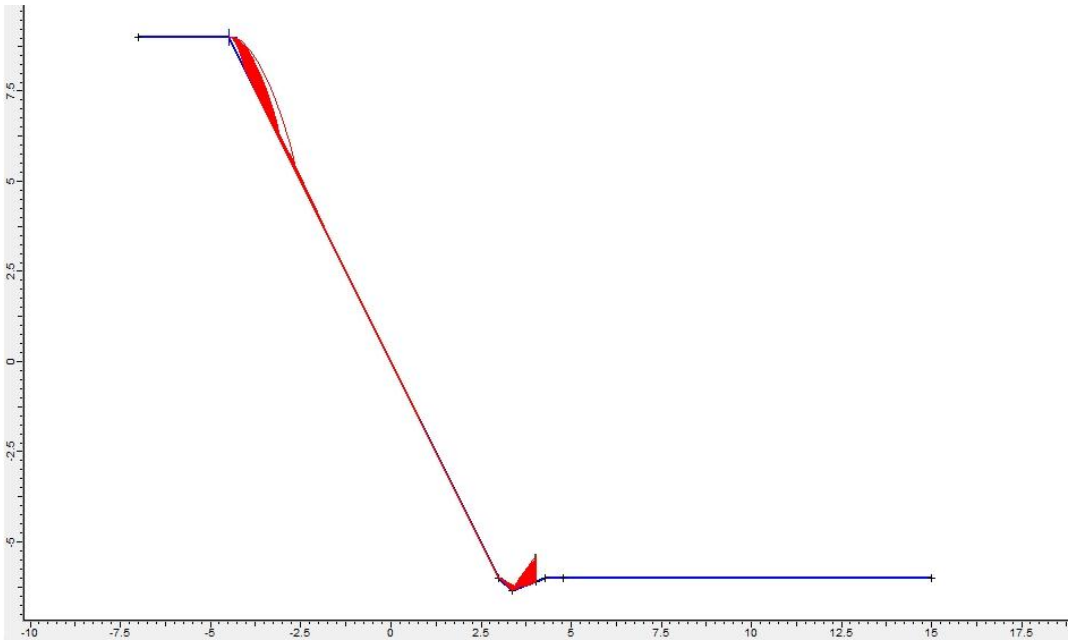

Figure 5.19. Rockfall analysis with 10 kg block and barrier solution for current slope condition.

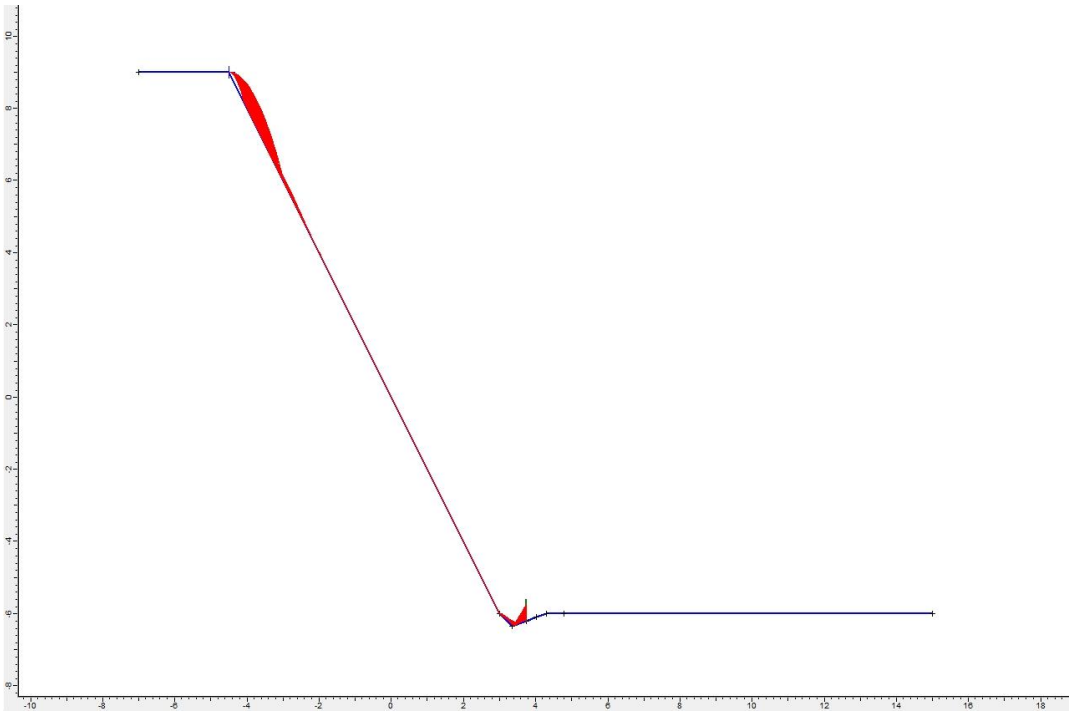

Figure 5.20. Rockfall analysis with 60 kg block and barrier solution for current slope condition.

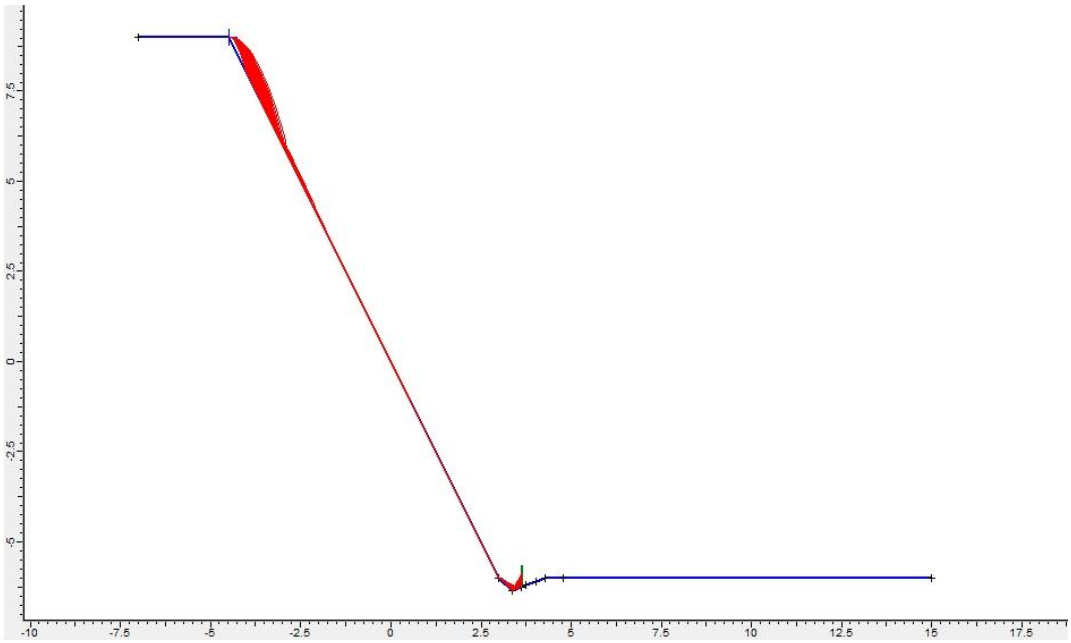

Figure 5.21. Rockfall analysis with 150 kg block and barrier solution for current slope condition.

5.3.2. Rockfall Analysis of the Cut Slope at Km: 25+600

For this part of the road, two remedial solutions, namely slope flattening and bench are considered. The reason to run these analyses was to be consistent with the General Directorate of Highway rules for the bench option and in order to see the effects of the remedial solutions suggested for Km: 25+900. There was no planar, wedge or toppling risk for this part of the road. So the slope flattening analyses is run according to the suggested slope change for Km: 25+900.

The calculation was done for 10 kg, 60 kg and 150 kg, for both slope flattening (Figures 5.22-5.24) and bench solutions (Figures 5.25-5.27). The slope angle is changed from 64° to 57°. The height of the bench is 10 m and the width is 5 m. As a result, the rocks always ended up in the road.

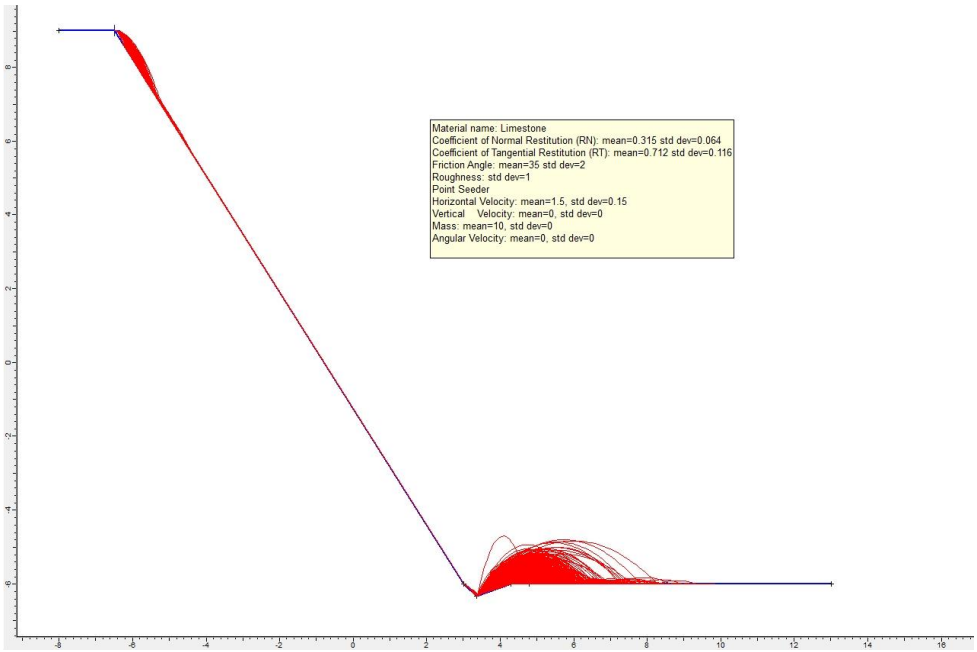

Figure 5.22. Rockfall analysis with 10 kg block and slope flattening solution at Km: 25+600.

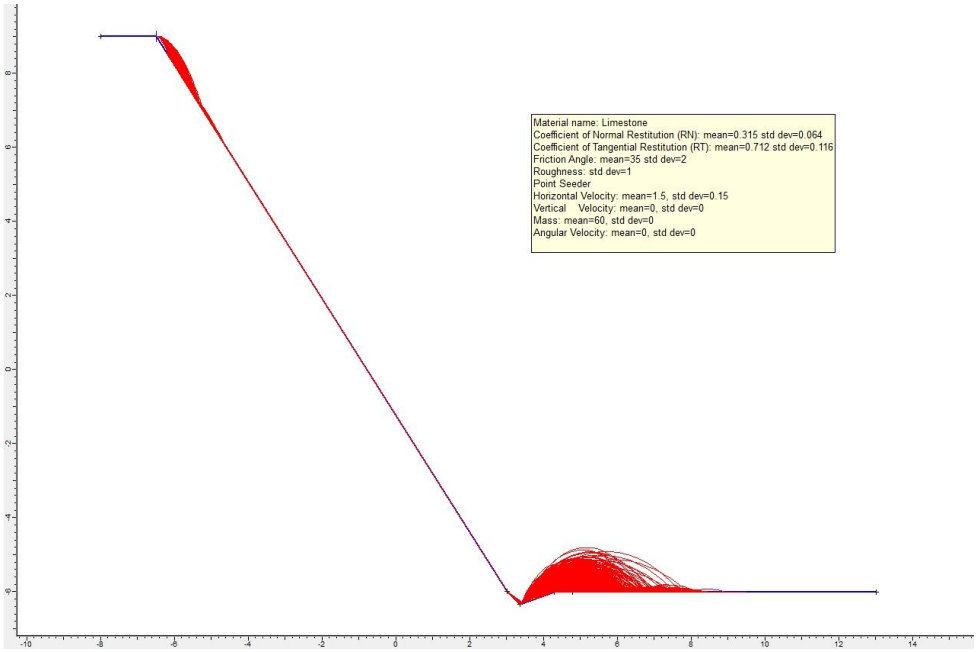

Figure 5.23. Rockfall analysis with 60 kg block and slope flattening solution at Km: 25+600.

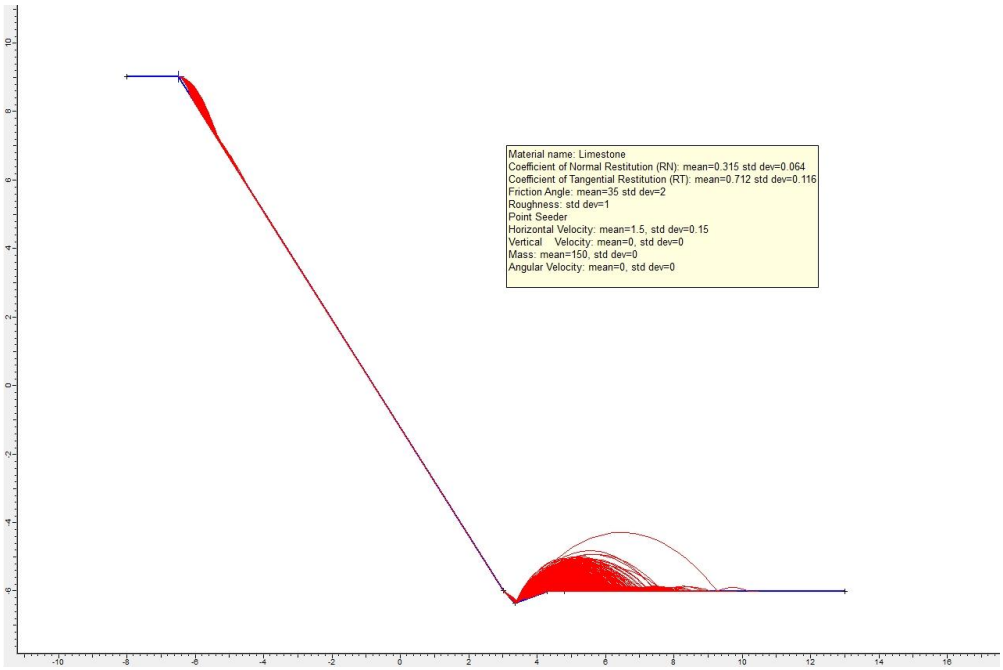

Figure 5.24. Rockfall analysis with 150 kg block and slope flattening solution at Km: 25+600.

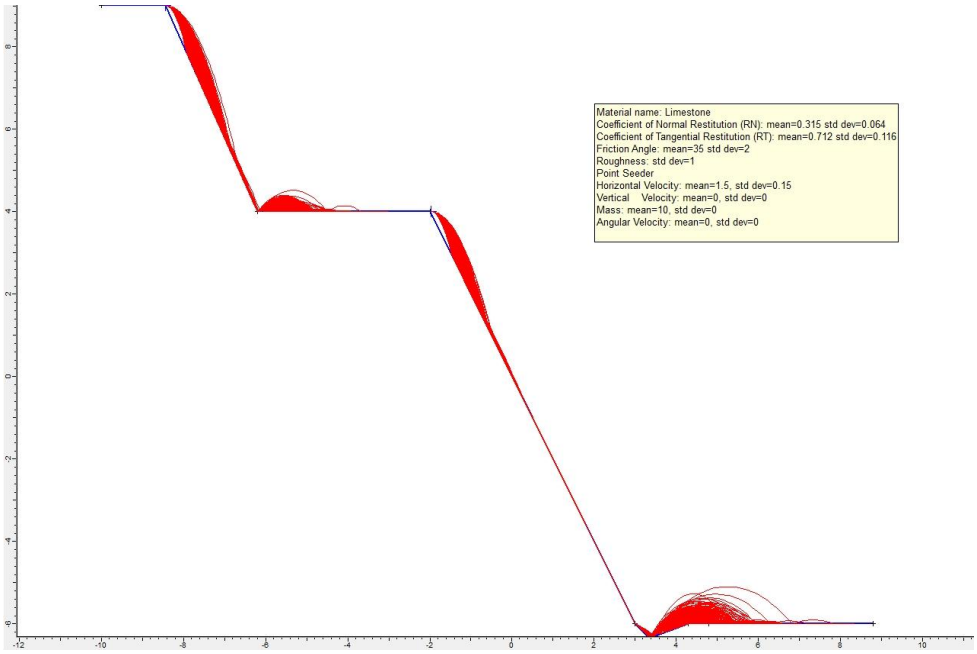

Figure 5.25. Rockfall analysis with 10 kg block and bench solution at Km: 25+600.

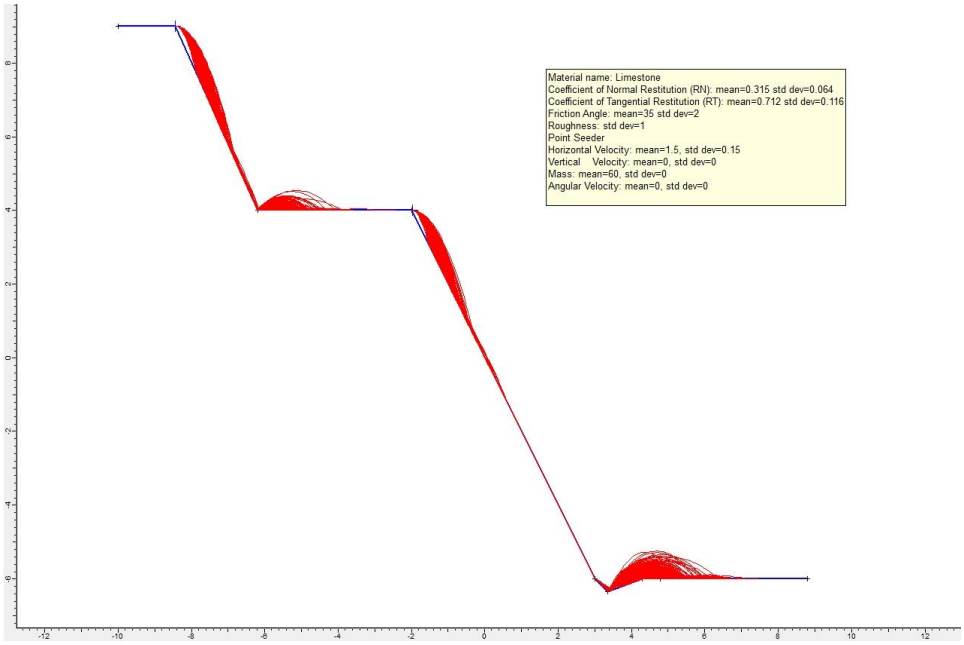

Figure 5.26. Rockfall analysis with 60 kg block and bench solution at Km: 25+600.

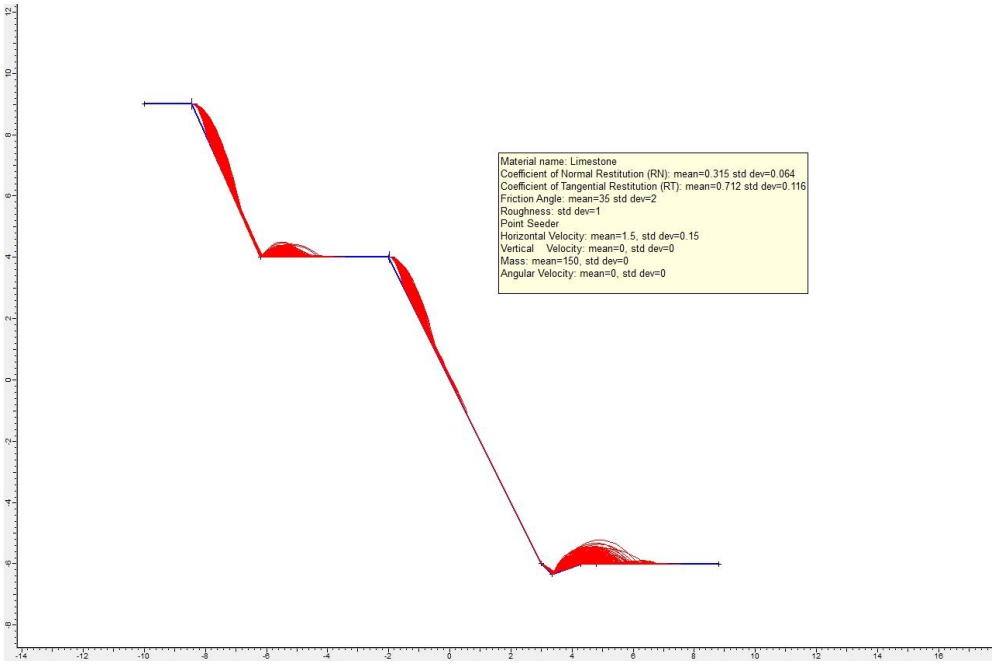

Figure 5.27. Rockfall analysis with 150 kg block and bench solution at Km: 25+600.

As a solution, catch barrier can also be thought here. In order to see the behavior of the individual rocks, the rockfall analysis is also done with slope flattening and the barrier (Figures 5.28-5.30), as well as bench and the barrier (Figure 5.31-5.33). Still, the barrier works well. However, it should be installed very close to the road.

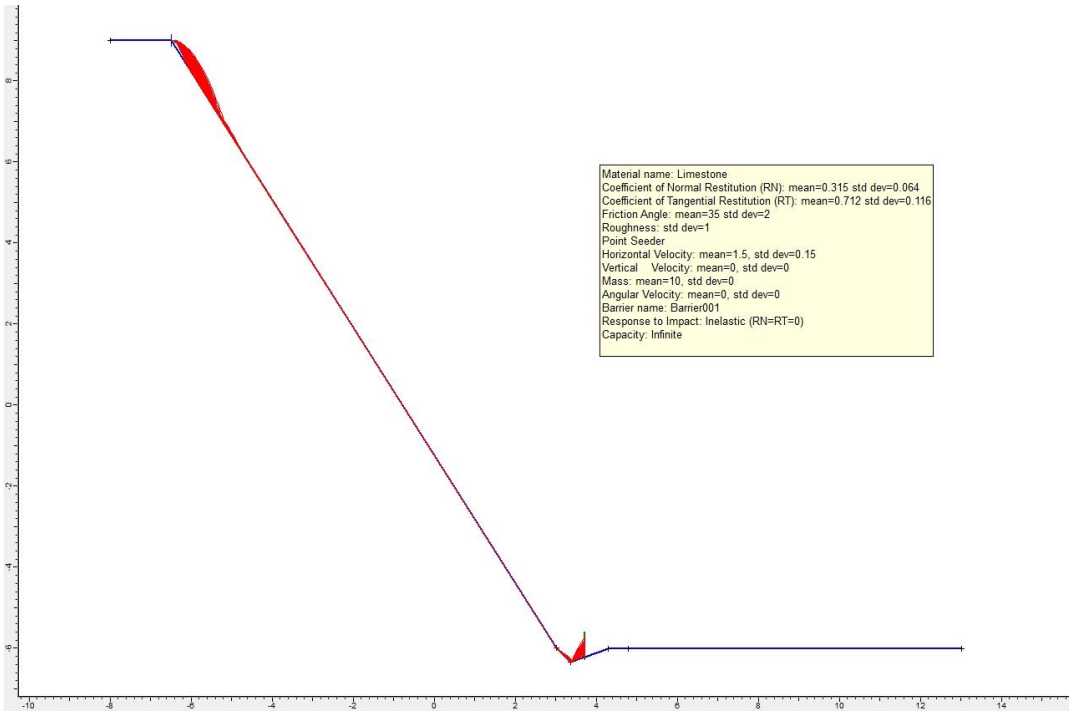

Figure 5.28. Rockfall analysis (10 kg block) with slope flattening and barrier solution at Km: 25+600.

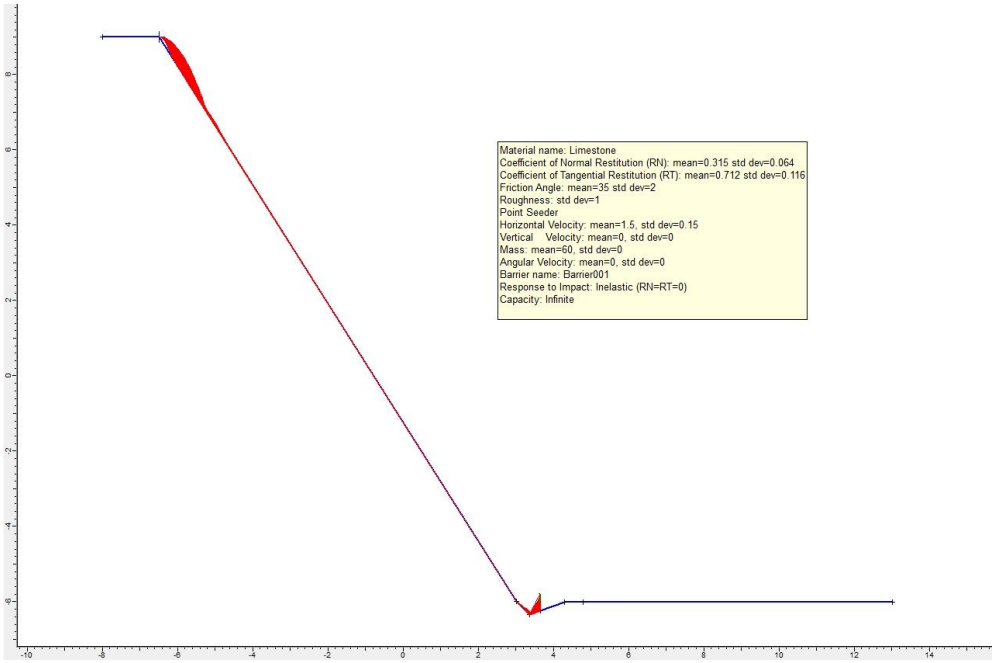

Figure 5.29. Rockfall analysis (60 kg block) with slope flattening and barrier solution at Km: 25+600.

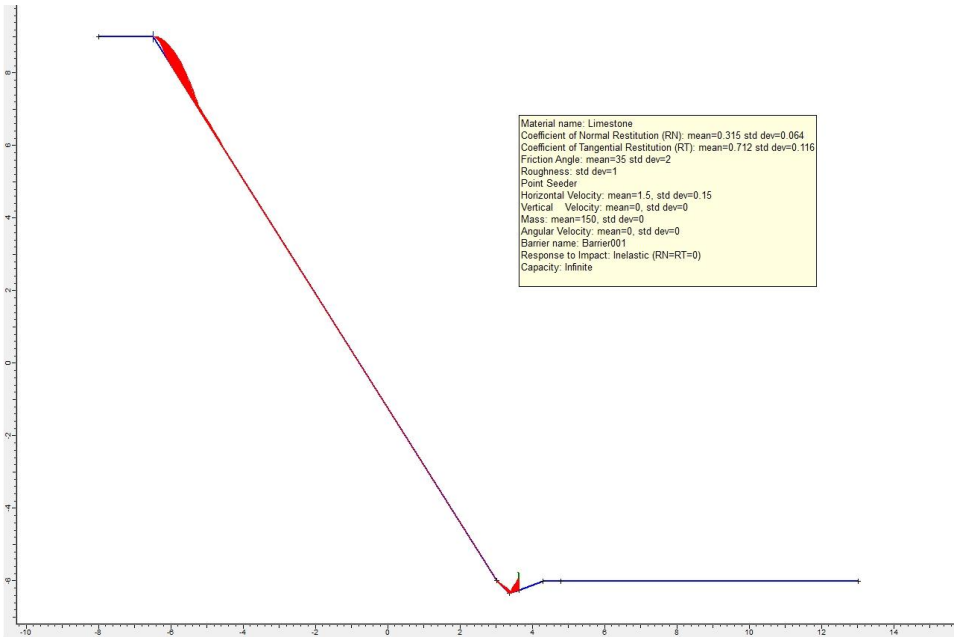

Figure 5.30. Rockfall analysis (150 kg block) with slope flattening and barrier solution at Km: 25+600.

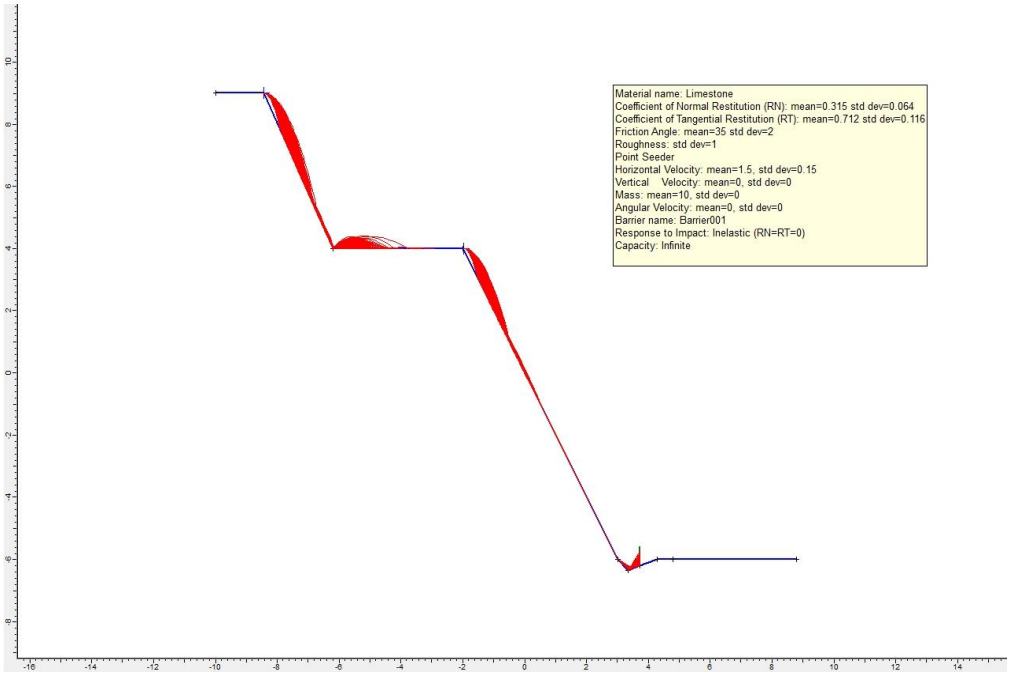

Figure 5.31. Rockfall analysis (10 kg block) with bench and barrier solution at Km: 25+600.

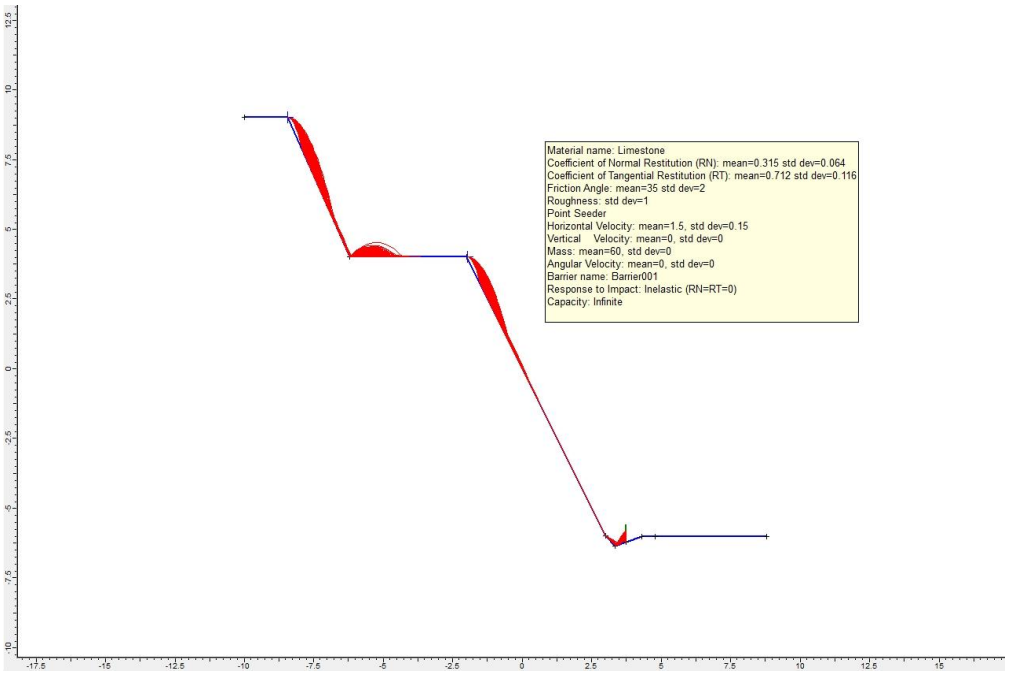

Figure 5.32. Rockfall analysis (60 kg block) with bench and barrier solution at Km: 25+600.

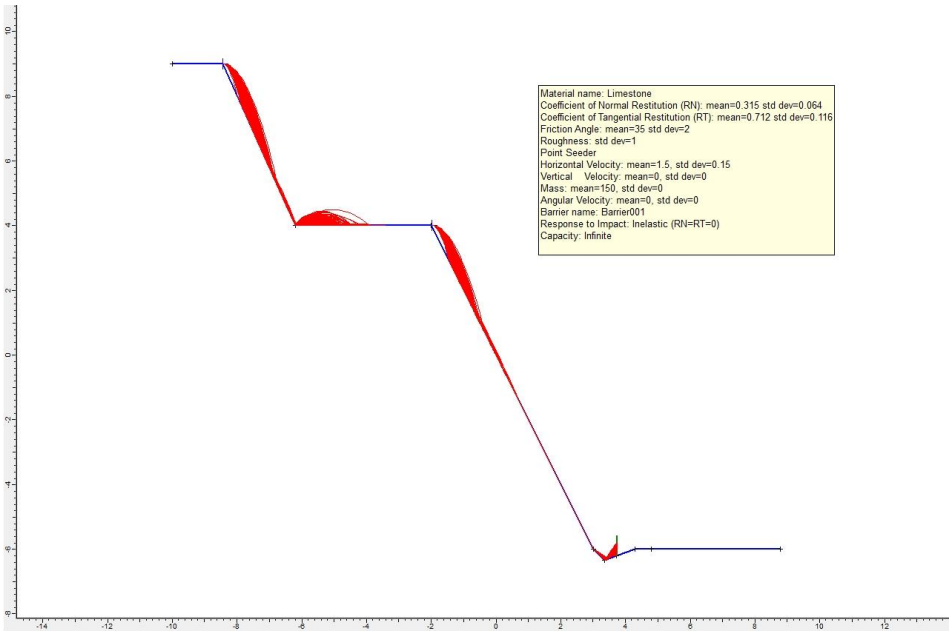

Figure 5.33. Rockfall analysis (150 kg block) with bench and barrier solution at Km: 25+600.

Based on the rockfall analyses, one can say that the rocks falling from the upper part of the slope do not fall to the road. The bench holds all the rocks. Therefore, benching may be suggested at Km: 25+600 for the upper part of the slope from rockfall point of view.

5.3.3. Rockfall Analysis of the Cut Slope at Km: 25+900

This part of the highway was found to be problematic according to the limit equilibrium analysis. In order to be consistent with those calculations and see the results of the solutions suggested for those slopes, the rockfall analyses were performed again. The calculation was done for 10 kg, 60 kg and 150 kg, for both slope flattening (Figures 5.34-5.36) and bench solutions (Figures 5.37-5.39). The slope angle was changed from 64° to 57°. The height of the bench is 10 m and the width is 5 m. The analyses reveal that the rocks always ended up in the road.

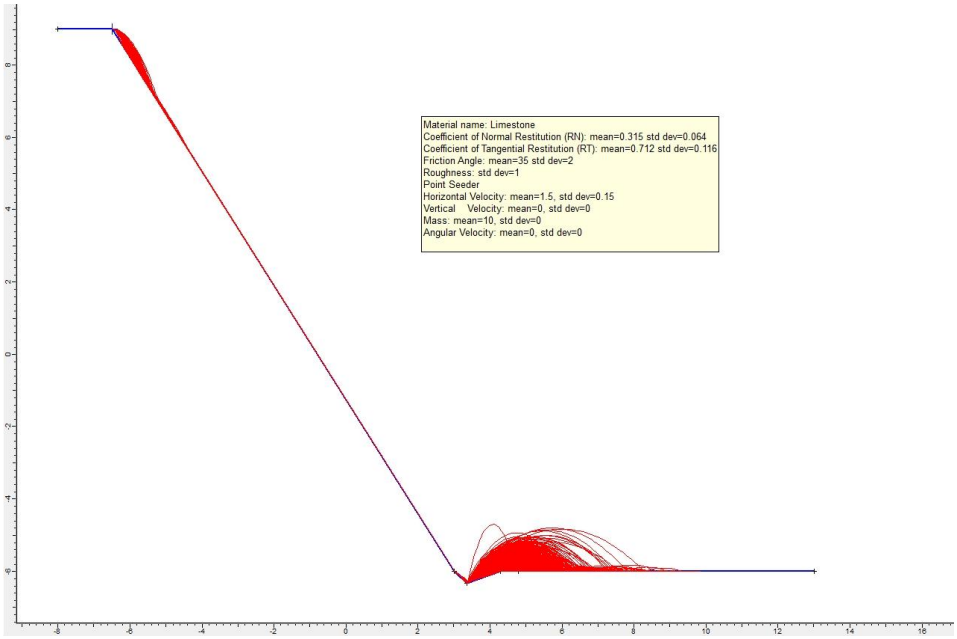

Figure 5.34. Rockfall analysis (10 kg block) with slope flattening solution at Km: 25+900.

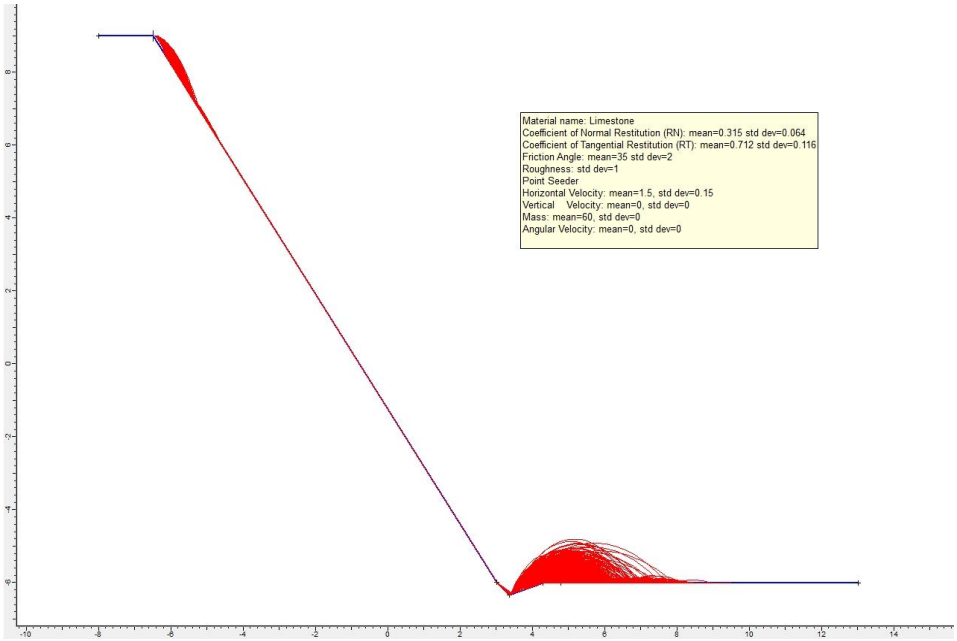

Figure 5.35. Rockfall analysis (60 kg block) with slope flattening solution at Km: 25+900.

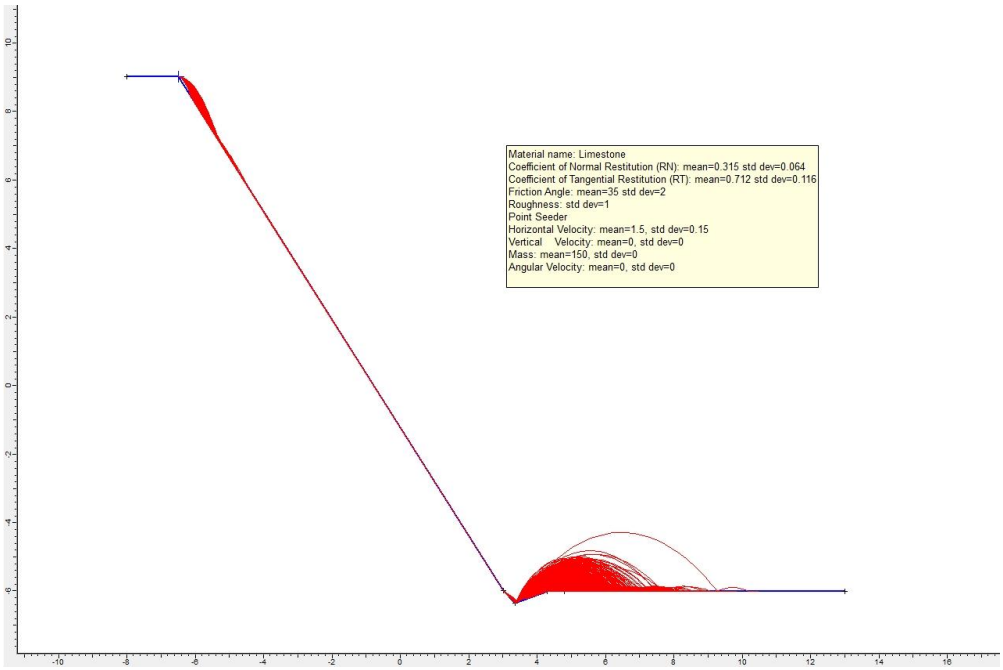

Figure 5.36. Rockfall analysis (150 kg block) with slope flattening solution at Km: 25+900.

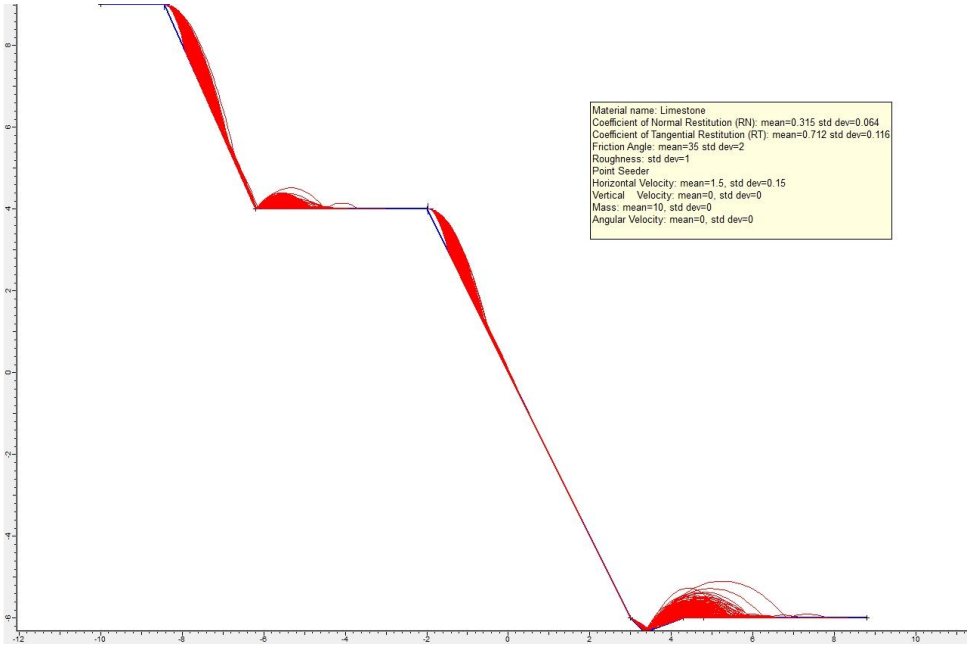

Figure 5.37. Rockfall analysis (10 kg block) with bench solution at Km: 25+900.

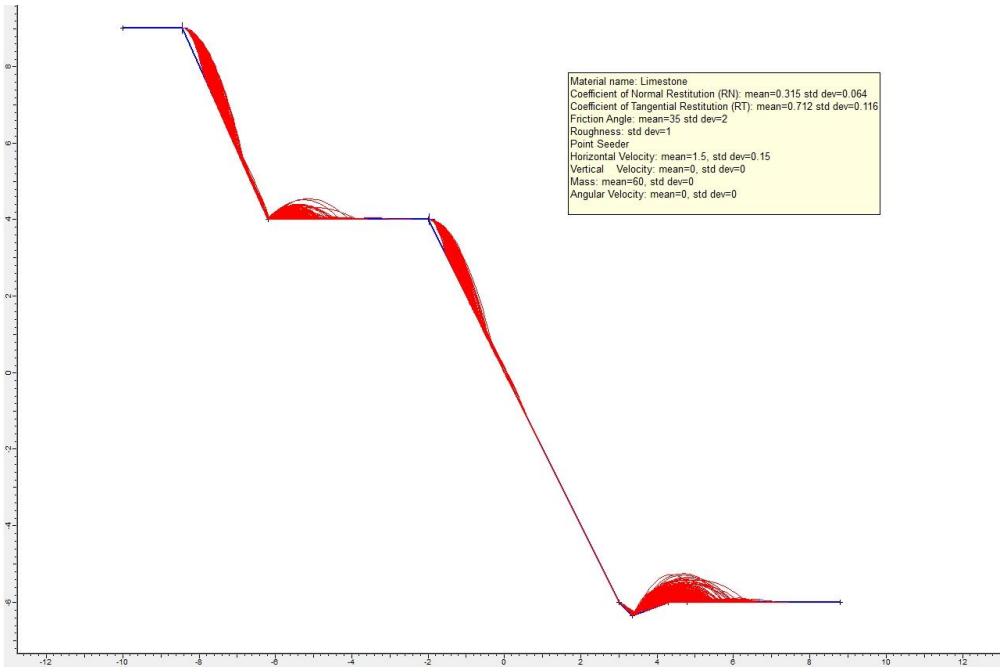

Figure 5.38. Rockfall analysis (60 kg block) with bench solution at Km: 25+900.

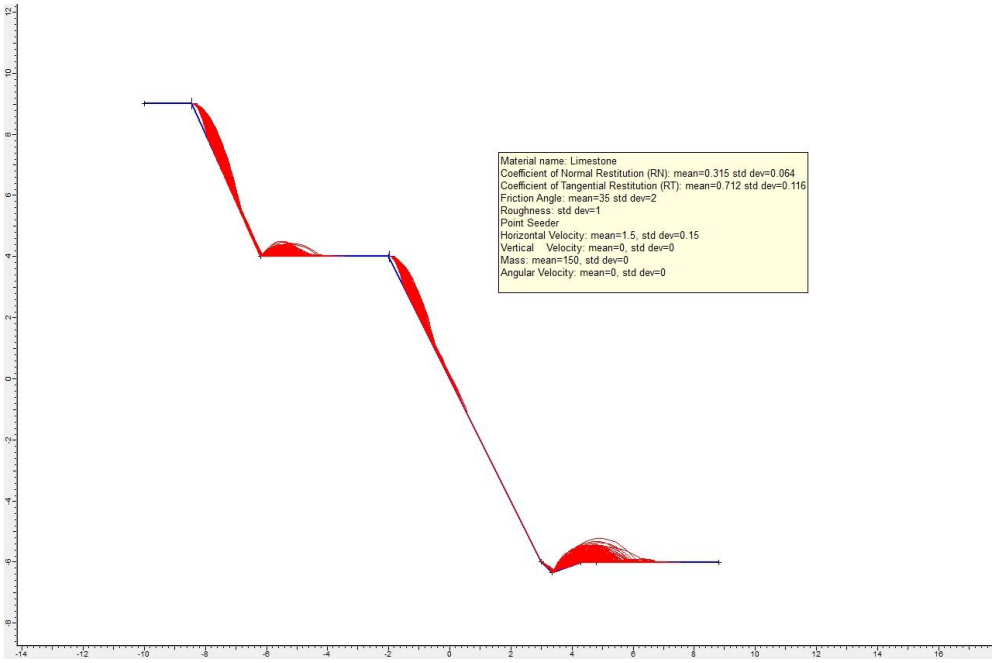

Figure 5.39. Rockfall analysis (150 kg block) with bench solution at Km: 25+900.

As a solution, catch barrier can be considered here. In order to see the behavior of the individual rocks, the rockfall analysis is also done with slope flattening and the barrier (Figures 5.40-5.42), as well as bench and the barrier (Figure 5.43-5.45). The only problem is that the barrier is very close to the road.

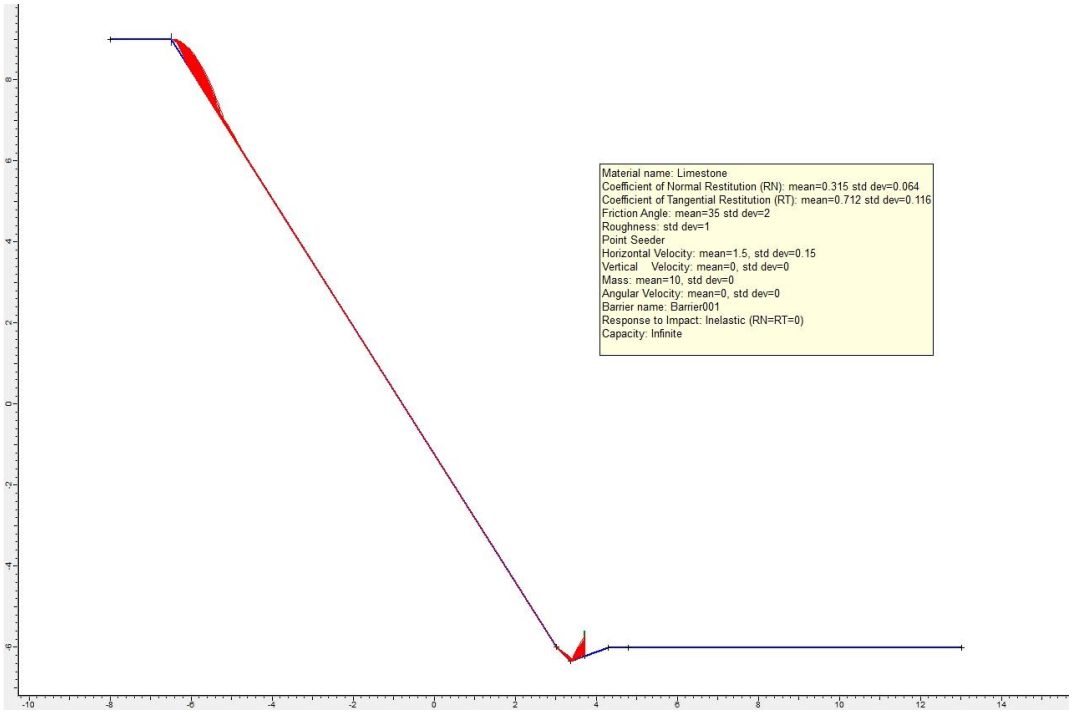

Figure 5.40. Rockfall analysis (10 kg block) with slope flattening and barrier solution at Km: 25+900.

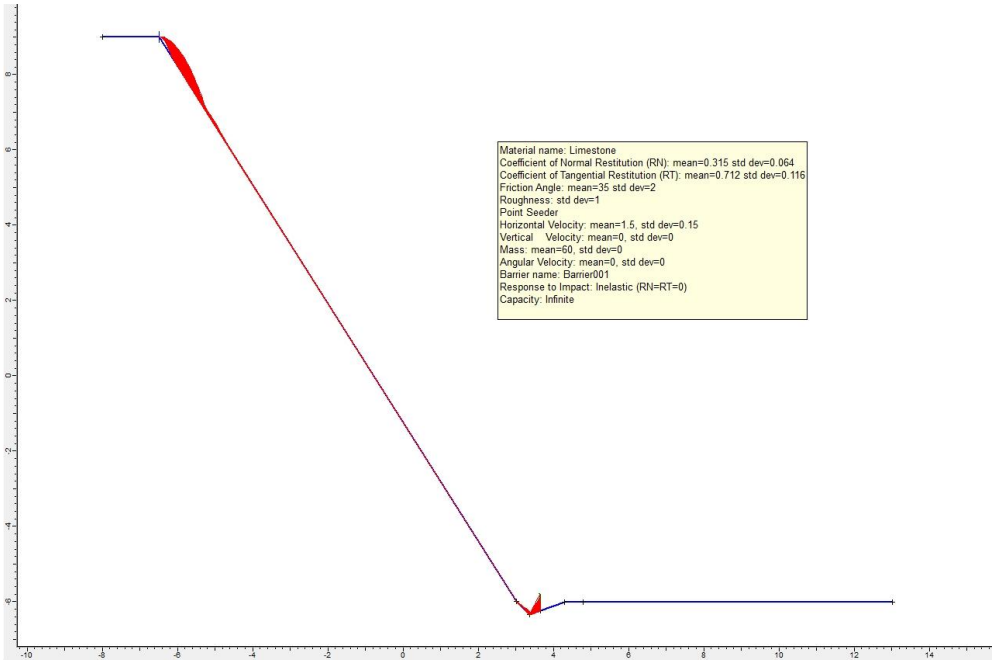

Figure 5.41. Rockfall analysis (60 kg block) with slope flattening and barrier solution at Km: 25+900.

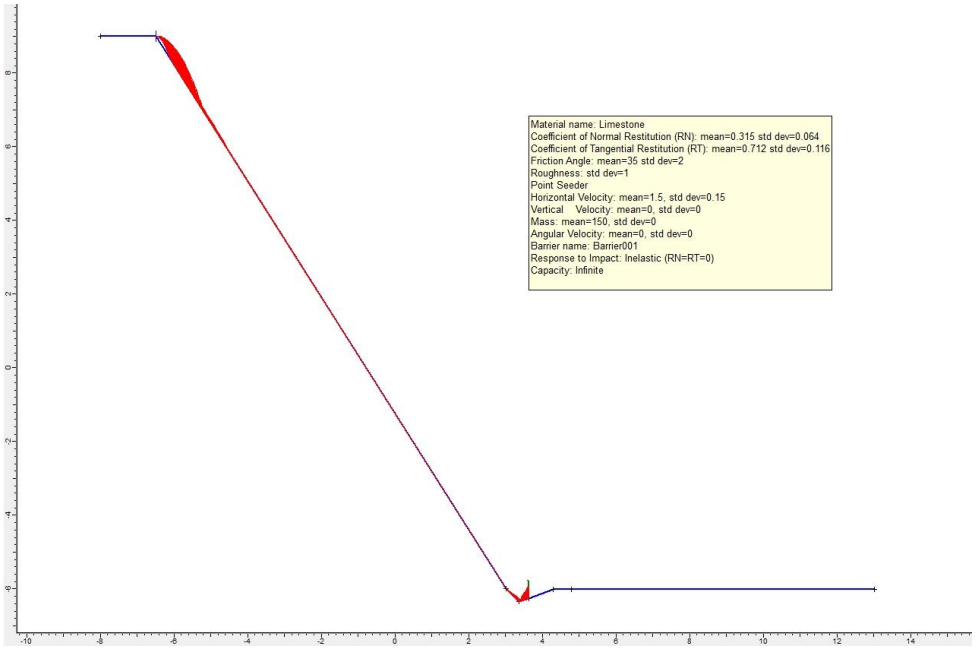

Figure 5.42. Rockfall analysis (150 kg block) with slope flattening and barrier solution at Km: 25+900.

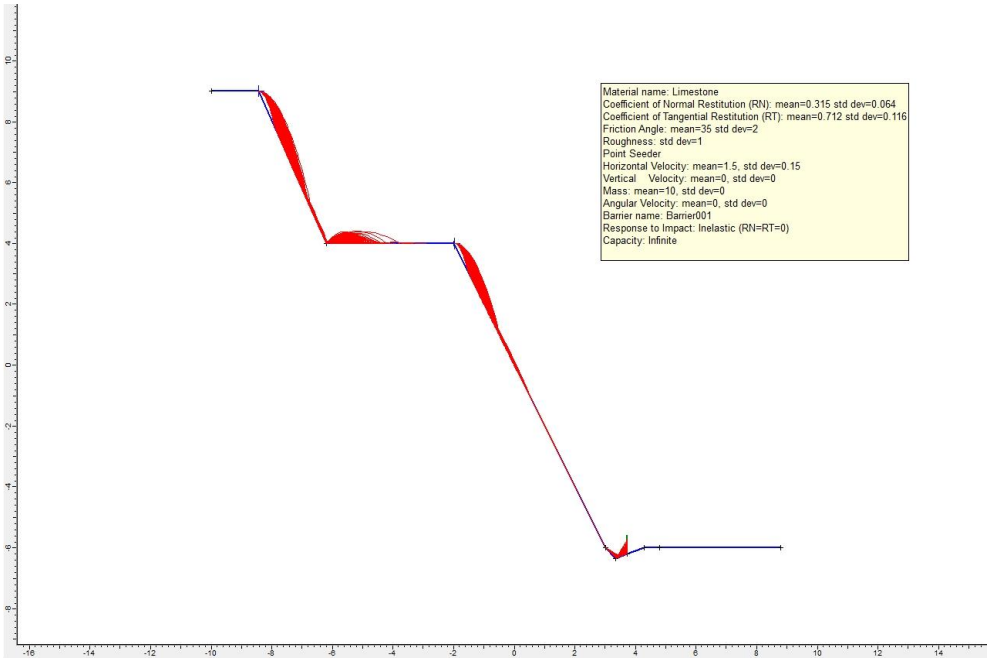

Figure 5.43. Rockfall analysis (10 kg block) with bench and barrier solution at Km: 25+900.

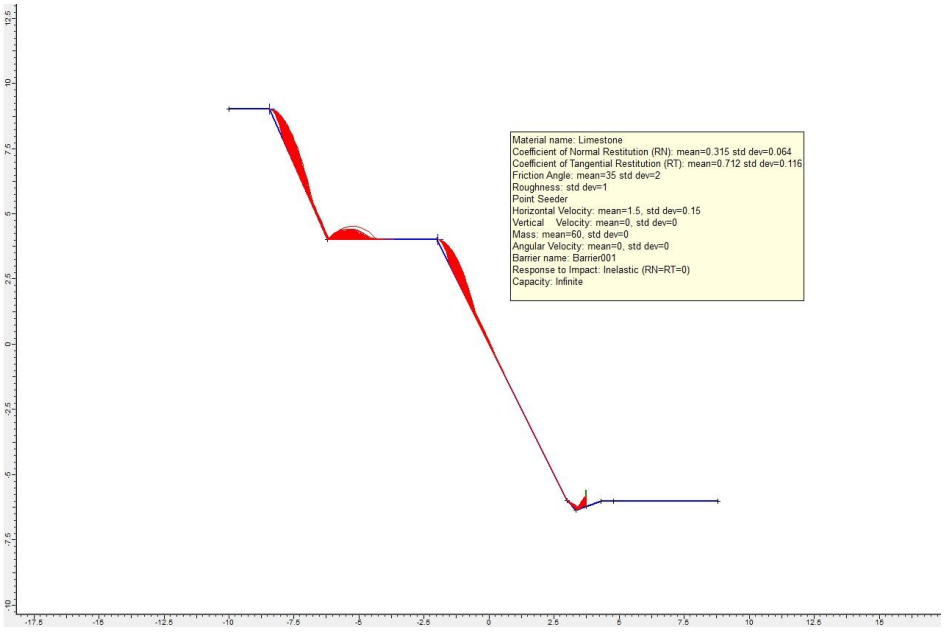

Figure 5.44. Rockfall analysis (60 kg block) with bench and barrier solution at Km: 25+900.

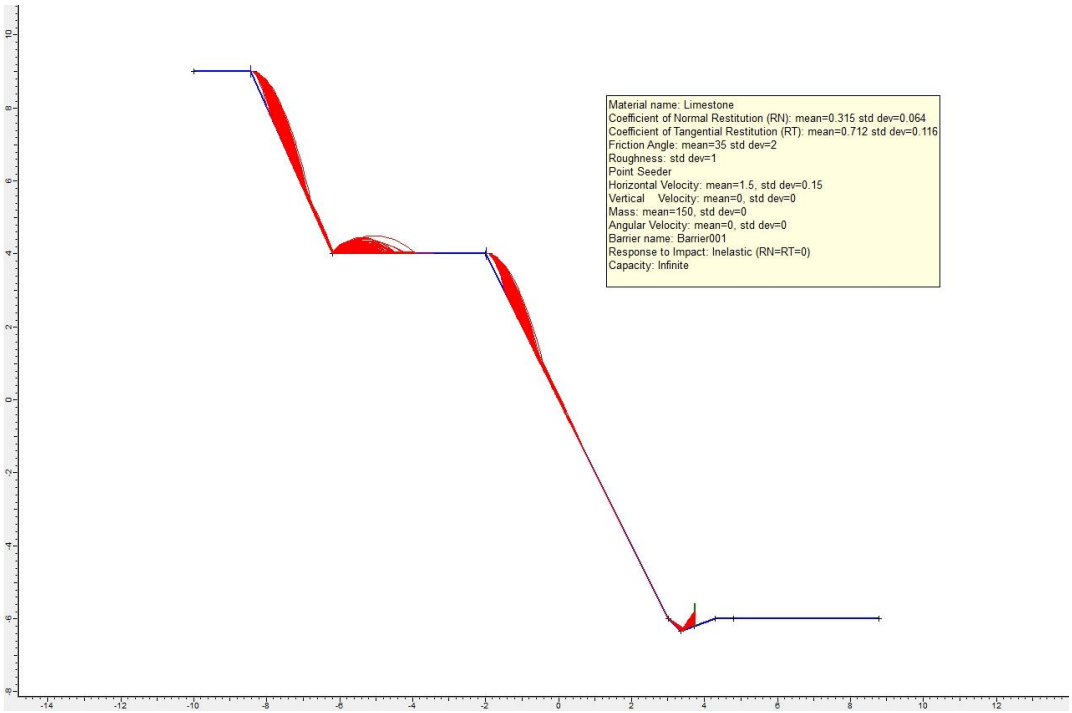

Figure 5.45. Rockfall analysis (150 kg block) with bench and barrier solution at Km: 25+900.

The rocks falling from the upper part of the slope do not fall again to the road. The bench holds all the rocks. As for the rockfall point of view, benching is suggested at Km: 25+900 for the upper part of the slope.

5.3.4. Rockfall Analysis of the Cut Slope at Km: 26+000

For this part, two remedial solutions, namely slope flattening and bench are considered during the rockfall analysis. The analysis was done for both slope flattening (Figures 5.46-5.48) and bench (Figures 5.49-5.51) solutions with the same block weights. The slope angle was changed from 64° to 57°. The height of the bench is 10 m and the width is 5 m. The rockfall analyses show that the falling rocks mainly reach the road.

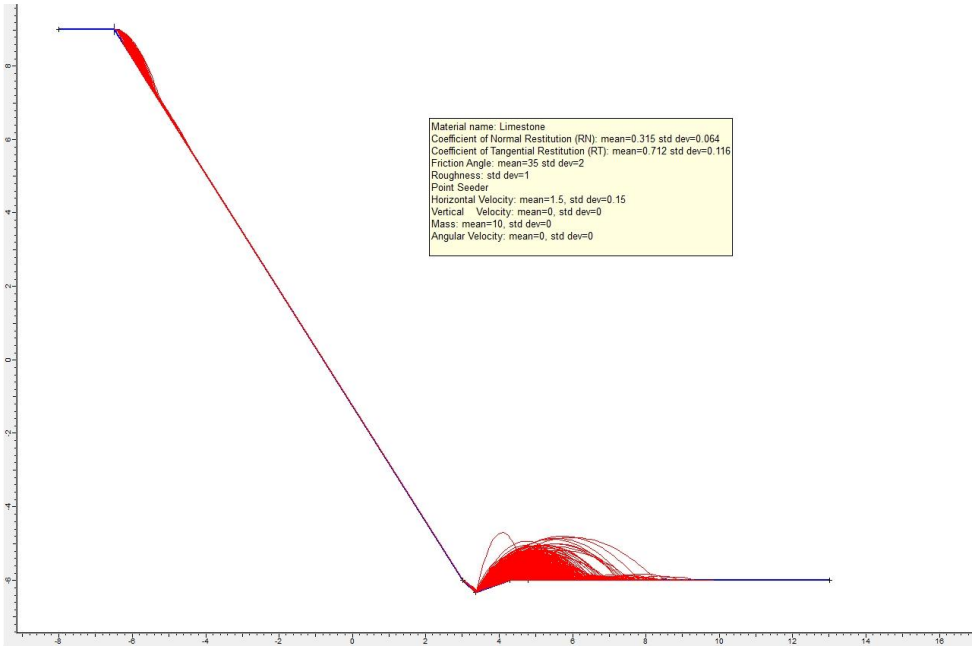

Figure 5.46. Rockfall analysis (10 kg block) with slope flattening solution at Km: 26+000.

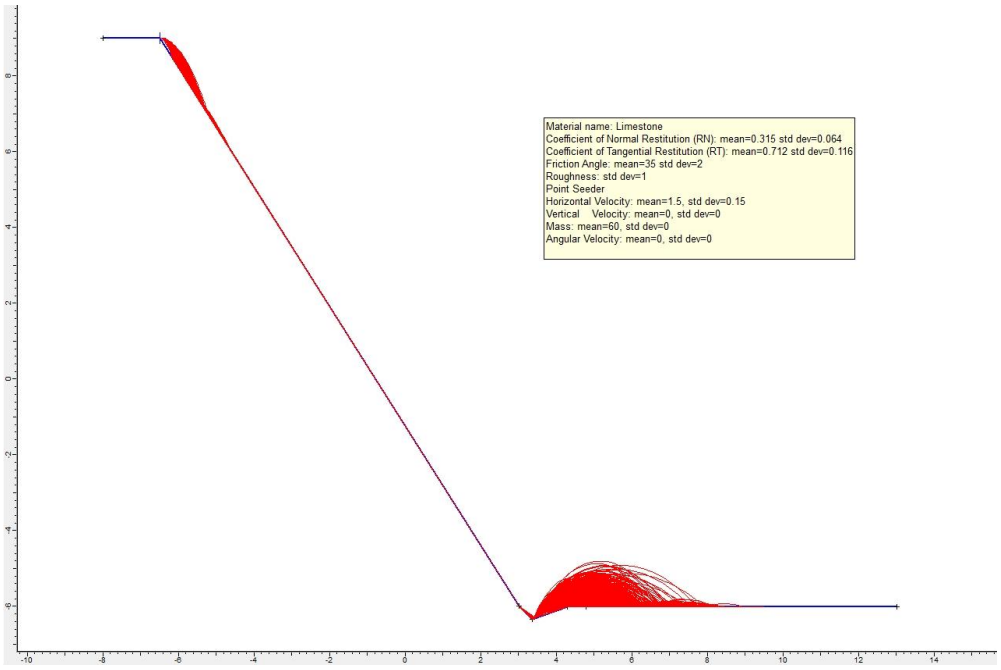

Figure 5.47. Rockfall analysis (60 kg block) with slope flattening solution at Km: 26+000.

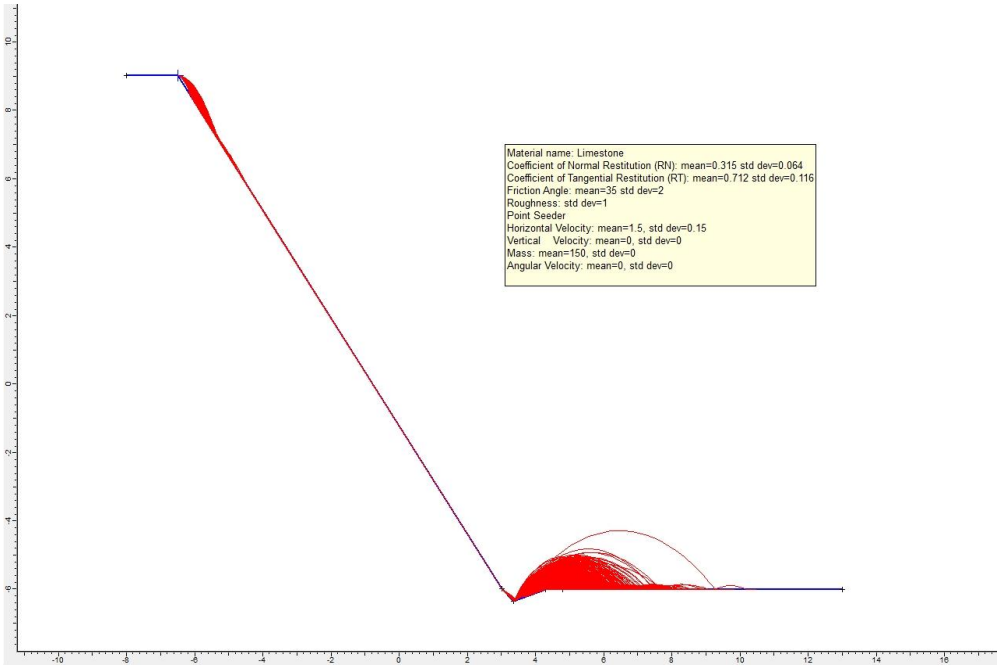

Figure 5.48. Rockfall analysis (150 kg block) with slope flattening solution at Km: 26+000.

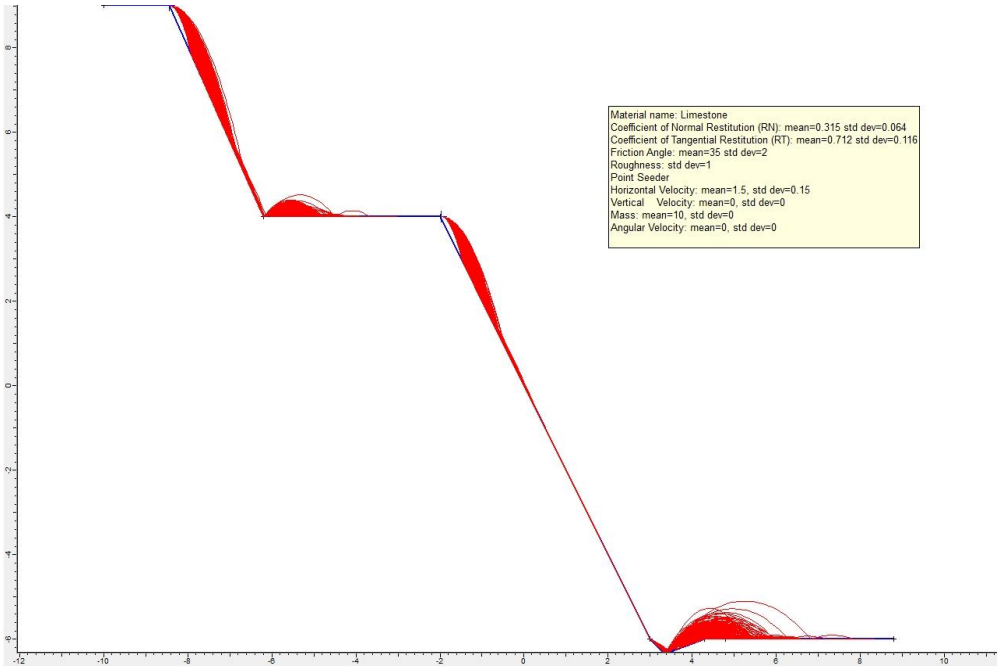

Figure 5.49. Rockfall analysis (10 kg block) with bench solution at Km: 26+000.

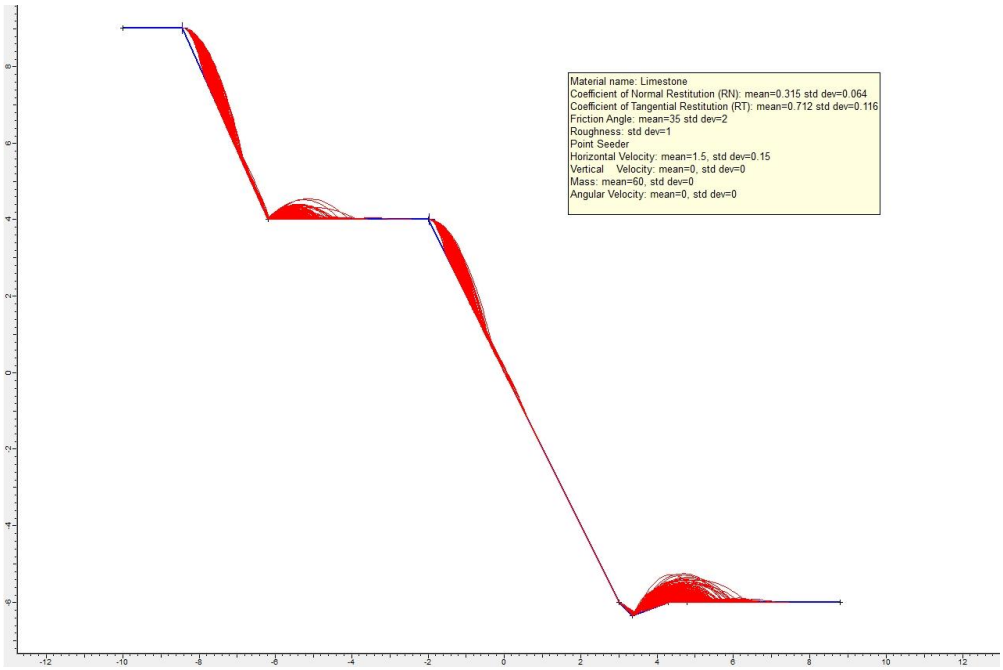

Figure 5.50. Rockfall analysis (60 kg block) with bench solution at Km: 26+000.

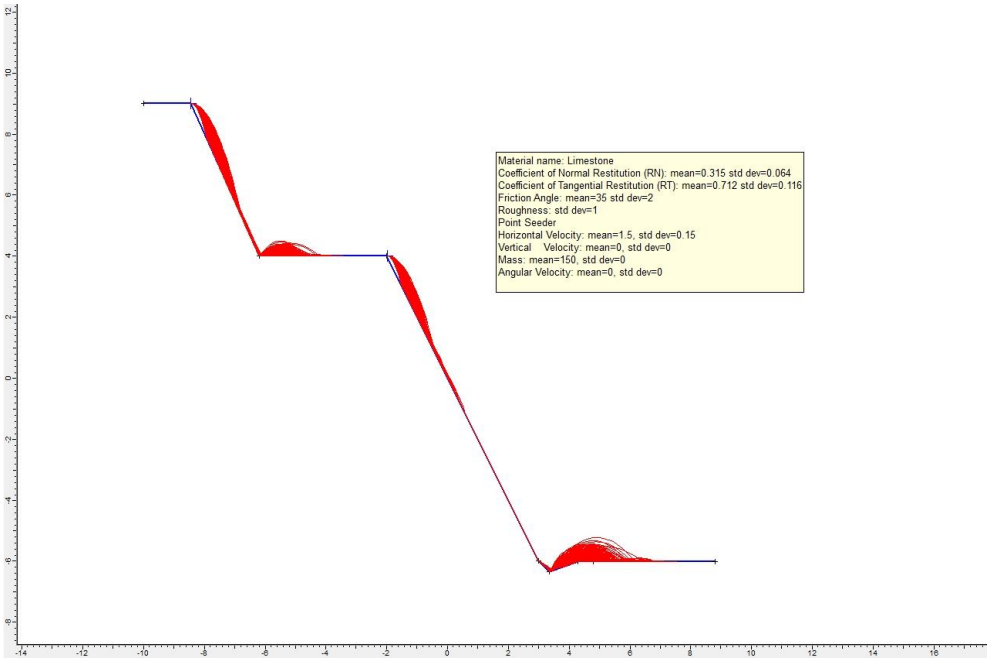

Figure 5.51. Rockfall analysis (150 kg block) with bench solution at Km: 26+000.

As a solution, catch barrier can be considered here. The rockfall analyses done with slope flattening and the barrier (Figures 5.52-5.54), and bench and the barrier (Figure 5.55-5.57) show that although the barriers solve the problem, they are very close to the road. Therefore, it is preferable to consider other alternatives if the ditch details do not change.

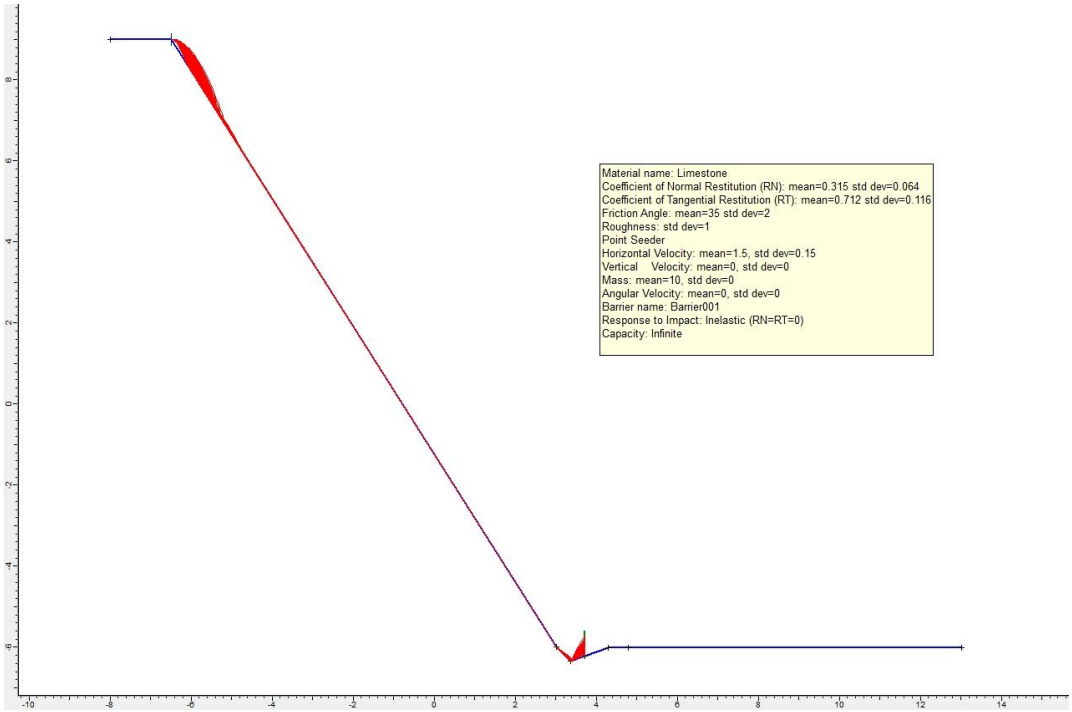

Figure 5.52. Rockfall analysis (10 kg block) with slope flattening and barrier solution at Km: 26+000.

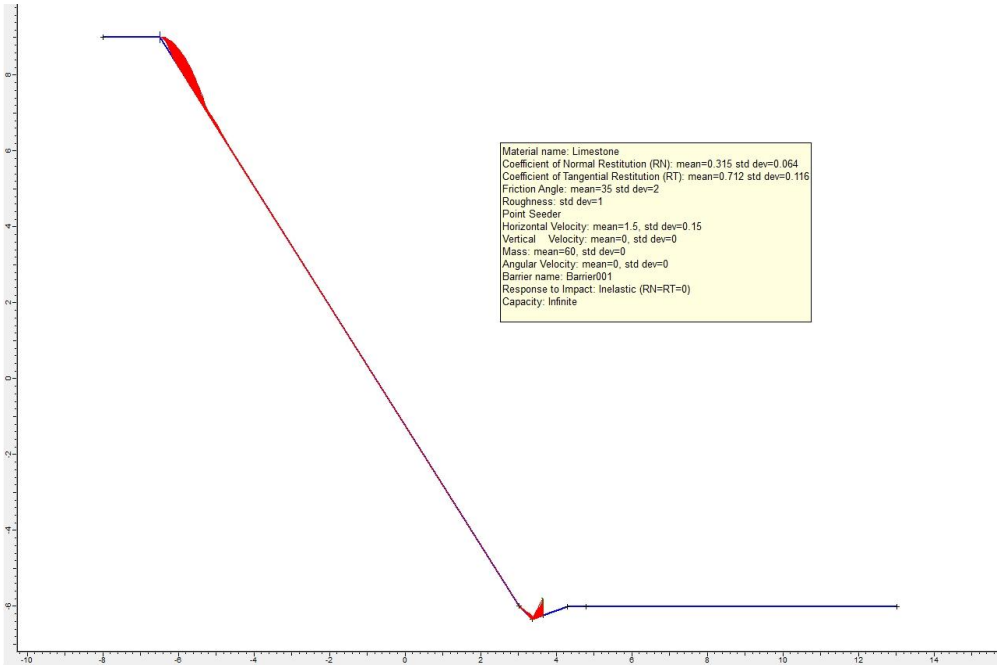

Figure 5.53. Rockfall analysis (60 kg block) with slope flattening and barrier solution at Km: 26+000.

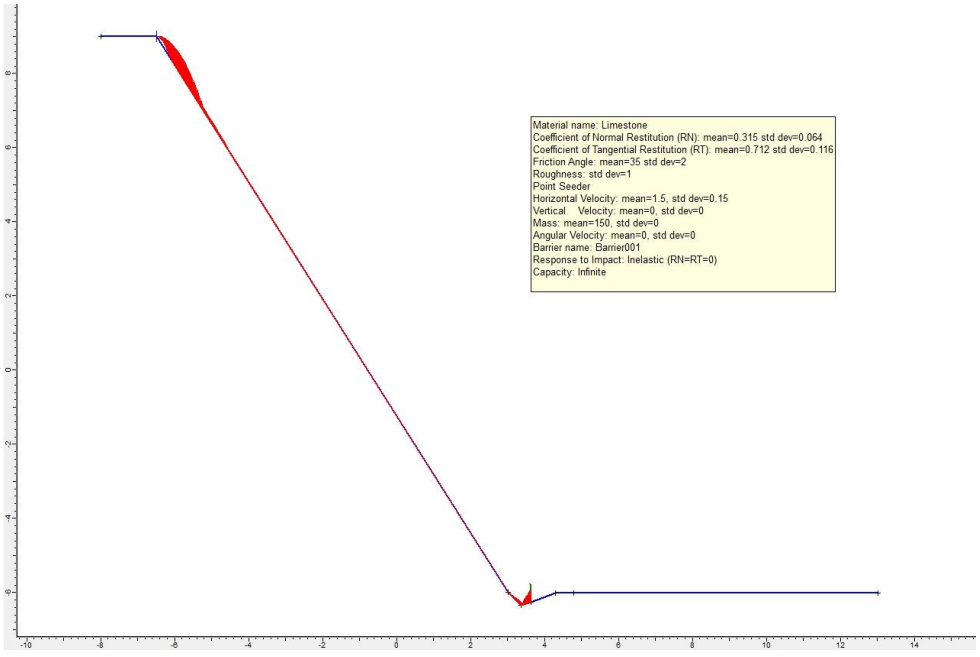

Figure 5.54. Rockfall analysis (150 kg block) with slope flattening and barrier solution at Km: 26+000.

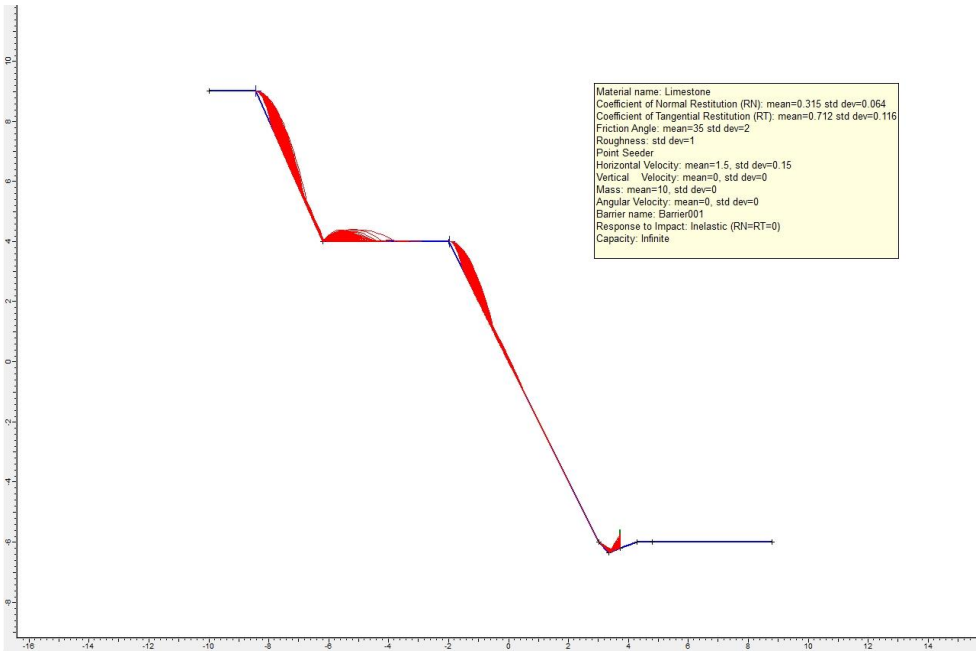

Figure 5.55. Rockfall analysis (10 kg block) with bench and barrier solution at Km: 26+000.

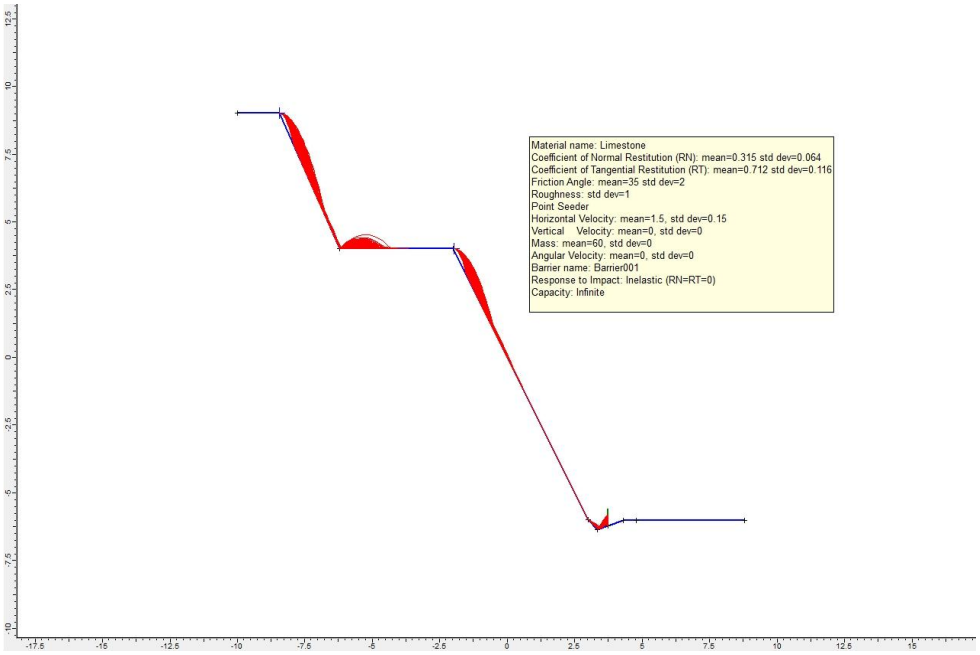

Figure 5.56. Rockfall analysis (60 kg block) with bench and barrier solution at Km: 26+000.

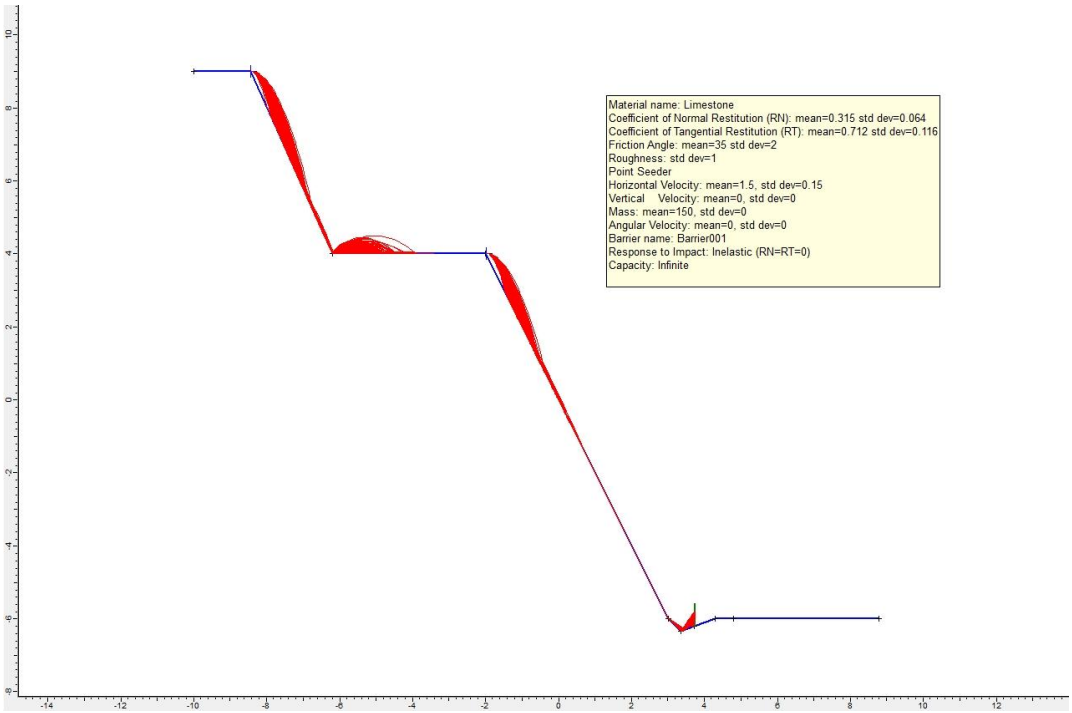

Figure 5.57. Rockfall analysis (150 kg block) with bench and barrier solution at Km: 26+000.

The rocks falling from the upper part of the slope do not fall again to the road. The bench holds all the falling rocks. Therefore, from rockfall point of view, benching is suggested at Km: 26+000 for the upper part of the slope similar to the other cases.

CHAPTER 6

DISCUSSION

This chapter is about the suggested solutions and their comparisons for the slope stability of the limestone cut slopes (nearly 15 m high) exposed at Km: 25+600-26+000. As mentioned before, the main concerns about this particular section of the road are planar failure and the rockfall issues. In order to eliminate these risks, a series of kinematic, limit equilibrium and rockfall analyses are done.

The outcrop in Km: 25+600-26+000 belongs to Limestone unit (JKyk) of the Çataltepe nappe. It is highly fractured and jointed. The rock mainly contains two joint sets and bedding plane as discontinuities. The main issue for this part of the road is the planar failure and rockfall that could assessed through limit equilibrium and rockfall analyses, and visual observations in the field.

For the current situation, it has been seen that there is no risk for mass failure. However, the planar failure is expected at Km: 25+900. This could be eliminated by 7^{o} slope flattening. Thus, the new slope may be 57^{o} instead of 64^{o}. Similarly, rock bolting may be applied to stabilize the slope. Due to the height of the cut slopes, there is a necessity to include a bench for the slopes studied. In this case, no planar failure is expected as validated by the limit equilibrium analysis. A comparison of

factor of safeties for different solutions and different parts of the section can be seen in Table 6.1.

Table 6.1. Comparison of the factor of safety values from the limit equilibrium analysis at Km: 25+900.

	Factor of Safety along Discontinuity	**Factor of Safety for Mass Failure**
Exsiting Slope	0.50	5.03
Slope with Bench	Stable	5.56
Slope Flattening	Stable	5.27
Slope with Rock Bolt	1.11	-

Although all of these approaches seem to solve the slope instability problem at this part of the highway, the analyses reveal that there is also rockfall problem. The falling rocks reach the highway (Table 6.2). The bench to be formed in the cut slope collects the falling rocks and does not allow the rocks to reach the highway. However, the rocks falling from the lower part of the bench reach the highway and create problems. As can be seen from Table 6.2, falling rocks travel 1.4-6.2m within the highway which cannot be accepted. Table 6.3 shows that the rockfall movements include free fall, bouncing and rolling for all cut slopes. During the field study, some rock pieces and blocks are also seen near or just beside the road. In order to eliminate this risk, a catch barrier needs to be installed, but it is very expensive and so close to the road (Table 6.4).

Table 6.2. Rockfall run-out distances for the cut slopes.

			Run-out Distance (m)	Rockfall Into The Road (m)	Slope Angle* (°)
Existing Condition		**10 kg**	5.7	1.4	64
		60 kg	10.4	6.1	64
		150 kg	10.3	6.0	64
25+600	**Slope Flattening**	**10 kg**	10.0	5.7	57
		60 kg	9.5	5.2	57
		150 kg	10.5	6.2	57
	Bench	**10 kg**	8.3	4.0	64
		60 kg	7.5	3.2	64
		150 kg	7.6	3.3	64
25+900	**Slope Flattening**	**10 kg**	10.0	5.7	57
		60 kg	9.5	5.2	57
		150 kg	10.5	6.2	57
	Bench	**10 kg**	8.3	4.0	64
		60 kg	7.5	3.2	64
		150 kg	7.6	3.3	64
26+000	**Slope Flattening**	**10 kg**	10.0	5.7	57
		60 kg	9.5	5.2	57
		150 kg	10.5	6.2	57
	Bench	**10 kg**	8.3	4.0	64
		60 kg	7.5	3.2	64
		150 kg	7.6	3.3	64

*Slope angle is measured from horizontal

Table 6.3. Types of rockfall movements at the cut slopes.

			Free Fall	Rolling	Bouncing
Existing Condition		**10 kg**	x	x	x
		60 kg	x	x	x
		150 kg	x	x	x
25+600	**Slope Flattening**	**10 kg**	x	x	x
		60 kg	x	x	x
		150 kg	x	x	x
	Bench	**10 kg**	x	x	x
		60 kg	x	x	x
		150 kg	x	x	x
25+900	**Slope Flattening**	**10 kg**	x	x	x
		60 kg	x	x	x
		150 kg	x	x	x
	Bench	**10 kg**	x	x	x
		60 kg	x	x	x
		150 kg	x	x	x
26+000	**Slope Flattening**	**10 kg**	x	x	x
		60 kg	x	x	x
		150 kg	x	x	x
	Bench	**10 kg**	x	x	x
		60 kg	x	x	x
		150 kg	x	x	x

Table 6.4. Comparison of the catch barrier distances from the road.

			From The Road (m)
Existing Condition		**10 kg**	0.6
		60 kg	0.7
		150 kg	0.8
25+600	**Slope Flattening**	**10 kg**	0.6
		60 kg	0.5
		150 kg	0.7
	Bench	**10 kg**	0.6
		60 kg	0.6
		150 kg	0.6
25+900	**Slope Flattening**	**10 kg**	0.6
		60 kg	0.5
		150 kg	0.7
	Bench	**10 kg**	0.6
		60 kg	0.6
		150 kg	0.6
26+000	**Slope Flattening**	**10 kg**	0.6
		60 kg	0.5
		150 kg	0.7
	Bench	**10 kg**	0.6
		60 kg	0.6
		150 kg	0.6

Regarding the remedial measures, any combination of slope flattening, benching, rock bolting, wire mesh and shotcrete application may be considered. Nevertheless, benching is compulsory for such heights of the cut slopes. No failure is expected in such a case based on the limit equilibrium analysis, but there is a problem of rockfall which may reach the road. Therefore, either catch barriers must be installed or individual rock pieces should be stabilized. The catch barriers are expansive and should be installed close to the highway if the ditch design is not changed. On the basis of all the field observations and stability-rockfall analyses, the author of this thesis suggests that after benching (10 m high and 5 m wide), the use of wire mesh+shotcrete is expected to eliminate the rockfall problems. Although various types of shotcrete exist, fibre-reinforced shotcrete is recommended for the cut slopes studied in this thesis because it is the most efficient method in slope stabilization, more adoptable to the topography and it reduces the amount of shotcrete mix to be used and labor cost (Ballou and Niermann, 2002).

CHAPTER 7

CONCLUSIONS AND RECOMMENDATIONS

This thesis is aimed to investigate the engineering geological properties of the units exposed for Km: 25+600-26+000 at three cut slopes along Antalya-Korkuteli road from the slope stability point of view. Based on the field studies as well as kinematic, limit equilibrium and rockfall analyses, the following conclusions and recommendations are achieved:

1. The main rock type exposed in the study area is limestone.

2. The limestone at the cut slopes are beige to gray, fine grained, fossiliferous, and highly jointed. The rock contains two joint sets and a bedding plane as main discontinuities. The discontinuities have close to wide spacing, tight to partly open aperture, planar rough to undulating rough discontinuity surfaces. It is slightly weathered mainly in the form of discoloration along discontinuity surfaces with some karstic cavities exists near the surface. The rock is medium strong and strong. The discontinuities are generally free of infilling. However, local calcite infilling may be seen. One of the joint set is bed confined. However, the other discontinuities are persistent. The cut slopes are dry.

3. Based on the kinematic analysis, planar failure is expected at Km: 25+900. Limit equilibrium analysis reveal that 7^{o} slope flattening

may solve the instability problem. Since bench with 10 m high and 5 m wide is required, then the slope becomes stable with the new slope geometry. Additionally, rockfall problems are expected at all three cut slopes. Benching eliminates rockfall from upper part of the cut slope, but the rockfalls from the lower part still reach the road.

4. As a remedial measure, following the bench construction with a slope angle of 64^{o}, covering the cut slope with wire mesh and fibre reinforced shotcrete will eliminate the rockfall problem.

REFERENCES

Antalya Agriculture, 2007, http://www.antalya-tarim.gov.tr/haber_detay.asp?ID=59&baslik_id=66, last accessed date: 10/09/2008

Antalya Municipality 2007a, Climate http://www.antalya.bel.tr/tr/kent_profili/iklim.cfm?tanitimId=761, last accessed date: 10/09/2008

Antalya Municipality 2007b, Vegetation http://www.antalya.bel.tr/tr/kent_profili/cografya.cfm?tanitimId=852, last accessed date: 10/09/2008

Ballou, M. and Matt Niermann, M., 2002, Soil and rock slope stabilization using fiber-reinforced shotcrete in North America, Shotcrete, 20-23.

Colin, H. J., 1962, Fethiye-Antalya-Kaş-Finike (Güneybatı Anadolu) Bölgesinde Yapılan Jeolojik Etüdler. Bulletin of the Mineral Research and Exploration Institute of Turkey, no. 59, 19-60

Cornforth, D.H., 2005, Landslides in practice. Wiley, Hoboken, 596 p.

DIPS, 2004, Scientific Software- Data Interpretation Package using Stereographic projection, Version 5.103, Rocscience Inc., Canada, 90 p

Form Jeoteknik, 2008, Antalya-Korkuteli Yolu Mühendislik Jeolojisi Raporu, Ankara

GDDA, 1996. Earthquake zoning map of Turkey, General Directorate of Disaster Affairs, Ministry of Reconstruction and Resettlement of Turkey.

GDH, 1995, Zemin arastırma işine ait teknik şartname. Karayolları Genel Müdürlüğü, Ankara

GDH, 2007, General Directorate of Highways website, http://www.kgm.gov.tr/, last accessed date: 10/09/2008

Google Earth, 2010, Maps and satellite images for complex or pinpointed regional searches

Hoek, E., Bray, J.W., 1981, Rock Slope Engineering, 3rd ed. Institute of Mining and Metallurgy, London. 358 p.

ISRM (International Society for Rock Mechanics), 1981, Rock characterization, testing and monitoring – ISRM Suggested Methods, Pergamon Press, Oxford, Brown, E.T.(ed), 211 p.

MTA, 2004, Türkiye 1:500.000 Ölçekli Jeoloji Haritası

Poisson, A. 1977, Recherches g.ologiques dans les Taurides occidentals. These Doct. D'Etat, Universitie de Paris-Sud, Orsay, 795 p.

Poisson, A. and Poignant, A.F., 1974, La formation ele Karabayır, base de la transgression Miocene dans la region de Korkuteli (Turquie). Bulletin of the Mineral Research and Exploration Institute of Turkey, no. 82, 67-71

Priest, S.D., 1993, Discontinuity analysis for rock engineering. Chapman & Hall, London, 496p.

RocFall, 2004, Scientific Software-Statistical Analysis of Rockfalls, Version 4.039, Rocscience Inc., Canada, 65 p

RocLab, 2007, Scientific Software-Rock Mass Strength Parameters, Version 1.031, Rocscience Inc., Canada, 25 p

SLIDE, 2004, Scientific Software-2D Limit Equilibrium Slope Stability Analysis, Version 5.104, Rocscience Inc., Canada, 199 p

Şenel, M., 1997, 1:100.000 Ölçekli Isparta K-10 Paftası. MTA Genel Müdürlüğü, pp. 3-10.

Şenel, M., Akdeniz, N., Öztürk, E. M., Özdemir, T., Kadınkız, G., Metin, Y., Öcal, H., Serdaroğlu, M., Örçen, S., 1994, Fethiye (Muğla)-Kalkan (Antalya) ve Kuzeyinin Jeolojisi. Maden Tetkik ve Arama Genel Müdürlüğü Jeoloji Etütleri Dairesi Başkanlığı, pp. 13-15.

Topal, T., Akin, M., 2009, Geotechnical assessment of a landslide along a natural gas pipeline for possible remediations (Karacabey-Turkey), Environmental Geology, 57 (3): 611-620.

Turner, A.K., Schuster, R.L., 1996, Landslides-investigation and mitigation. Transportation Research Board, National Research Council, Special Report, vol. 247. National Academy Press, Washington, DC. 673 p.